NUMERICAL STUDY OF THREE-DIMENSIONAL CIRCULATION AND HYDROGRAPHY IN HALIFAX HARBOUR USING A NESTED-GRID OCEAN CIRCULATION MODEL

by

Shiliang Shan

Submitted in partial fulfillment of the requirements
for the degree of Master of Science

at

Dalhousie University
Halifax, Nova Scotia
December 2010

DALHOUSIE UNIVERSITY

DEPARTMENT OF OCEANOGRAPHY

The undersigned hereby certify that they have read and recommend to the Faculty of Graduate Studies for acceptance a thesis entitled "NUMERICAL STUDY OF THREE-DIMENSIONAL CIRCULATION AND HYDROGRAPHY IN HALIFAX HARBOUR USING A NESTED-GRID OCEAN CIRCULATION MODEL" by Shiliang Shan in partial fulfillment of the requirements for the degree of Master of Science.

Dated: December 14, 2010

External Examiner: _____
Dr. Brian Petrie

Supervisor: _____
Dr. Jinyu Sheng

Readers: _____
Dr. Keith Thompson

_____
Dr. David Greenberg

_____
Dr. David Scott

DALHOUSIE UNIVERSITY

DATE: December 14, 2010

AUTHOR: Shiliang Shan

TITLE: NUMERICAL STUDY OF THREE-DIMENSIONAL CIRCULATION
            AND HYDROGRAPHY IN HALIFAX HARBOUR USING A
            NESTED-GRID OCEAN CIRCULATION MODEL

DEPARTMENT OR SCHOOL: Department of Oceanography

DEGREE: MSc   CONVOCATION: May   YEAR: 2011

_____
Signature of Author

TABLE OF CONTENTS

LIST OF TABLES

LIST OF FIGURES

ix

ABSTRACT

Halifax Harbour is one of the world's largest natural harbours and has significant environmental and economic value. A good understanding of oceanographic processes is required for pollution control and sustainable development of the Harbour. A five-level nested-grid coastal ocean circulation model known as the Nested-grid Coastal Ocean Prediction System for Halifax Harbour (NCOPS-HFX) is used to reconstruct the three-dimensional circulation and hydrography and associated temporal and spatial variability of the Harbour. The NCOPS-HFX is driven by tides, meteorological forcing, and buoyancy forcing associated with river and sewage discharges. Model performances are assessed by comparing model results with available observations including sea level from tide gauges, CTD observations, current meter records and monthly mean climatology of temperature and salinity. Model results are also used to examine the main physical processes affecting circulation and hydrography in the Harbour. It is found that the near-surface currents in the Harbour are significantly affected by tides and wind forcing with an intense tidal jet in the Narrows and a salinity front in the upper layer of Bedford Basin. The time-mean circulation produced by the model is characterized by a typical two-layer estuarine circulation with seaward flow in the upper layer and landward flow in the lower layer. The model also reproduces reasonably well the seasonal changes of temperature and salinity in the Harbour. Dispersion and retention in the Harbour are studied based on numerical passive tracer and particle tracking experiments. The e-folding flushing time is about 40 and 90 days in the upper and entire Bedford Basin respectively, 2-5 days over the Inner and Outer Harbour, and about 1 day in the Narrows.

LIST OF ABBREVIATIONS AND SYMBOLS USED

2D	two-dimensional
3D	three-dimensional
BIO	Bedford Institute of Oceanography
CANDIE	CANadian version of DIEcast
CHS	Canadian Hydrographic Service
CTD	Conductivity, Temperature, and Depth
DFO	Fisheries and Oceans Canada
HFX	Halifax Harbour
HHWQMP	Halifax Harbour Water Quality Monitoring Project
KPP	K Profile Parameterization
LOBO	Land/Ocean Biogeochemical Observatory
MATLAB	MATrix LABoratory
MSC	Meteorological Service of Canada
NAO	North Atlantic Oscillation
NCOPS-HFX	Nested Coastal Ocean Prediction System for Halifax Harbour
NCOPS-LB	Nested Coastal Ocean Prediction System for Lunenburg Bay
POM	Princeton Ocean Model
SCRUM	S-Coordinate Rutgers University Model
SLP	Sea Level Pressure
STP	Sewage Treatment Plant
UTC	Coordinated Universal Time
VAC	Volume Averaged Concentration

ACKNOWLEDGEMENTS

CHAPTER 1

INTRODUCTION

1.1 Background

Halifax Harbour is one of the world's largest ice-free natural harbours and is situated on the south coast of Nova Scotia, Canada. The Harbour is an elongated estuary which consists of the Outer Harbour, Inner Harbour, Northwest Arm, Eastern Passage, Narrows and Bedford Basin (Figure 1.1). Untreated sewage and wastewater had been flushed into Halifax Harbour through several outfalls for centuries. A new sewage treatment plant (STP) was constructed and began operation in February 2008, leading to a brief period of significant improvement of the water quality in the Harbour. However, the STP was shut down in January of 2009 due to an extended local area power outage and multiple mechanical malfunctions (*Bousquet*, 2009). As a result, raw sewage was again discharged directly into the harbour. On June 24, 2010 the STP was back on line (http://www.halifax.ca/mediaroom/ pressrelease/pr2010/100624HarbourCleanupisbackontrack.html). Nevertheless, due to the processing capacity of the STP, raw untreated sewage and storm water are only screened and pumped directly into the Harbour during intense precipitation periods associated with storms such as the recent Hurricane *Earl* in September, 2010.

   The release of raw sewage and wastewater into Halifax Harbour over the last 200 years has led to many environmental problems. For example, an area of $\sim$93 km^2 in the Harbour was closed to shellfish harvesting due to high bacterial concentrations of Harbour waters, resulting in $27 million of lost revenue between 1965 and 2000 (*Wilson*, 2000). Poor water quality also interferes with military dive training operations (*CBC News*, 2009). Floatable waste not only causes aesthetic offence but also is a hazard to some marine animals. The long-term dumping of sewage into Halifax Harbour has resulted in the buildup of deposits

of organic contaminants, heavy metals and toxic and hazardous chemicals in the sediments (*Buckley and Winters*, 1992; *Fournier*, 1990); these can also contribute to environmental deterioration. All of these problems have a negative effect on the reputation of the Harbour region, and carry both economic as well as environmental impacts.
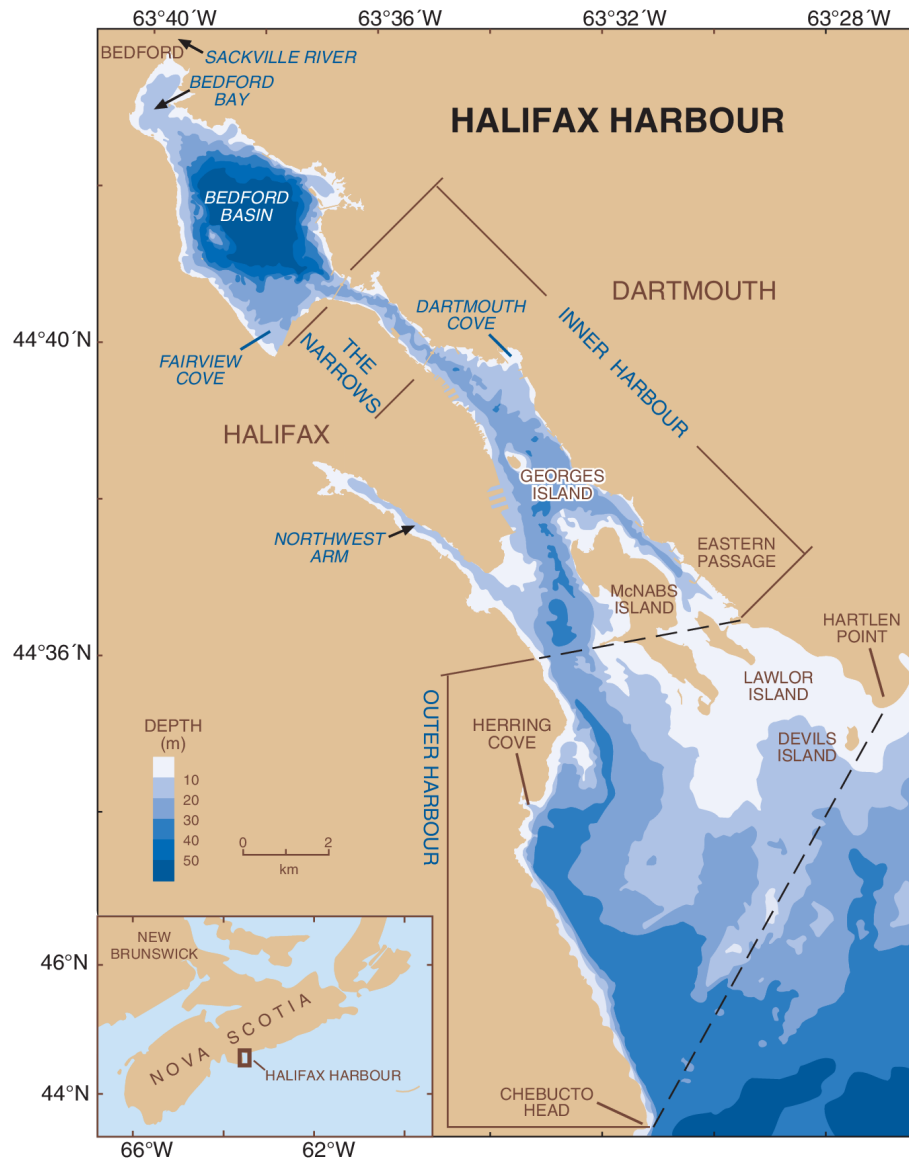
Figure 1.1: Map of Halifax Harbour, Nova Scotia, Canada (from *Fader and Miller* 2008).

Circulation plays a fundamental role in advecting and diluting wastewater and the transport and deposition of water-borne particles in coastal waters. A better knowledge of major physical, chemical and biological processes is needed to predict the possible pollution effects of sewage discharge in Halifax Harbour. Reliable prediction of the water movement is also essential for an effective ecosystem-based management of natural resources in the region. This places an emphasis on the development of numerical circulation models with reasonable predictive capability that can adequately represent the physical oceanography and its effects on dilution and flushing of effluent on time scales ranging from a few hours to several months.

1.2   Literature Review

Halifax Harbour has been the focus of various studies in the past, in part due to the fact that the Harbour is a convenient test bed for oceanographers in the region including scientists at Bedford Institute of Oceanography (BIO) and Dalhousie University, but also because the Harbour is important to local and national industry, the military, civilians and tourism. The following is a brief summary of major oceanographic research activities and their findings related to Halifax Harbour.

Significant efforts have been made in monitoring oceanographic conditions in Halifax Harbour. An early study of the ocean circulation and hydrography in the Harbour was made by *Huntsman* (1924) and *Hachey* (1935) collected in-situ temperature and salinity observations. There were two comprehensive field observation programs and some of their observations will be used in this study. The first field program was conducted from July 1969 to September 1971 with temperature and salinity measurements made monthly at eight cross-sections from the head to the mouth of Halifax Harbour (*Jordan*, 1972). The second field program is an on-going program that started in 2004 with weekly or bi-weekly CTD (conductivity, temperature, and depth) observations made by Halifax Harbour Water Quality Monitoring Project (HHWQMP, http://www.halifax.ca/harboursol/waterqualitydata.html). Sea level observations have been made by two tide gauges in Halifax Harbour, and they are also used in this study. The two tide gauges are the Canadian Hydrographic Service (CHS) station 490 near the Naval Dockyard and CHS station 491 near the Bedford Institute of Oceanography.

There are several moorings inside Halifax Harbour providing mainly biological oceanographic measurements. A Land/Ocean Biogeochemical Observatory (LOBO) was deployed in the Northwest Arm in January of 2007 to provide hourly biogeochemical parameters (http://lobo.satlantic.com). In 1991, the Bedford Institute of Oceanography started a monitoring program which collects weekly plankton samples in Bedford Basin (http://www2.mar.dfo-mpo.gc.ca/science/ocean/BedfordBasin/index.htm). In October 2009, Dalhousie University deployed a coastal ocean monitoring buoy known as the Bedford Basin Ocean Monitoring Buoy (BBOMB http://bbomb.ceotr.ca/index.php). This buoy is equipped with many advanced sensors in order to develop a rigorous understanding of important ecological processes in the Basin and the adjacent ocean.

Along with field observations, several numerical models of different complexity have been developed for Halifax Harbour over the past 20 years. Most of the models were used in process studies of hydrodynamics and some were used to assess the water quality implications of various sewage treatment options. A simple box model based on the conservation of mass and salt was developed by *Petrie and Yeats* (1990) in a study of metal, suspended solids and nutrients distributions in Halifax Harbour. Using this box model and salinity observations (*Jordan*, 1972) as input, *Petrie and Yeats* (1990) demonstrated that the time-mean circulation in the Harbour is a classical two-layer estuarine type; the modelled distributions of copper, suspended solids, nitrate and phosphate using this box model agree well with observations. A simple water quality model was developed by ASA Consulting Limited as part of a numerical study of concentrations and distributions of fecal coliform bacteria and suspended particulate matter in the Harbour (*Fournier*, 1990). A two-dimensional (2D) baroclinic circulation model was developed by *Tee and Petrie* (1991) to simulate winter circulation in 1970 in the Harbour. They demonstrated that the mean estuarine circulation in the Harbour is driven primarily by the Sackville River and enhanced by the wind forcing but reduced by sewage input. A 2D hydrodynamic model was developed by *MacLaren Plansearch Limited and Martec Limited* (1991) to simulate tides and wind-driven circulation in Halifax Harbour. The model is based on the depth-averaged Navier-Stokes equations and a finite difference numerical scheme. The horizontal resolution of this model was 400 by 400 m which poorly resolves the narrow area of the Harbour. In addition, the tidal forcing specified in the model was only the principal lunar semi-diurnal constituent M_2, and the wind forcing was idealized. A three-dimensional

(3D) hydrodynamic model for Bedford Basin (*Zhang*, 1998) based on the S-Coordinate Rutgers University Model (SCRUM, *Song and Haidvogel* 1994) was developed. This model was used to simulate the circulation patterns and hydrography distributions driven by freshwater discharge and wind forcing over a few days in Bedford Basin. The model results of *Zhang* (1998) indicate the importance of baroclinic effects associated with freshwater discharges in Bedford Basin. A finite element model was used by *Greenberg et al.* (1993) to simulate a tsunami due to the 1917 Halifax Harbour explosion. A 3D linear harmonic finite element model (resolution varying between 20 m and 1000 m) was developed by *Greenberg* (1999) to simulate the M_2 tide in the Harbour. A tidal prediction program known as WebTide which contains several datasets, including Halifax Harbour datasets (http://www.mar.dfo-mpo.gc.ca/science/ocean/coastal_hydrodynamics/WebTide/ Install/halifax_data.html), was developed to provide predictions of five tidal constituents (M_2, K_1, N_2, S_2 and O_1) for any location inside Halifax Harbour based on tidal harmonic constants pre-determined from the model output of *Greenberg* (1999).

Although previous observational and numerical studies have been very useful in revealing the basic features of tidal and sub-tidal circulations and hydrographic distributions in Halifax Harbour, a better understanding and quantification of the 3D circulation and hydrography, and their temporal and spatial variability in the Harbour is required.

1.3   Objectives

As mentioned earlier, Halifax Harbour has a complex topography with a narrow channel connecting to Bedford Basin to the northwest and the Scotian Shelf to the southeast. Circulation in the Harbour is affected by tides, wind forcing, surface heat fluxes and fresh water discharges. The Nova Scotia Current can also affect the circulation and hydrography in the Harbour and adjacent coastal waters. A better understanding of the main physical processes in the Harbour is required for pollution control and sustainable development of the region. The main objectives of this study are:

  i) To develop a five-level nested-grid 3D baroclinic ocean circulation model for Halifax Harbour based on the coastal circulation model for Lunenburg Bay, Nova Scotia, Canada developed earlier by *Yang and Sheng* (2008).

 ii) To conduct a process study using the nested-grid modelling system to determine the main physical processes affecting circulation and hydrography in Halifax Harbour.

iii) To quantify flushing time, dispersion and retention in Halifax Harbour using passive tracers and passive particles that are carried by 3D flow fields produced by the nested-grid modelling system.

In this study, numerical model results of the 3D circulation and hydrography in 2006 produced by the nested-grid modelling system are used to examine the main physical processes affecting circulation and associated variability in the Harbour. As a result, the general meteorological and oceanographic conditions in Halifax Harbour, especially in 2006, and the impact of climate change of the general circulation in the Harbour will be discussed.

1.4   Structure of Thesis

Chapter 2 describes the main meteorological and oceanographic conditions in Halifax Harbour, including gridded monthly mean temperature and salinity climatology constructed from scattered hydrographic observations. Chapter 3 describes the model and summarizes the setup, external forcing and validations of the nested-grid modelling system. Chapter 4 presents model results and the major physical processes affecting the 3D circulation and hydrography in Halifax Harbour. Chapter 5 discusses the local flushing time, dispersion and retention in Halifax Harbour based on numerical passive tracer and particle tracking experiments. The final chapter provides a summary and discussion.

CHAPTER 2

METEOROLOGICAL AND OCEANOGRAPHIC CONDITIONS IN HALIFAX HARBOUR

Halifax Harbour is an elongated ice-free estuary, consisting of a deep basin (Bedford Basin) connecting to the open ocean via a narrow channel (Figure 1.1). The main navigation channel is located on the western side of the Harbour, which shoals from 40 m at its entrance to about 25 m through out most of the Harbour. The Narrows, which is about 500 m wide and 3 km long, with a mean water depth of ~20 m, connects the Inner Harbour to Bedford Basin. Bedford Basin, which is a small fjord-type estuary, is approximately 6 km long and 4 km wide with a surface area of ~17 km^2 and a maximum depth of ~71 m. The Sackville River, the only major freshwater river in the study region, discharges into the northwestern end of Bedford Basin. The Northwest Arm is the western component of the Inner Harbour and is approximately 5 km long and several hundred meters wide, with water depths varying between 10 and 15 m.

2.1 Meteorological and Hydrological Conditions

Halifax Harbour is marked by a continental climate influenced significantly by the adjacent Atlantic Ocean. The daily mean air temperatures range from -9–0 °C in January to 14–23 °C in August*. The time-mean precipitation between 1971 and 2000 is about 1,510 mm annually with the lowest rate in summer. Snow falls and melts alternate from

---

*source: Canadian Climate Normals and Averages 1971–2000 of Halifax Citadel http://climate. weatheroffice.gc.ca/climate_normals/index_e.html

November through April. Spring is usually cool and foggy, and summer can vary from hot and dry to cool and rainy. Early fall is often sunny and warm. The dominant wind direction in the region is from the northwest in winter and from the southwest in summer. The mean wind speed varies from 10–11 knots (∼5.14–5.66 m/s) in winter to 7–8 knots (∼3.60–4.12 m/s) in summer (*MacLaren Plansearch Limited*, 1991). Halifax Harbour also generally experiences several strong snow storms in winter and tropical storms or hurricanes occasionally in summer and fall. For example, Hurricane *Juan* made landfall west of Halifax with estimated maximum sustained winds of 44 m/s on September 29, 2003 (*Fogarty et al.*, 2006) .

2.1.1 Wind

Winds can affect the circulation, mixing and hydrography of Halifax Harbour. Figure 2.1 shows the monthly mean sea level pressure (SLP) fields for January and July over North America. From the large-scale monthly mean SLP distributions, mean wind directions in a region can be estimated based on the principle that geostrophic winds are tangential to the SLP contour lines with high pressure on the right-hand side in the Northern Hemisphere. In January, there is an intense low pressure centre located around Iceland called Icelandic Low and a high pressure centred close to Bermuda called the Bermuda High (Figure 2.1a). The dominant wind direction is northwesterly in Halifax Harbour in January. From a local point of view, the mean wind blows nearly along the longitudinal axis of the Harbour pointing offshore during winter. As time progresses from winter to summer, the Icelandic Low weakens. Over the North Atlantic Ocean, the Bermuda High strengthens in summer. The changes in position and strength of the low and high pressure centres result in a southerly shift of the dominant wind direction in Halifax Harbour. The southwesterly wind blows roughly along the Atlantic coast of Nova Scotia during the summer.

The windroses presented in Figure 2.2 summarize the wind speed, direction and frequency information for 2006 at McNabs Island in Halifax Harbour. They demonstrate that wind forcing exhibits strong seasonal variability in Halifax Harbour. In spring and fall, winds are mainly from two directions: southeast and northwest respectively. In winter winds blow predominantly from the west or northwest and tend to be stronger than other seasons. This is due mainly to the higher intensity of weather systems which pass through this region in winter. During summer, the prevailing wind undergoes a shift to a

more southerly wind. These southerly winds occur more frequently than from any other direction.
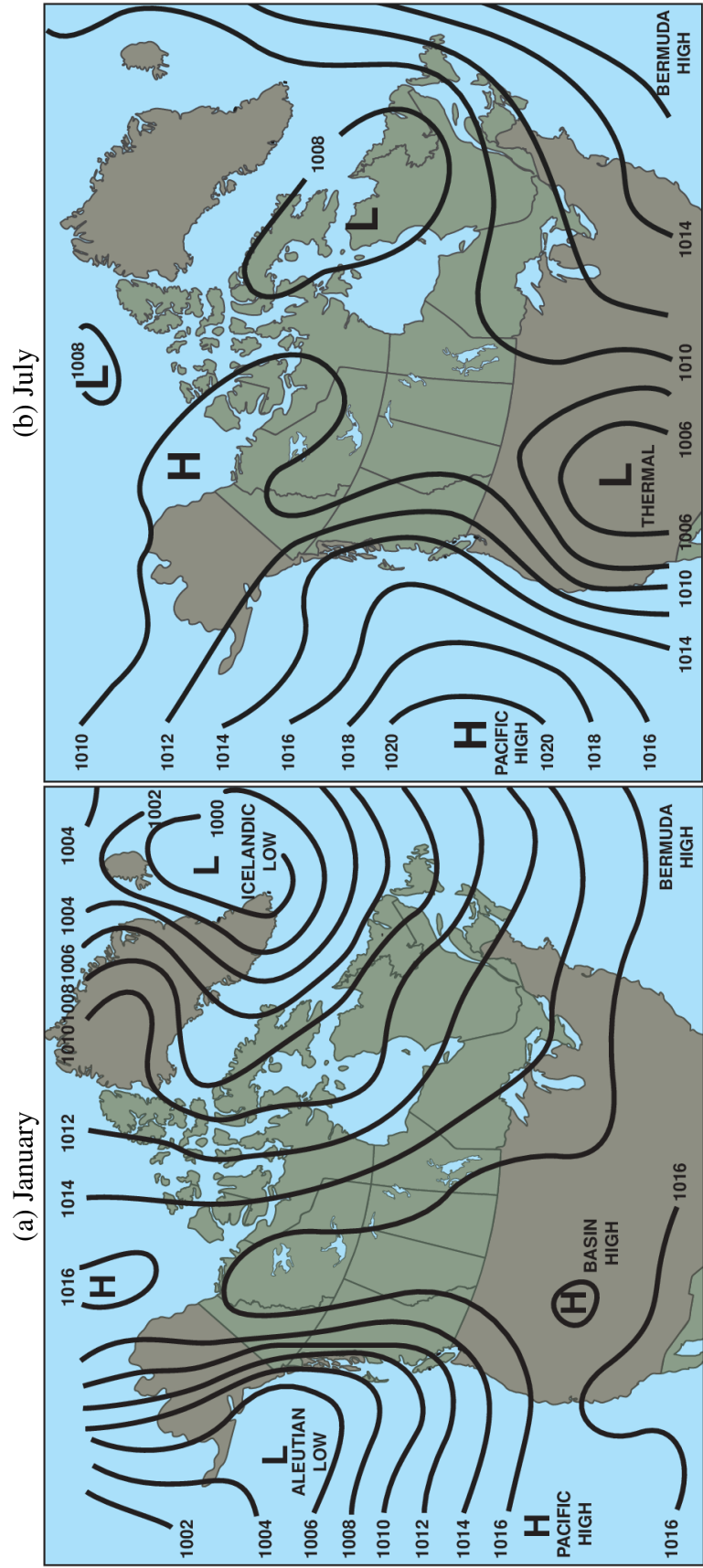
Figure 2.1: Monthly mean sea level pressure distributions averaged from instantaneous fields over a number of years in (a) January and (b) July (*Robichaud and Mullock*, 2001)

2006 Annual Windrose

Spring (Mar/Apr/May)

Summer (Jun/Jul/Aug)

Fall (Sep/Oct/Nov)

Winter (Dec/Jan/Feb)
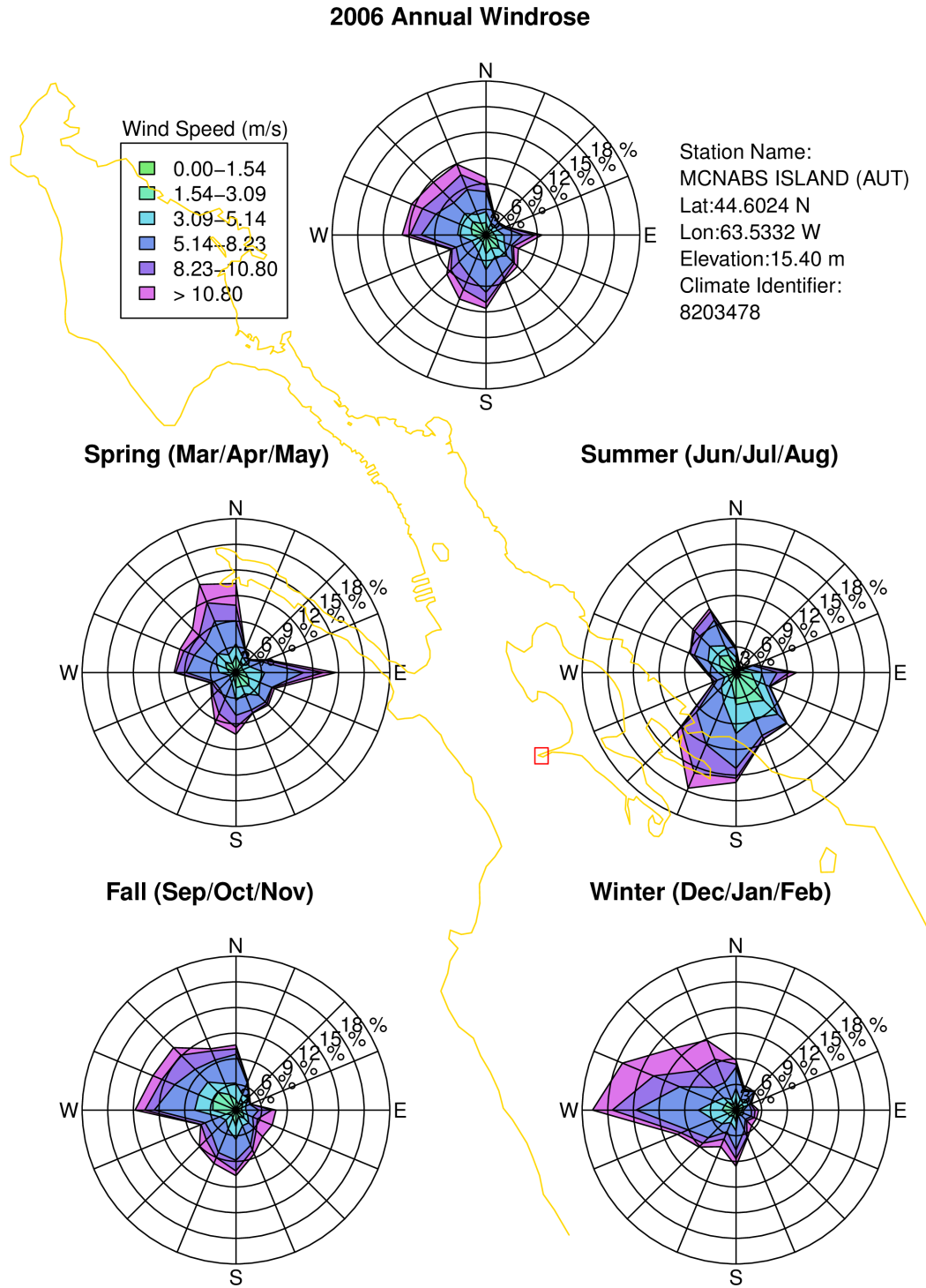
Figure 2.2: Windroses for Halifax Harbour based on weather station records from McNabs Island in 2006. Each of the extending arms on the windrose represents the direction from which wind is blowing. Data were extracted from the National Climate Data and Information Archive of Canada, http://climate.weatheroffice.gc.ca/climateData/canada_e. html.

2.1.2   River, Sewage and Distributed Water Discharges

The circulation and hydrography of Halifax Harbour are also affected by freshwater discharge from the Sackville River, several sewage outfalls and small streams. Their locations and discharges are shown in Figure 2.3 and listed in Table 2.1.

The annual mean discharge from the Sackville River is relatively small at $\sim$5 m^3/s (*Buckley and Winters*, 1992). It is the largest single component and alone accounts for $\sim$1/3 of the total freshwater inflow. The climatological monthly mean discharges of the River have two peaks each year, one occurring in April and the other in November (Figure 2.4). The 2006 daily discharge time series feature several large discharge events with a rapid increase in discharge followed by a gradual decay. The water storage capacity of the Halifax area is large in winter, with much of the surface and ground water is locked up as ice, and the precipitation stored by snow cover (*Forrester*, 1983). As the ice and snow melt in spring, the runoff increases rapidly, resulting in a discharge peak between April and May as shown in Figure 2.4. Real-time water level data of the Sackville River can be found from http://www.wateroffice.ec.gc.ca/graph/graph_e.html?stn=01EJ001.
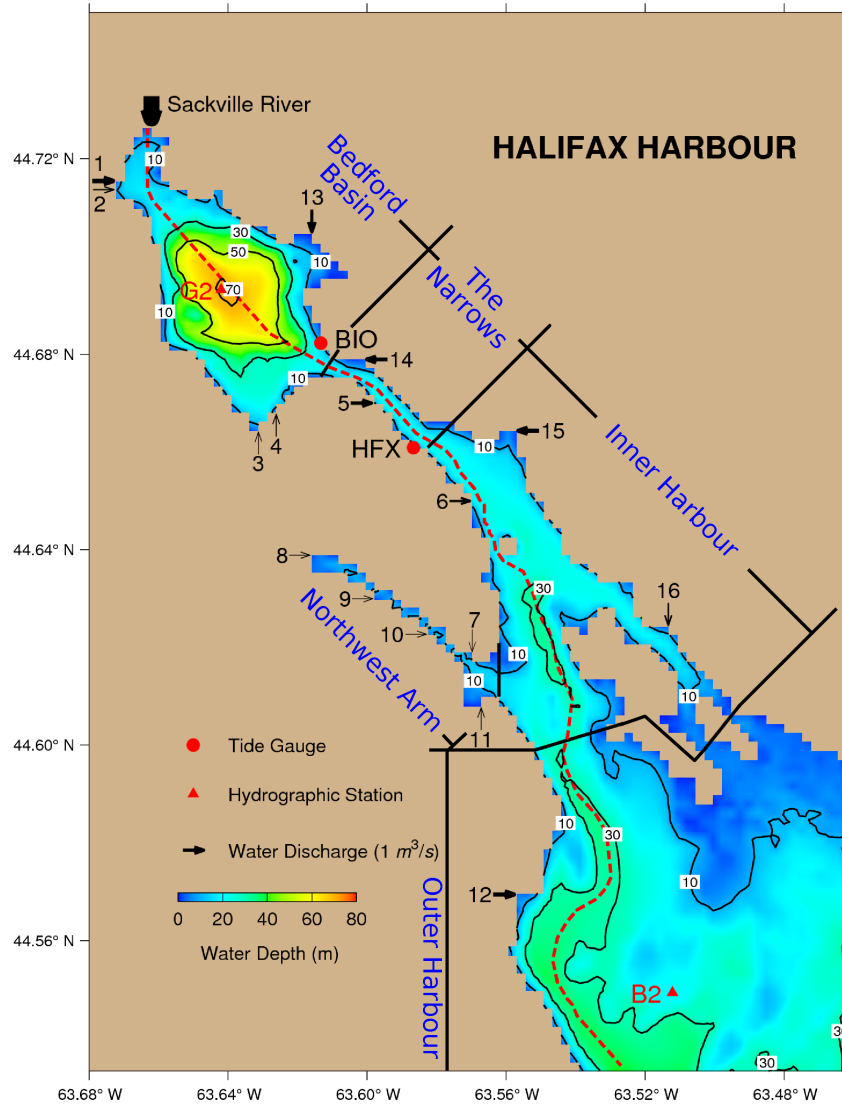
Figure 2.3: Gridded ($\sim$200 m) topography of Halifax Harbour and adjacent waters. Five geographic divisions labelled in blue text are used in this study. Red dots indicate positions of two tide gauges: CHS station 490 near the Naval Dockyard (HFX) and CHS station 491 near the Bedford Institute of Oceanography (BIO). Red triangles represent positions of two hydrographic stations: G2 in Bedford Basin and B2 in the Outer Harbour. Water discharge locations are numbered 1 to 16; discharge values are indicated by scaled arrows. The thick bold arrow at the head of Bedford Basin represents the climatological annual mean discharge (1971–2007) of the Sackville River, about 5.04 m^3/s. Fluvial and sewage discharges along the shore are listed in Table 2.1. The red dashed line represents a transect from the mouth of the Sackville River through Bedford Basin following the deep channel to the open sea; this transect is used in the discussion of climatology and model results in later sections.
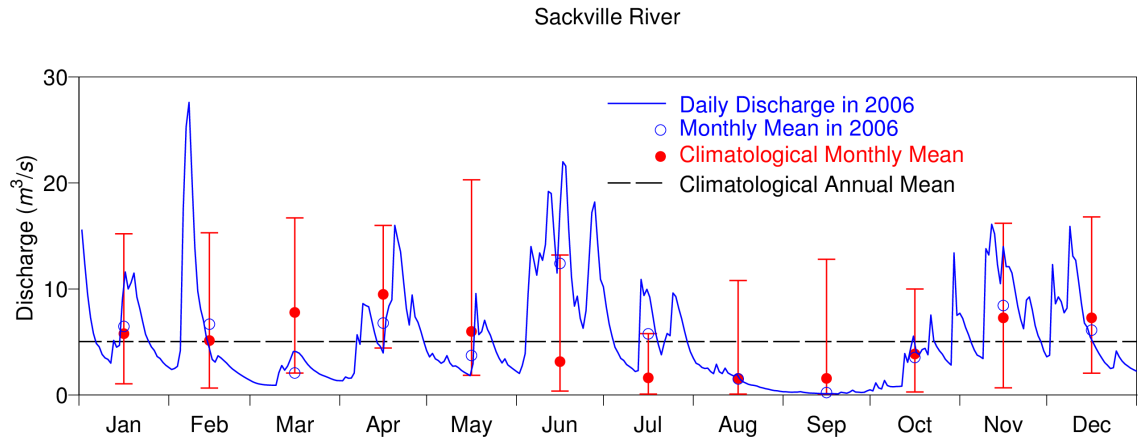
Sackville River

Figure 2.4: Climatological monthly mean discharges from the Sackville River. The climatological monthly mean values were calculated from 1971–2007 flow observations. For comparison, the freshwater discharge from the Sackville River in 2006 is also presented (blue). Discharge of the Sackville River was extracted from Canada's HYDAT database (http://www.wsc.ec.gc.ca/hydat/H2O/index_e.cfm?cname=main_e.cfm). Vertical red lines show the monthly minimum and maximum river discharges between 1971–2007.

Table 2.1: Fluvial and sewage effluent discharges into Halifax Harbour[†]

Number	Location	Average discharge (m^3/s)
	Head of Bedford Basin	
	Sackville River	Daily
	Western Bedford Basin	
1	Paper Mill Lake flume	1.38±0.01
2	Bedford-Sackville sewage treatment plant	0.37±0.01
3	Fairview Cove storm and sewer	0.19±0.01
4	Fairview Cove storm drain	0.27±0.01
	Western middle harbour	
5	Duffus Street sewer	1.02±0.01
6	Duke Street sewer	0.68±0.01
	Northwest Arm	
7	Point Pleasant sewer	0.14±0.01
8	Chocolate Lake flume	0.24±0.01
9	Frog Lake Brook	0.20±0.01
10	Williams Lake Brook	0.20±0.01
	Western lower middle harbour (Georges Island to York Redoubt)	
11	Purcells Lake Brook	0.21±0.01
	Western outer harbour	
12	Herring Cove sewer and Powers Pond flume	1.29±0.02
	Eastern Bedford Basin	
13	Wrights Brook	0.94±0.01
	Eastern middle harbour	
14	Tufts Cove sewer	1.18±0.01
15	Dartmouth Cove sewer	1.24±0.01
	Eastern lower middle harbour (Georges Island to Eastern Passage)	
16	Eastern Passage sewage treatment plant	0.46±0.01

[†]The discharges were adapted from *Buckley and Winters* (1992). The distributed discharges along shoreline discharges were equally add to discharge locations in the correspond subregions.

2.2 Oceanographic Conditions

As mentioned in the introduction, Halifax Harbour is a semi-enclosed estuary influenced strongly by tides, wind forcing and water discharges from the Sackville River, sewage and distributed water along the coast. The time-mean density-driven circulation in Halifax Harbour is a typical two-layer estuarine type (*Huntsman*, 1924), with relatively fresh upper layer water moving toward the open sea and a salty lower layer water moving toward Bedford Basin and mixing with fresh upper layer water at the interface (Figure 2.5). Based on the salinity observations in monthly surveys over a two-year period, *Petrie and Yeats* (1990) confirmed the existence of this classical two-layer estuarine circulation in Halifax Harbour (Figure 2.6) using a simple box model. The box model results also demonstrate that strong horizontal currents occur in the Narrows and McNabs Island area. The largest vertical exchanges occur over the Narrows during low discharge periods and over the McNabs Island area during high discharge periods.
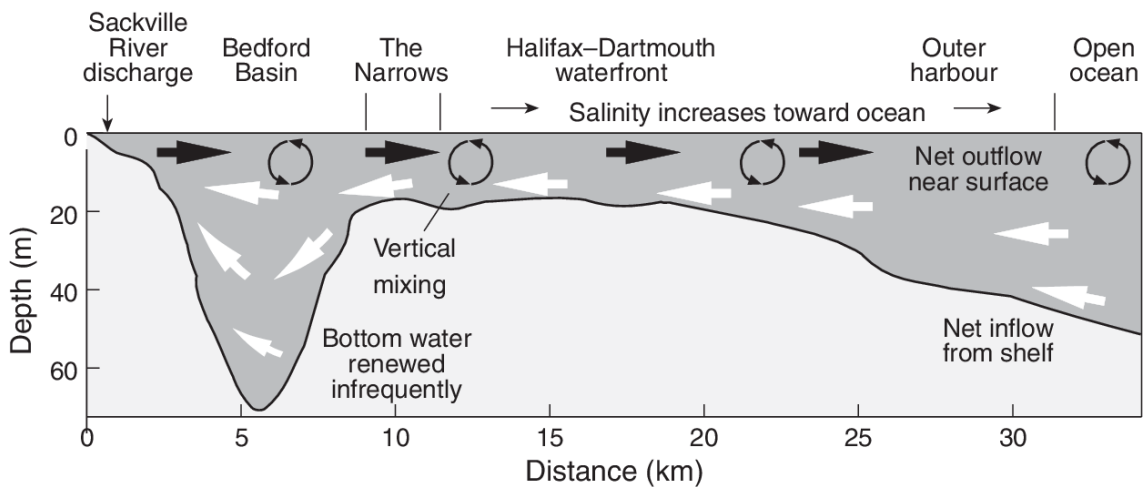
Figure 2.5: Schematic showing a two-layer circulation structure in Halifax Harbour (from *Fader and Miller* 2008).

Tides in Halifax Harbour are mainly semi-diurnal (*MacLaren Plansearch Limited*, 1991). Mean and maximum tidal ranges are ∼1.3 m and ∼2.1 m, respectively. The M_2 has an amplitude about 63.3 cm and accounts for 60% of the tidal elevation (*Lawrence*, 1989). Figure 2.7 shows the depth-averaged flood and ebb M_2 tides in Halifax Harbour produced by *Greenberg* (1999). Note the relatively large tidal currents at the Narrows, and over the east and west side of McNabs Island. The M_2 current is the largest tidal constituent
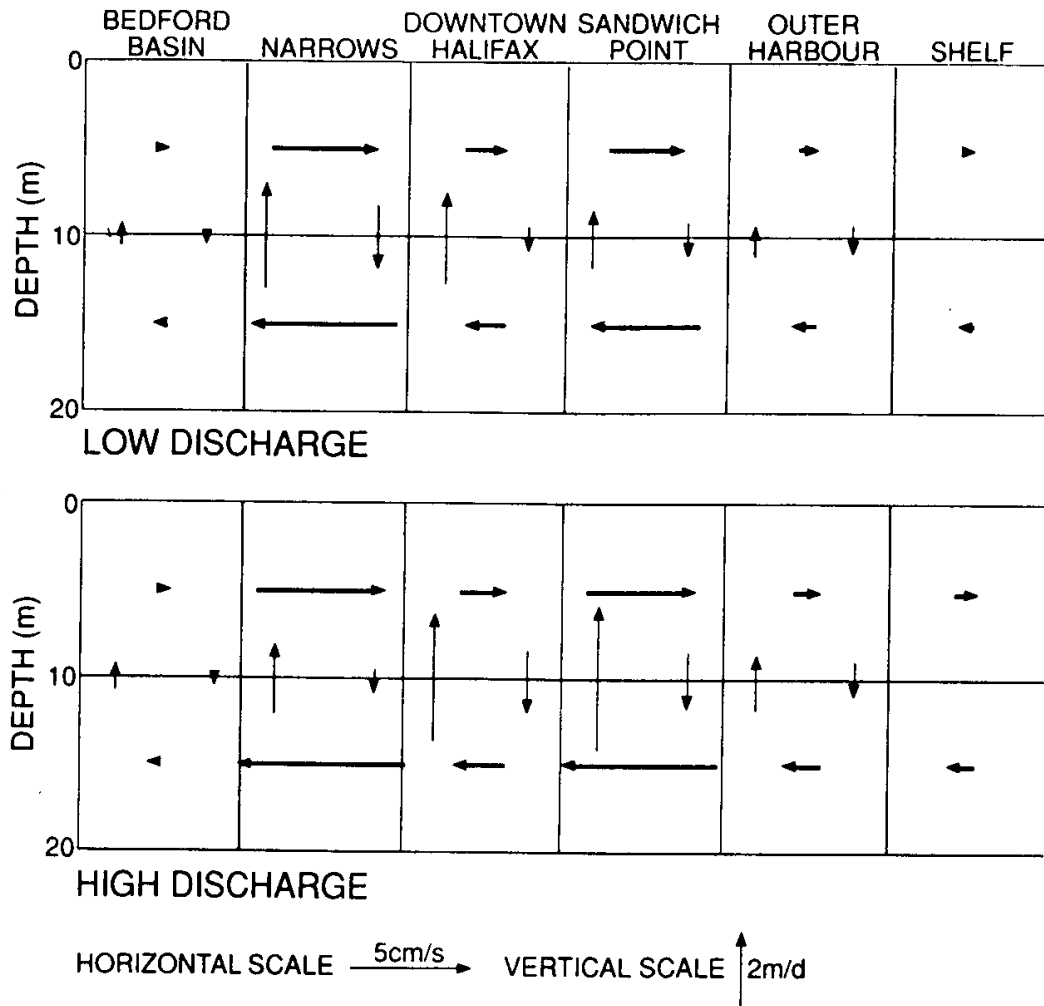
Figure 2.6: The time-mean two-layer circulation in Halifax Harbour produced by *Petrie and Yeats* (1990) using a box model and based on salinity observations collected by *Jordan* (1972) from periods of high and low freshwater discharges from the Sackville River.

in the Harbour, and can reach up to 15–35 cm/s in the Narrows and 5–15 cm/s along the boundary of the Inner and Outer Harbour extending to Chebucto Head in the Outer Harbour (*MacLaren Plansearch Limited*, 1991). Current meter records in the Narrows (*McGonigal et al.*, 1974) show the currents are mostly tidal. Tidal ellipses in the Narrows are nearly rectilinear with the major axis aligned with the channel axis.

A seiche is the free oscillation of the water in a closed or semi-enclosed basin at its natural period (*Forrester*, 1983). Seiche oscillations in Halifax Harbour and other Atlantic coastal waters have been observed and studied (*McGonigal et al.*, 1974; *Smith*
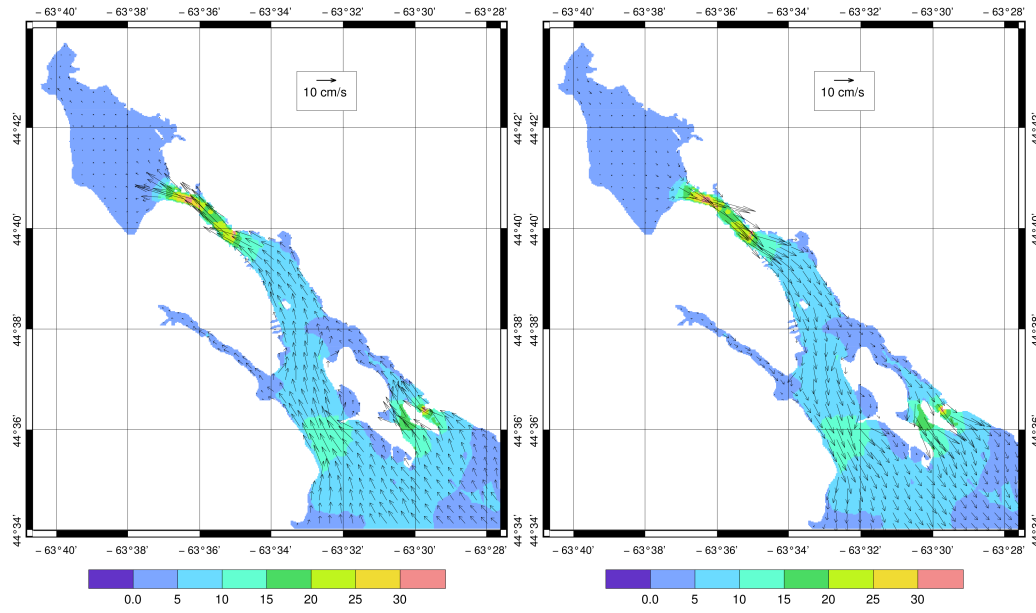
Figure 2.7: Flood (left) and ebb (right) M_2 tidal currents in Halifax Harbour (in units of cm/s) produced by a finite element model (*Greenberg*, *Personal Communication*, 2010).

and Miyaoka, 1999 and *Mullarney et al.*, 2008). The primary period of observed seiches in Halifax Harbour is about 2.2 hours estimated from observed time series for 2006 at tide gauges CHS491 and CHS490 using power spectrum analysis.

Circulation in Halifax Harbour is also affected by wind forcing, particularly during winter and tropical storms, and hurricanes. It was found that wind-driven currents can override the tidal currents in the Harbour (*ASA Consulting Limited*, 1991). The dominant southwesterly wind in summer is favourable for upwelling along the south coast of Nova Scotia (*Petrie et al.*, 1987). Using satellite images (Figure 2.8), *Petrie et al.* (1987) captured the development of a band of cool water along the southshore of Nova Scotia during a month-long period of upwelling favorable winds. Their results suggest that the wavelike features (Figure 2.8d) are primarily due to baroclinic instability of the upwelling-associated base state.

Temperature and salinity distributions in Halifax Harbour are affected by net heat and freshwater fluxes at the sea surface, freshwater discharge from the Sackville River and sewage, and advection of offshore waters from the Scotian Shelf (*MacLaren Plansearch Limited*, 1991). Abrupt changes in temperature and salinity caused by onshore and offshore movements of water in response to passing storm systems were observed in Halifax Harbour (*Hachey*, 1935). The salinity observations made on August 16, 1971 (*Jordan*,
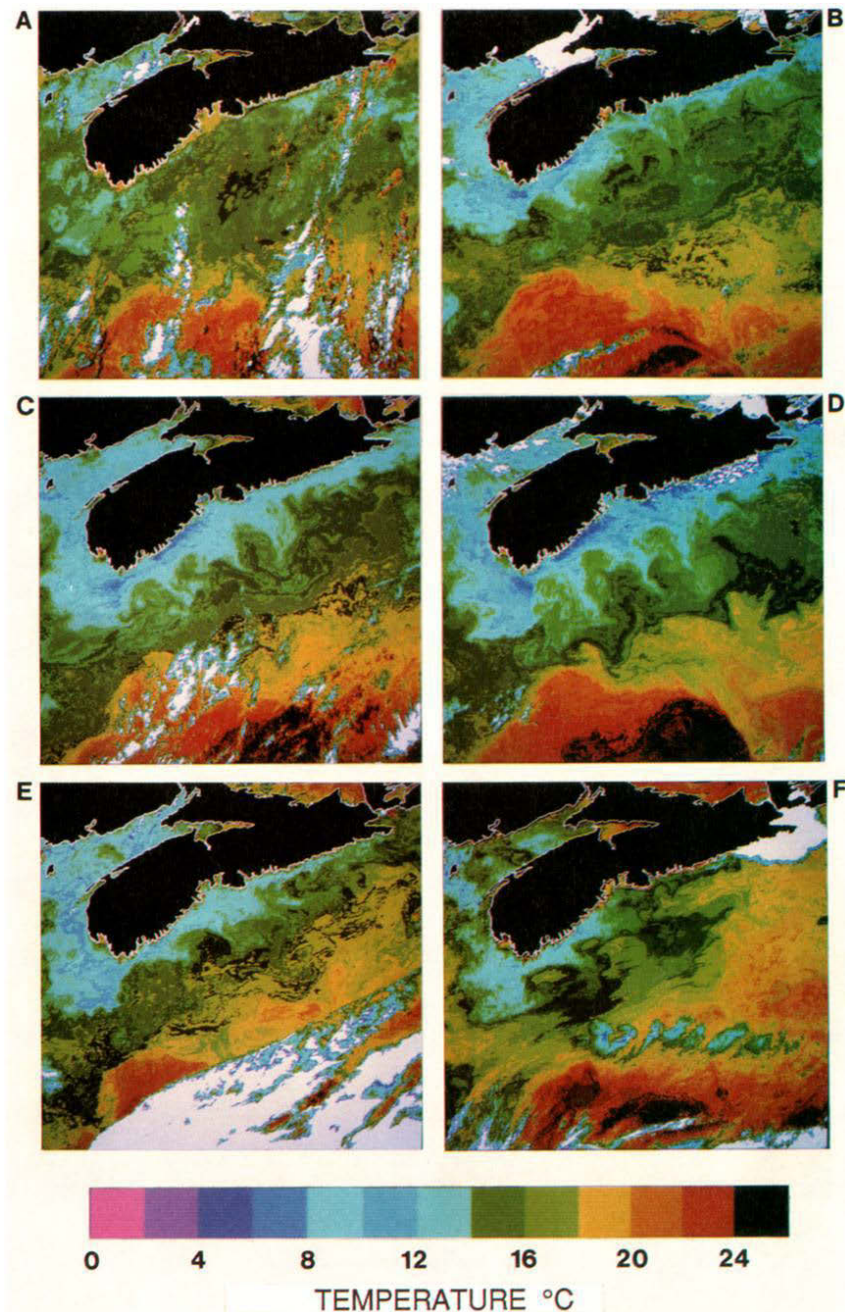
Figure 2.8: Satellite Infrared imagery of the sea surface temperatures on (a) July 7, (b) July 14, (c) July 21, (d) July 25, (e) July 31, and (f) August 6, 1984 (from *Petrie et al.* 1987).

1972) also demonstrated that decreasing of surface salinity in the Harbour occurred after Hurricane Beth, which brought 20.3–22.9 cm rainfall in a period of 30 hours (*DeIure*, 1983). Based on a 14-year record of weekly physical and biological observations in Bedford Basin, *Li and Harrison* (2008) found that the intra-annual variations of vertical

density stratification in Bedford Basin are mainly determined by temperature variations, while inter-annual changes in vertical density stratification are related to changes in salinity.

The large-scale circulation on the inner Scotian Shelf can also affect the circulation and hydrography in Halifax Harbour through the Outer Harbour. There are three major currents outside Halifax Harbour: the Nova Scotia Current near the coast, the Labrador Current over the shelf break and the Gulf Stream off the slope water of the Scotian Shelf. Figure 2.9 demonstrates the general southwestward movement of coastal current (known as the Nova Scotia Current) outside Halifax Harbour, and the two-layer estuarine circulation (at station i) over the Outer Harbour. From drift bottle experiments, *Huntsman* (1924) speculated that a single large weak cyclone eddy exists to the south of Halifax Harbour and constantly renews salt water at the entrance of the Harbour down to Bedford Basin (Figure 2.10).
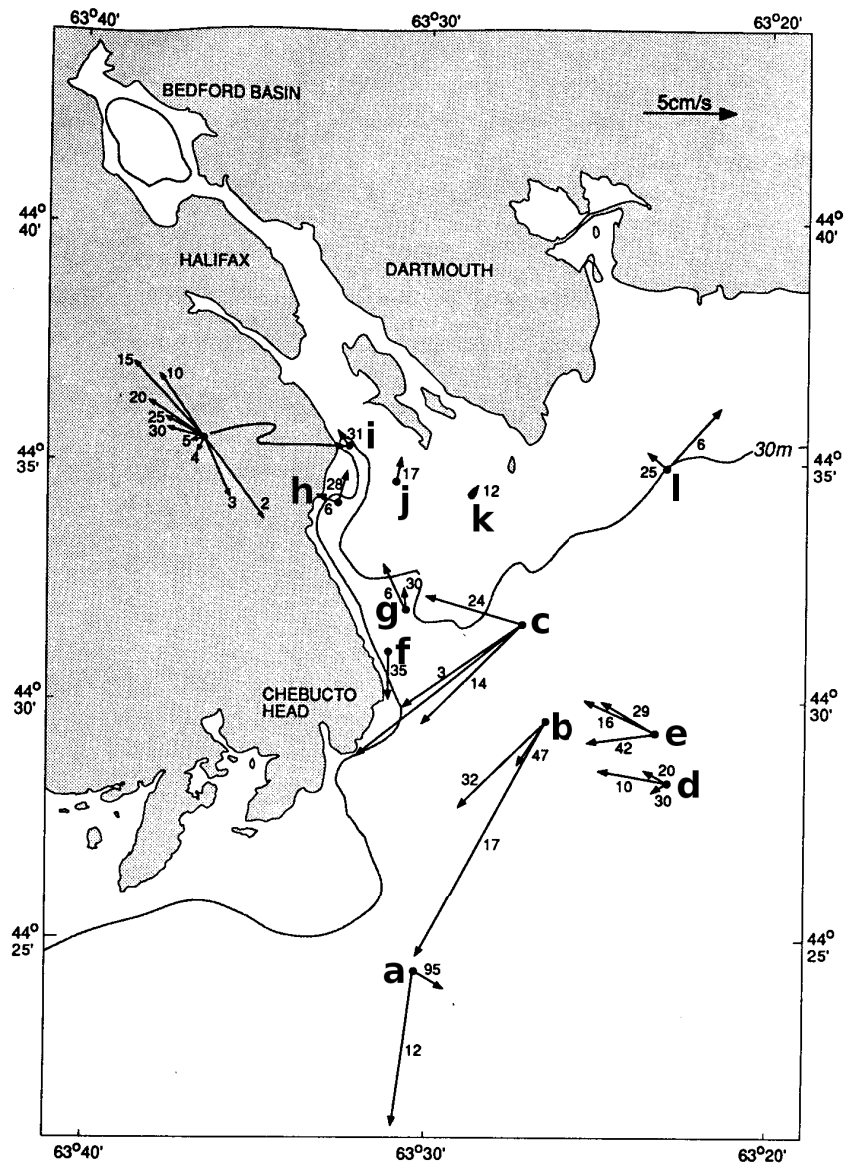
Figure 2.9: Time-mean observed currents in the Outer Harbour and adjacent inner Scotian Shelf based on archived current meter records collected over a 22 y period before 1990. Record lengths vary from about 3 weeks to 8 months. The number beside the arrow indicates the depth (m) at which the data were recorded. The 30 m isobath is shown. (Modified from *Petrie and Yeats* 1990).
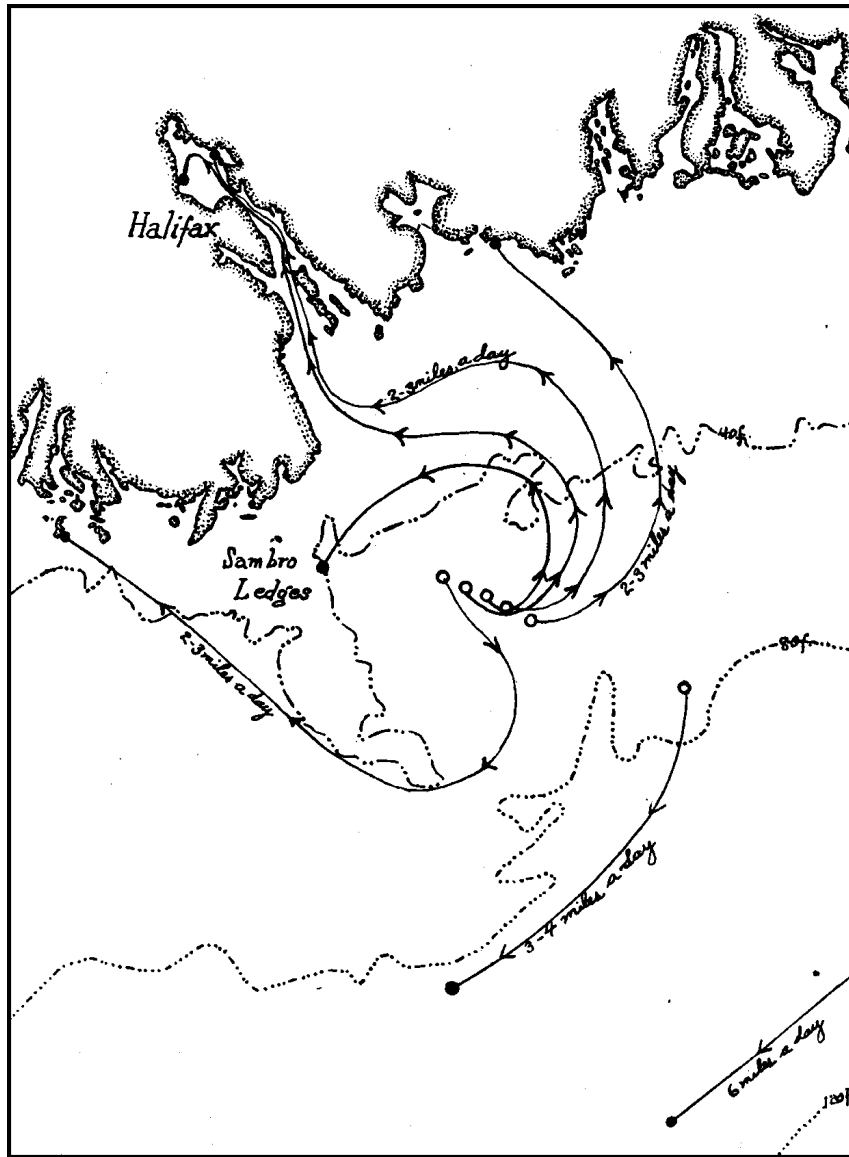
Figure 2.10: Possible drifter tracks outside Halifax Harbour proposed by *Huntsman* (1924).

2.3 Monthly Mean Temperature and Salinity Climatology

To examine the general distribution and seasonal variability of hydrography in Halifax Harbour and also to initialize the coastal circulation model, we constructed a 3D monthly mean temperature and salinity climatology from a database which contains 501,156 temperature and salinity observations made between 1915 and 2008. The database includes hydrographic observations taken from various sources: (1) weekly or bi-weekly CTD observations from 2004 to 2007 made by the Halifax Harbour Water Quality Monitoring Project (HHWQMP); and (2) observations in Halifax Harbour and adjacent areas extracted from the Hydrographic Climate Database of Fisheries and Oceans Canada (http://www.mar.dfo-mpo.gc.ca/science/ocean/database/climapp.html). Since the hydrographic observations are sparse in space and time, an interpolation scheme modified from Barnes' algorithm (*Daley*, 1993) was used to generate the gridded monthly mean climatology from temperature and salinity observations using a 3D grid with a horizontal resolution of $\sim$110 m and a vertical resolution of 1 m. We followed *Geshelin et al.* (1999) and *Spencer et al.* (1999) and specified the weight function to be space- and time-dependent. At each grid point $\mathbf{r}_i$, the interpolated field at the jth iteration $f_A^j(\mathbf{r}_i)$ is given as

$$f_A^j(\mathbf{r}_i) = f_A^{j-1}(\mathbf{r}_i) + \sum_{k=1}^{K_i} W_{ik}[f_O(\mathbf{r}_k) - f_A^{j-1}(\mathbf{r}_k)] \tag{2.1}$$

for $j \geq 1$. The subscripts A and O in the above equation denote analyzed and observed fields respectively, $\mathbf{r}_k$ is the position vector of the kth observation, K_i is the number of observations inside the search area for the ith grid point, and W_{ik} is the weight function of the kth observation at the ith grid point defined as

$$W_{ik} = \frac{w_{ik}}{\sum_{k=1}^{K_i} w_{ik}} \tag{2.2}$$

with

$$w_{ik} = e^{-\frac{R_{xy}^2}{\lambda^2} - \frac{R_z^2}{\beta^2} - \frac{R_t^2}{\tau^2}} \tag{2.3}$$

where λ, β and τ are the horizontal, vertical and temporal decorrelation scale at each iteration for the ith grid point, R_{xy}, R_z and R_t are the horizontal, vertical and temporal distance between the ith grid point of the mid-month and the kth observation. In this study

j is set to 3, and the decorrelation scales used in the calculation are

$$\lambda_1 = 7.5 \text{ km}, \quad \lambda_2 = 5 \text{ km}, \quad \lambda_3 = 4.5 \text{ km} \tag{2.4}$$

$$\beta_1 = \beta_2 = \beta_3 = 5 \text{ m} \tag{2.5}$$

$$\tau_1 = \tau_2 = \tau_3 = 15 \text{ days} \tag{2.6}$$

The constructed monthly mean temperature and salinity climatology in Halifax Harbour are shown in Figures 2.11–2.14.

The gridded hydrographic climatologies demonstrate that the near-surface water temperatures in Halifax Harbour have significant month-to-month variability. In winter, the near-surface temperatures are cold and about $-1°$C just above the freezing point due mainly to the strong net heat loss to the atmosphere. The near-surface water temperatures could rise up to 15°C in summer, due mainly to the positive surface heat flux gained by the sea water. The near-surface water temperatures in Bedford Basin are higher than those in the Outer Harbour from April to August. From September to March, the near-surface water temperatures over the whole Halifax Harbour are almost uniform horizontally.

We next examine vertical distributions of temperature along a transect which runs roughly along the deep channel in Halifax Harbour (Figure 2.3). It should be noted that vertical distributions shown in Figure 2.12 are based on the gridded climatology and therefore vertical stratifications shown in the figure could be weaker than the real stratifications in the region. Surface layer waters are cooler than the lower layer waters in January, February and March due to the continuous negative heat flux for the ocean water. The temperatures in the upper water column of the Harbour decrease from 8°C in November to 1°C in March. Temperatures of waters deeper than 30 m in Bedford Basin are around 3°C, with relatively small month-to-month variability. Warm waters in the upper 10 m occur from the head of Bedford Basin to the open sea from April to August, during which vertical temperature stratification is reestablished in the Harbour. Temperature stratification in the Harbour is strongest in September, and gradually diminishes due to the heat loss and large vertical mixing associated with vertical convection in late fall. From November to March, water temperatures are almost uniform vertically in the upper layer due to winter convection and strong mixing.

The near-surface salinity climatology in Halifax Harbour, particularly in Bedford Basin,

also has significant month-to-month variability (Figure 2.13). Typically, the near-surface salinity is relatively low in Bedford Basin and relatively high in the Outer Harbour. The near-surface salinities vary from higher values of about 30.8 psu in March to lower values of about 27.5 psu in December. From January to March, the near-surface salinity in the Outer Harbour increases with time due to the intrusion of offshore saltier waters from the Scotian Shelf. From April to June, freshwater spreads from the head of Bedford Basin due mainly to ice and snow melt in spring as reflected in the climatological discharge of the Sackville River (Figure 2.4). From July to September, near-surface salinities in Bedford Basin and the Northwest Arm increase significantly due mainly to low precipitation. From October to December, near-surface salinities in Bedford Basin and the Northwest Arm decrease due mainly to the increase of precipitation in the region. The near-surface salinities reach a minimum in December in Halifax Harbour.

Figure 2.14 shows that vertical stratification of salinity has significant month-to-month variability, particularly in the top 10 m. Salinity below 10 m is generally greater than 30 psu and has weaker seasonal variability. Over the Outer Harbour, the salinity of the whole water column is 30 psu or greater with the bottom salinity of greater than 31 psu. There is a low-salinity estuarine front at the head of Bedford Basin associated with freshwater discharge from the Sackville River. The estuarine front advances and retreats seasonally (Figure 2.14). The relatively stronger salinity stratification in the Harbour occurs in May and December due mainly to ice and snow melt in spring, and large precipitation in fall. Salinity in the deeper waters of Bedford Basin is higher ($\sim$31.5 psu) in December than other months. Based on the vertical distribution of salinity, three types of water mass can be identified in Halifax Harbour: (1) relatively fresh upper layer water near the Sackville River; (2) salty water mass in the deeper layer of Bedford Basin; and (3) the salty water intrusion from the Scotian Shelf.

To further examine the seasonal evolution of hydrography in Halifax Harbour, we examine time-depth distributions of temperatures and salinities at stations G2 in Bedford Basin and B2 in the Outer Harbour (Figure 2.15). The shallow water temperatures at G2 are cold and near 0 °C in winter due mostly to negative surface heat fluxes. The upper water column at G2 in winter is well mixed due mainly to strong wind and vertical convection. The cooling gradually penetrates into the deep layer at this site in spring and early summer. As a result, cooling of the surface water in Bedford Basin in winter partially determines

the near-bottom water temperature in the coming summer months. Due to positive surface net heat fluxes in spring and summer, surface water temperatures rise gradually with time since April and reach a maximum in September. At station B2 where the water depth is about 20 m, temperature is almost uniform through the whole water column in late fall and winter. The water temperatures at B2 are $\sim$16°C in summer and $\sim$1°C in winter. There is a transition period from July to August, featuring the redevelopment of the seasonal thermocline. The depth of thermocline increases with time until reaching the bottom at this site in September. As mentioned earlier, the near-surface salinity is highly affected by river runoff, evaporation and precipitation. In Bedford Basin, there are two low salinity periods in the upper water column (about 0–5 m), with one in spring between April-June, the other in fall between October-December. The time-depth distributions of salinity in the upper water column at G2 are very similar to those at B2. The differences in salinity between the two locations can be explained by the effect of freshwater discharges in different geographic locations and the lateral transport and mixing from G2 to B2 between the two layers of the estuarine circulation.

It is interesting to note that the near-bottom salinities at G2 are relatively higher in late fall and winter than those in other seasons, which suggests that the offshore salty water intrusion along the deep channels into Bedford Basin occurs and maintains the salty water mass in the deeper layer of Bedford Basin in late fall and winter. The near-bottom salinity at B2 in the Outer Harbour does not show the similar seasonal variability. We also examined bottom salinities at three other stations (B1, B3, B4) in the Outer Harbour, none of which have the higher near-bottom salinity in late fall and winter. The fact that the near-bottom salinity in the Outer Harbour does not have the similar trend as that at G2 in Bedford Basin could be explained by the hypothesis that high salinity water intrusion from offshore to Bedford Basin does not occur all the time and may not be reflected in the weekly or bi-weekly hydrographic observations used in constructing the monthly hydrographic climatology.

To examine the inter-annual variability of temperature and salinity in Halifax Harbour, we compare the multi-year observations of temperature and salinity at station G2 and B2 made by the HHWQMP with vertical profiles of gridded temperature and salinity climatology at the same sites in Figure 2.16. The observed temperatures in the deeper layer of Bedford Basin have significant inter-annual variability, with the maximum variability

of about 4 °C from in summer and fall. The observed temperature profiles in February 2006 are relatively warm in comparison with profiles made in other years, especially in the upper layer of Bedford Basin due mainly to a mild winter of 2005/2006. Consequently, the observed temperatures profiles in spring and summer months in 2006 are abnormally warm in the deeper layer of Bedford Basin. By comparison, November temperature profiles in 2006 are abnormally cold in the upper layer of Bedford Basin. The observed salinity profiles also demonstrate significant inter-annual variability of about 0.7 psu in the upper layer. The freshwater runoff, vertical mixing and sporadic shelf water intrusion may be the dominant mechanism that controls the inter-annual variability of the salinity in deeper layer of Bedford Basin. At station B2 in the Outer Harbour, the observed temperatures vary about 5 °C and salinities vary about 1 psu in the same months of different years. In particular, the pronounced temperature (salinity) stratification occurs in August (May). In winter, temperature and salinity are well mixed in the whole water column. However, the profiles in November of 2006 show warm and salty water near the bottom which may indicate the intrusion of offshore waters. Figure 2.16 also demonstrates the monthly mean climatology represents reasonably well the mean states observed hydrography in each month indicating that modified Barnes' objective analysis method performs reasonably well in constructing the gridded hydrographic climatology from sparse observations in Halifax Harbour.
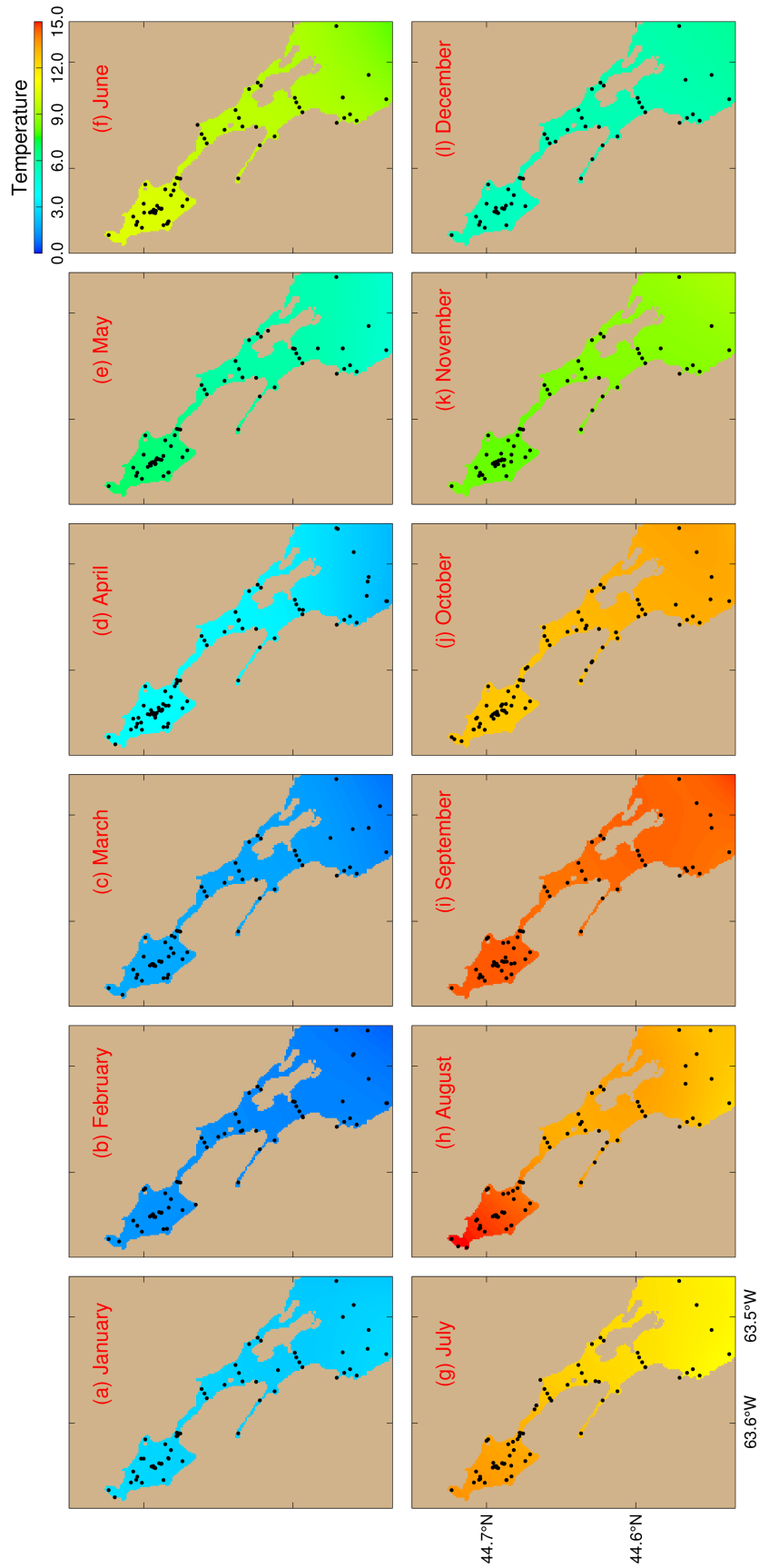
Figure 2.11: Gridded monthly mean near-surface (2 m) temperature (°C) in Halifax Harbour interpolated from observations made from 1915 to 2008 using Barnes' algorithm. Black dots represent observation locations.
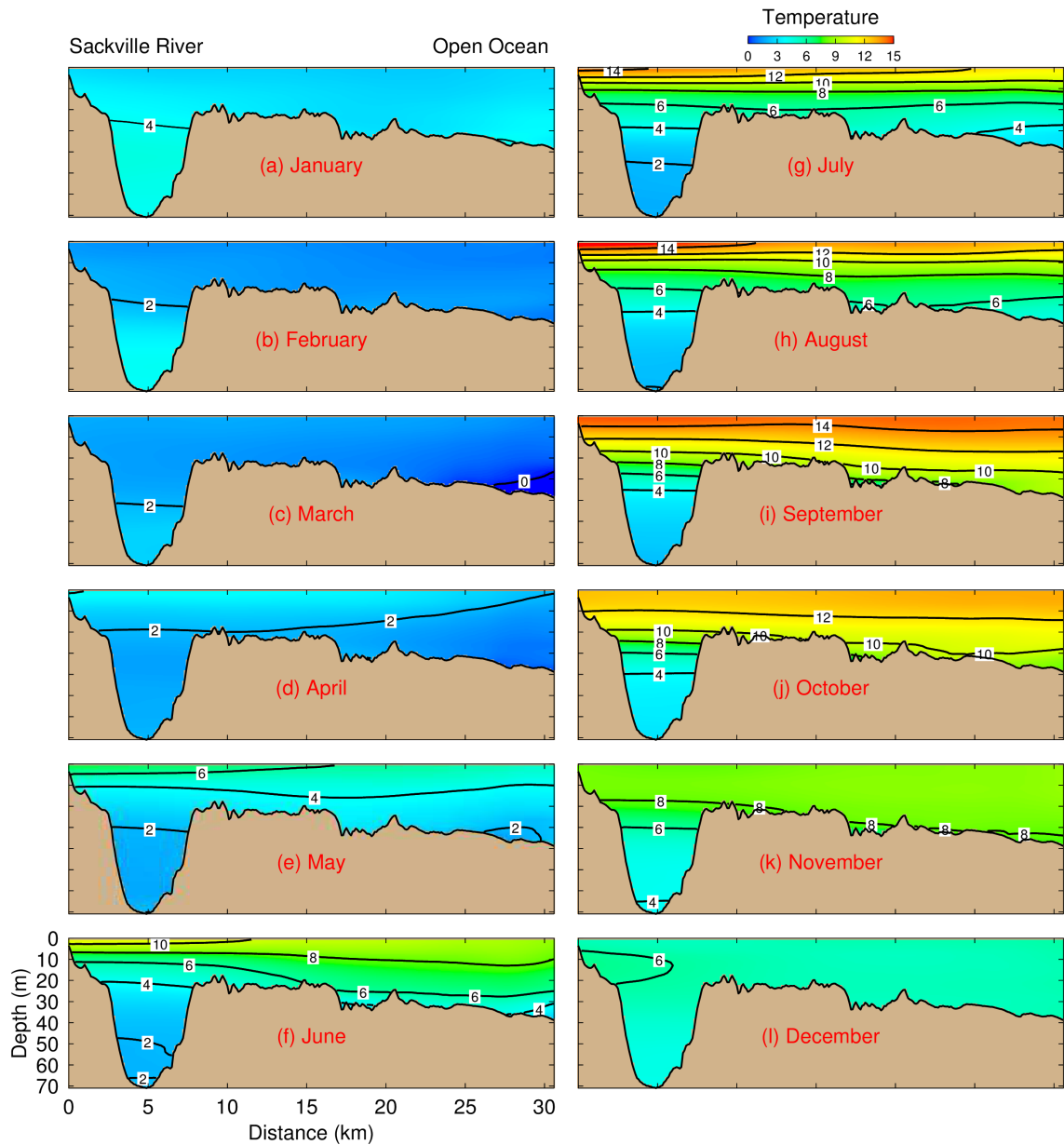
Figure 2.12: Vertical distribution of monthly mean temperatures (°C) along a transect from the Sackville River to the open sea (see Figure 2.3) interpolated from the gridded climatology of monthly mean hydrography.
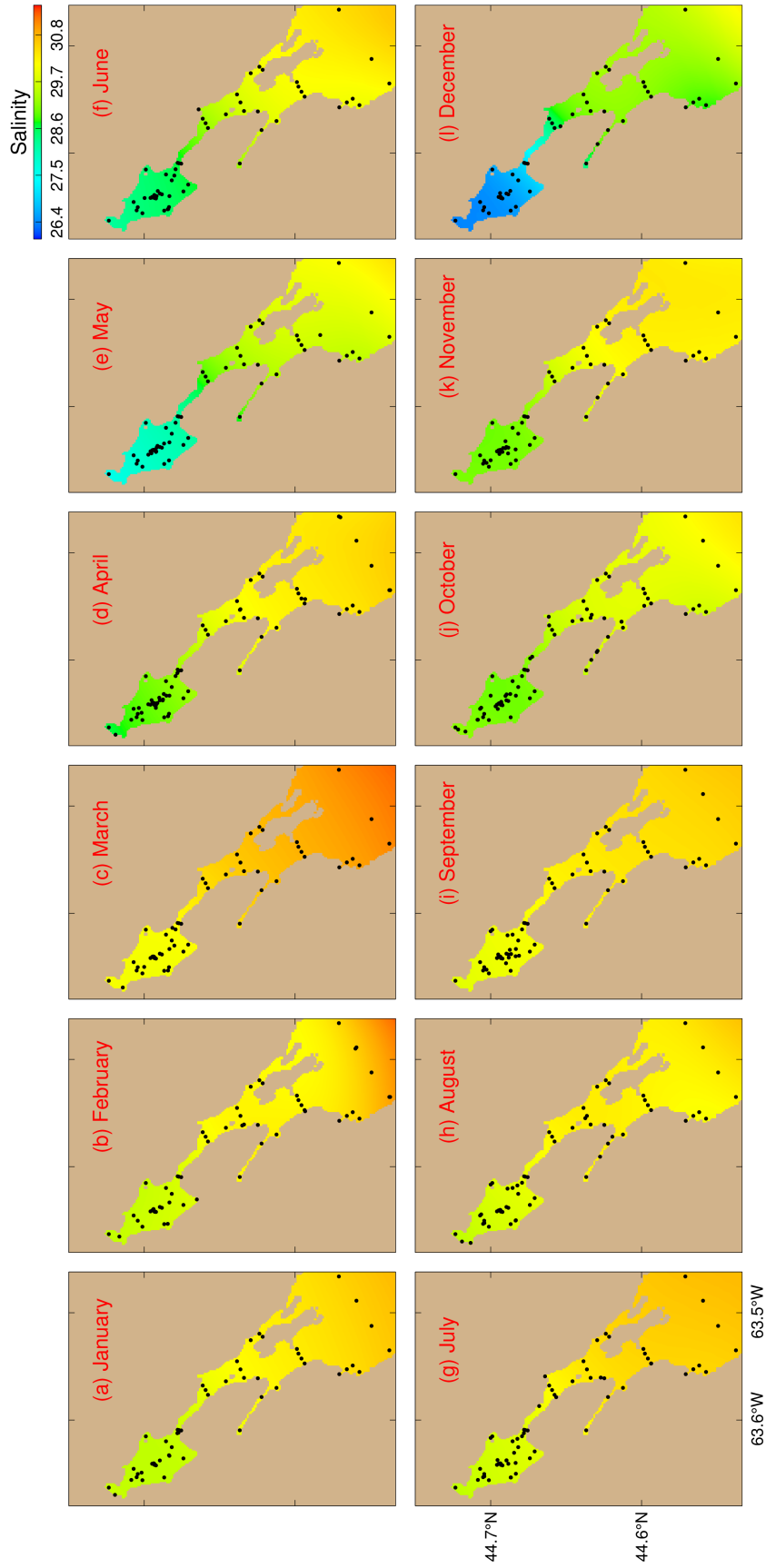
Figure 2.13: Gridded monthly mean near-surface (2 m) salinity (psu) in Halifax Harbour interpolated from observations made from 1915 to 2008 using modified Barnes' algorithm. Black dots represent observation locations.
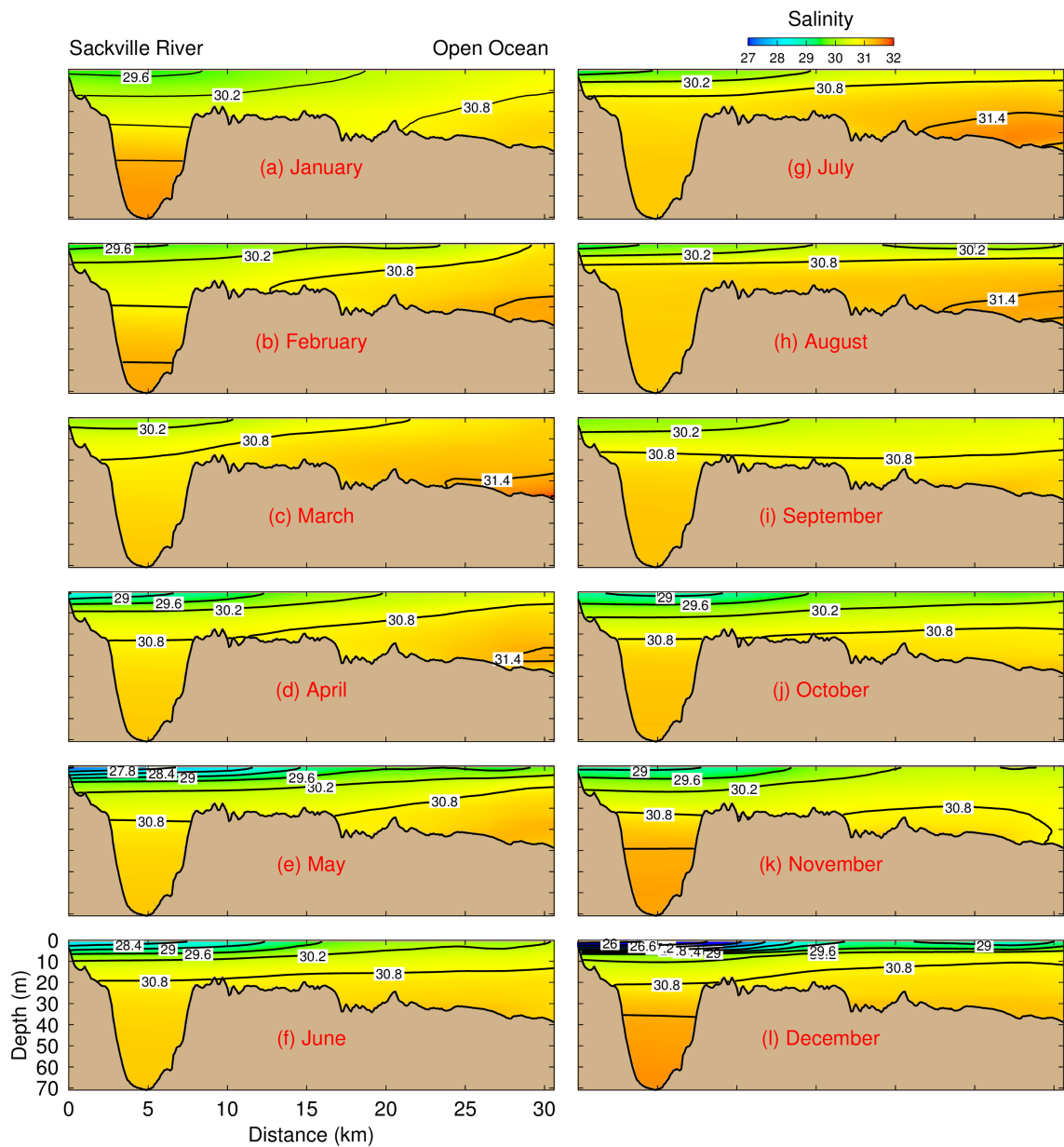
Figure 2.14: Vertical distribution of monthly mean salinities (psu) along a transect from the Sackville River to the open sea (see Figure 2.3) interpolated from the gridded climatology of monthly mean hydrography.
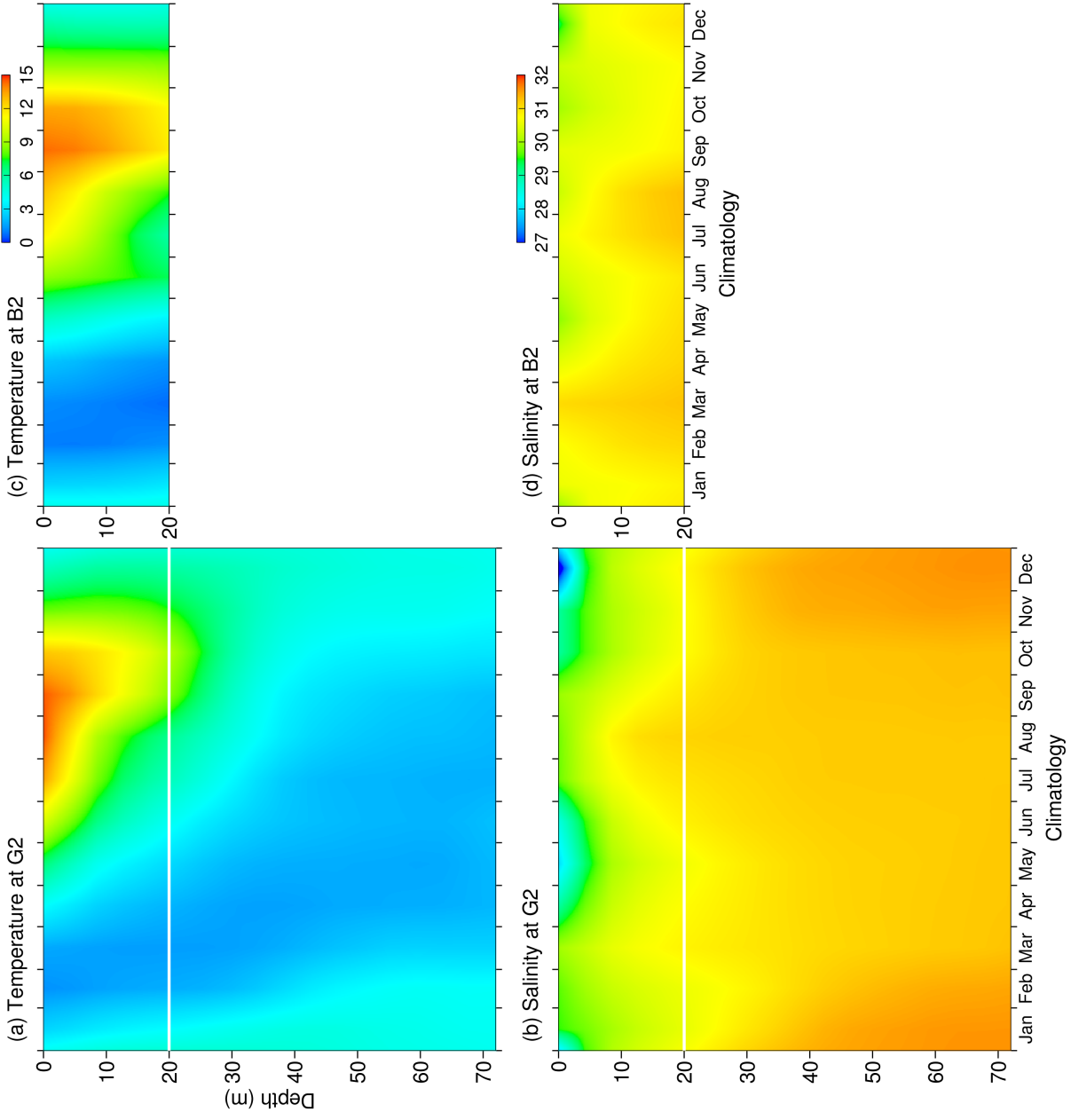
Figure 2.15: Time-depth distributions of temperature and salinity at (a, b) stations G2 in Bedford Basin and (c, d) B2 in the Outer Harbour based on gridded monthly mean climatology. Locations of these two stations are marked in Figure 2.3.

Figure 2.16: Vertical profiles of observed temperature and salinity at station G2 in Bedford Basin and B2 in the Outer Harbour.
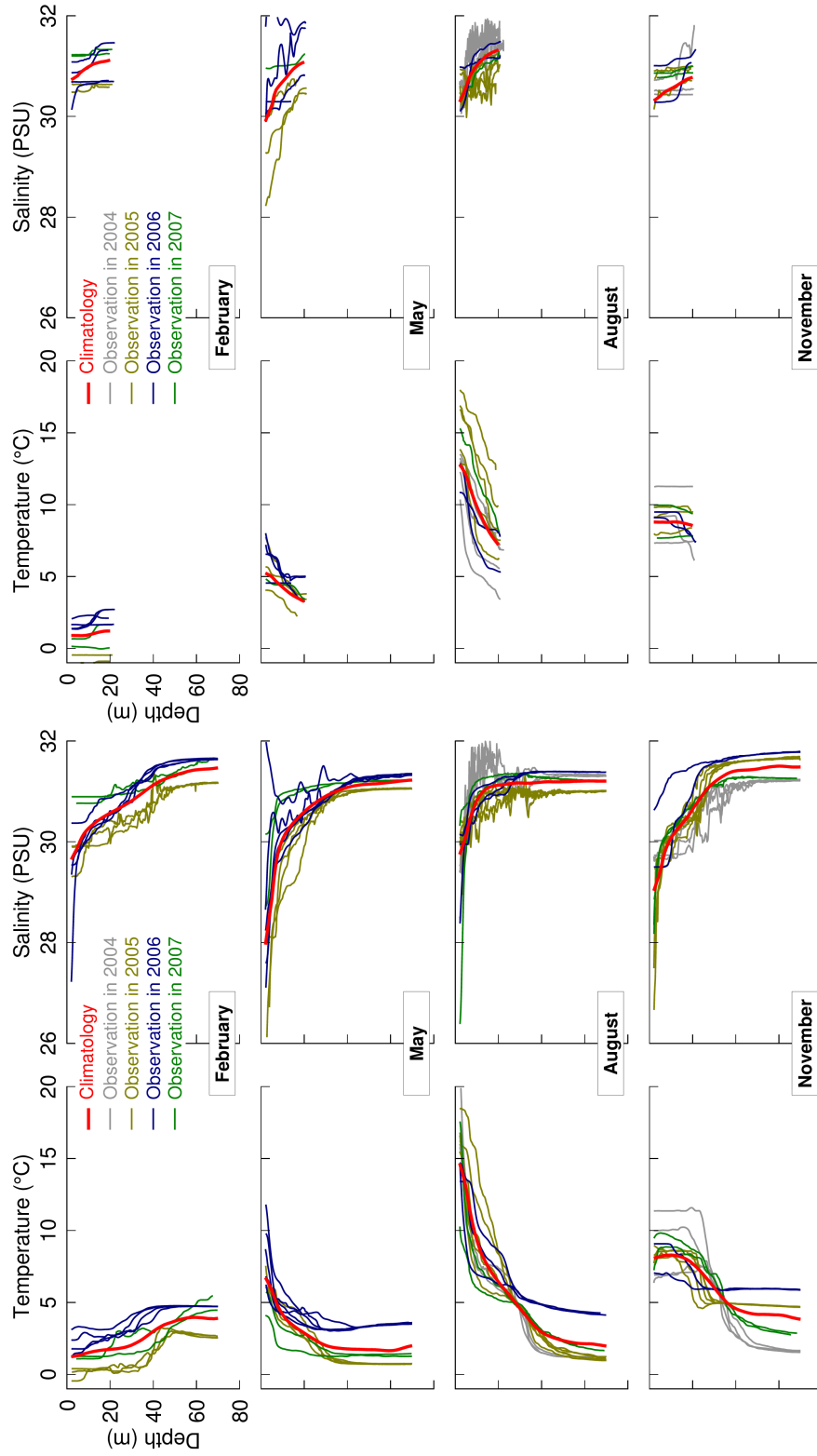
Station G2 in Bedford Basin

Station B2 in the Outer Harbour

CHAPTER 3

NESTED-GRID OCEAN CIRCULATION MODEL, EXTERNAL FORCING AND VALIDATION

Dynamic downscaling techniques have increasingly been used in simulating circulation and hydrography of coastal waters. The key to dynamic downscaling is a nested-grid model which contains one or several realistic submodels with increasing horizontal resolution over smaller model domains. The main benefit gained from a nested-grid model is that relatively fine circulation features can be resolved by fine-resolution submodels using dynamically consistent open boundary conditions provided by larger domain and coarse-resolution submodels. A five-level nested-grid coastal circulation modelling system is used in this study. The nested-grid model was developed previously by *Yang and Sheng* (2008) for Lunenburg Bay, Nova Scotia, Canada known as the Nested-grid Coastal Ocean Prediction System for Lunenburg Bay (NCOPS-LB). This five-level nested-grid modelling system is modified with the two inner-most submodels relocated to Halifax Harbour and adjacent area. Consequently, the modified version of the modelling system is named as the NCOPS-HFX. The nested-grid modelling system has the outer-most storm surge model covering the eastern Canadian shelf which allows the wind-induced coastal currents and sea level over the Gulf of St. Lawrence and Newfoundland Shelf to propagate into Halifax Harbour. The other important feature of the NCOPS-HFX is its operational capability.

3.1 NCOPS-HFX Setup

The NCOPS-HFX is a five-level nested-grid coastal ocean circulation modelling system with five nested domains of progressively smaller areas and finer horizontal resolutions (Figure 3.1). Submodels L1 and L2 are based on DalCoast (*Thompson et al.*, 2007) constructed from the Princeton Ocean Model (POM). Submodel L1 is a two-dimensional (2D) and barotropic[*] storm surge model covering the eastern Canadian shelf from the Labrador Shelf to the Gulf of Maine with a horizontal resolution of 1/12°. Submodels L2–L5 are three-dimensional (3D) and baroclinic[†] with horizontal resolutions of 1/16°, ∼2 km, ∼500 m, ∼200 m, respectively. Submodel L2 is a 3D shelf circulation model covering the Gulf of St. Lawrence and the Scotian Shelf with 30 σ-levels. Submodels L3-L5 using 32 unevenly-spaced z-levels are based on the free surface version of CANDIE (*Sheng et al.*, 1998), which is a 3D, z-coordinate, primitive equation, A-grid, ocean circulation model using a fourth-order advection scheme.

The submodel L5 domain covers Halifax Harbour and adjacent waters, and uses the newly generated gridded topography of Halifax Harbour (Figure 2.3) with a horizontal resolution of ∼200 m. The gridded topography of L5 was constructed using Barnes' algorithm from (1) ungridded water depth data provided by David Greenberg at BIO, (2) the coastline data of Halifax Harbour and adjacent areas, and (3) 2-minute gridded relief dataset (ETOPO2, http://www.ngdc.noaa.gov/mgg/fliers/01mgg04.html) for the inner Scotian Shelf. The gridded topography shown in Figure 2.3 resolves major topographic features in Halifax Harbour and adjacent areas, such as the deep depression in Bedford Basin and the deep channel from the Sackville River extending to the open sea. It should be noted that the newly generated topography does not resolve well the fine-scale topography over the eastern part of the Outer Harbour around McNabs Island and Lawlor Island due to the poor coverage of original water depth data in that area.

The Smagorinsky scheme (*Smagorinsky*, 1963) is used for horizontal sub-grid-scale mixing. This scheme provides shear and grid size dependent eddy viscosity coefficients for submodels L1-L5. Vertical mixing of momentum, heat and salt in submodel L2 is parameterized by the Mellor-Yamada level-2.5 turbulent closure scheme (*Mellor and Yamada*, 1982); an enhanced version of the K profile parameterization (KPP) scheme

---

[*]Model temperature and salinity are set to be spatially uniform and time-invariant.
[†]Model temperature and salinity are allowed to vary in time and space.
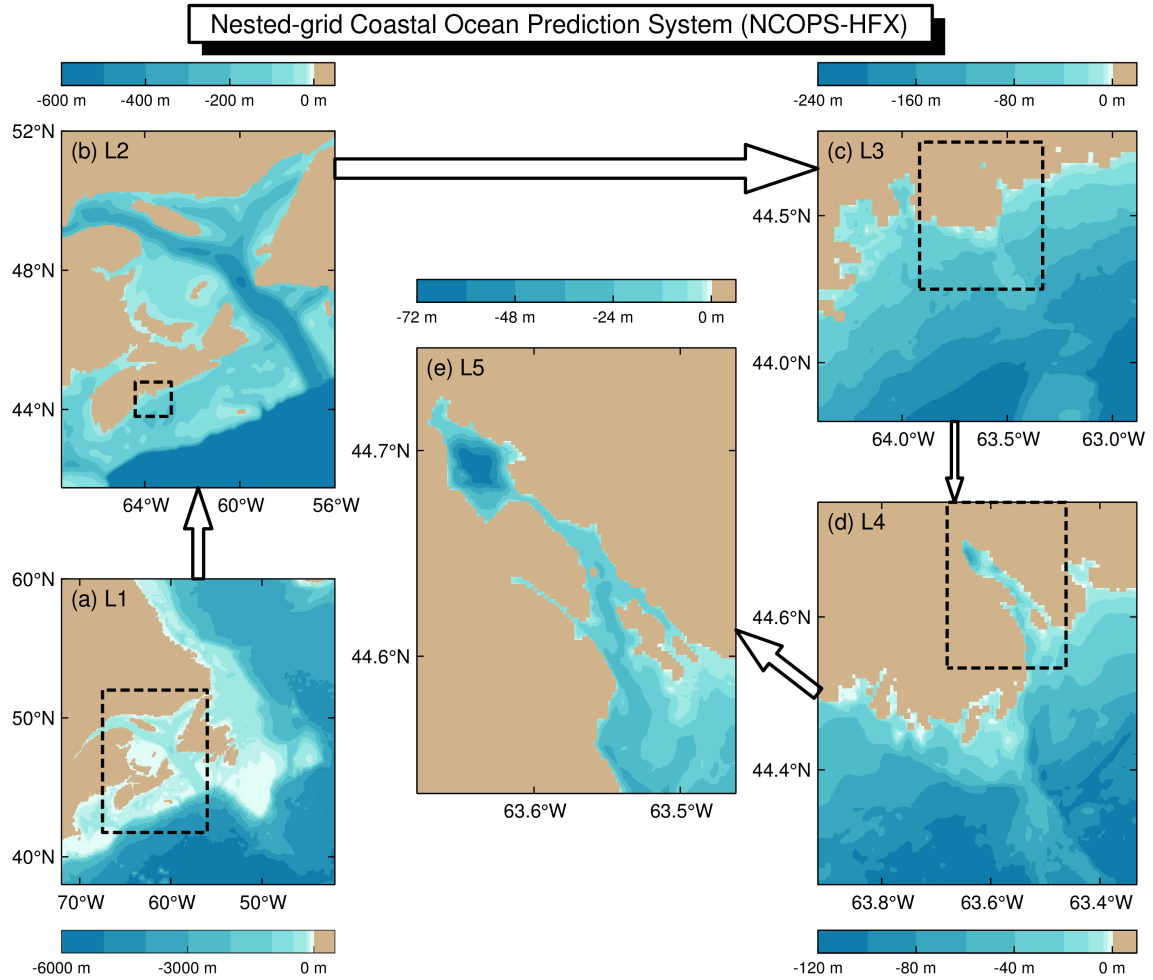
Figure 3.1: Domains and major bathymetric features of the five submodels of the nested-grid ocean circulation model known as the NCOPS-HFX. (a) Submodel L1 (horizontal resolution 1/12 °, ∼9 km) and (b) submodel L2 (1/16 °, ∼7 km) are DalCoast; (c) submodel L3 (∼2 km), (d) submodel L4 (∼500 m) and (e) submodel L5 (∼200 m) are based on CANDIE. Land is marked by the tan color.

suggested by *Durski et al.* (2004) is used in submodels L3-L5.

3.2   Model Forcing

The nested-grid modelling system is driven by tides, meteorological forcing, surface heat fluxes, and river and sewage discharges. Surface freshwater fluxes in the modelling system are parameterized in terms of surface salinity restoring to be discussed later.

The atmospheric forcing used to drive NCOPS-HFX includes three-hourly sea level pressure (SLP) and surface wind fields taken from numerical weather forecasts provided by the Meteorological Service of Canada (MSC). The bulk formula of *Large and Pond* (1981) is used to convert wind speeds to wind stress. Figure 3.2a presents time series of wind stress in Halifax Harbour for January and February 2006. This figure demonstrates significant temporal variability of wind stress at the position of HFX tide gauge. During this two-month period several winter storms affected Halifax Harbour and adjacent waters, with maximum wind stress exceeding 0.2 Pa on January 20 and February 1 in 2006. Figure 3.3 shows the spatial patterns and time evolution of a winter storm passing the Scotian Shelf on February 1, 2006. The three-hourly atmospheric forcing is linearly interpolated onto each model time step and mapped to each submodel grid using Barnes' algorithm.

The net heat flux (Q_{net}) at the sea surface is specified in submodels L2-L5 of the nested-grid modelling system according to

$$Q_{net} = Q_I + Q_B + Q_L + Q_S \tag{3.1}$$

where Q_I is the absorption of solar radiation, Q_B is the net upward flux of long-wave radiation from the ocean, Q_L is the latent heat flux carried by evaporated water, Q_S is the sensible heat flux due to conduction. In this study, Q_I, Q_B, Q_L, Q_S are taken from six-hourly NCEP reanalysis data downloaded from the NOAA/OAR/ESRL/PSD, website at http://www.esrl.noaa.gov/psd/data/gridded/data.ncep.reanalysis.surfaceflux.html. The formula provided by *Paulson and Simpson* (1977) is used to parametrize shortwave penetration (Q_I) in the water column. Time series of the net surface heat flux in January and February of 2006 are shown in Figure 3.2b, which demonstrates that the ocean waters lose heat to the atmosphere during this two-month period except for several short episodes. Similar to wind forcing in the Harbour, the net surface heat flux also has large fluctuations

on synoptic timescales during this period. The surface heat flux field is also linearly interpolated onto each model time step and mapped to each submodel grid point using Barnes' algorithm.
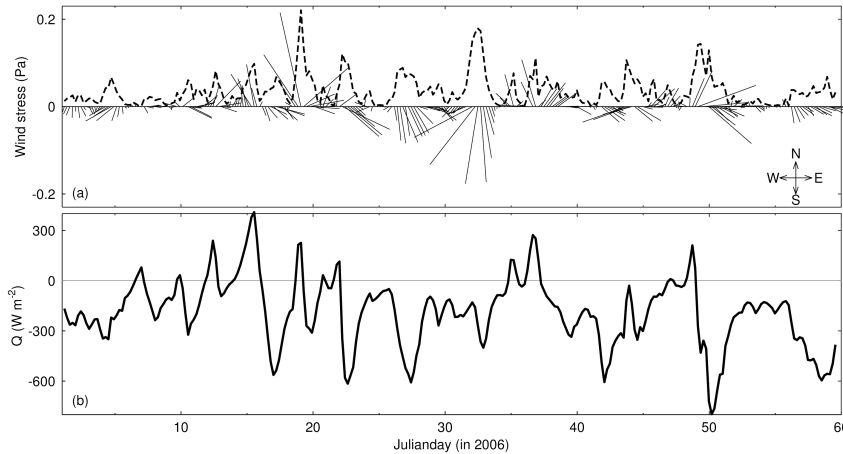
Figure 3.2: Time series of atmospheric forcing: (a) the stick plot of wind stress forcing and (b) the net heat flux at HFX tide gauge for January and February in 2006. The dashed line represents the wind stress amplitude.

The buoyancy forcing associated with freshwater runoff from the Sackville River, sewage and distributed discharges are also specified in submodel L5. The daily observed discharge of the Sackville River (Figure 2.4) is linearly interpolated onto each model time step. Sewage is the flow of used water and wastes generated by the community, and contsists of 99.9% water and only 0.1% solids (*Fournier*, 1990). As a result, sewage is treated the same as freshwater discharge in the NCOPS-HFX. The locations (Figure 2.3) and values (Table 2.1) of fluvial and sewage effluent in Halifax Harbour are adapted from *Buckley and Winters* (1992).

A simple numerical scheme based on the salt and volume conservation is used to specify the salinity and surface elevation at each discharge head in the NCOPS-HFX (*Yang et al.*, 2007). The water discharge location is denoted by one grid cell wide ($\sim$200 m) and three grid cells long ($\sim$600 m) in the top z-level. The salt balance at the head of each freshwater source is specified as

$$S^h = \frac{S^m V^c + S^r V^r}{V^c + V^r} \tag{3.2}$$

where S^h is the model salinity at the head, S^m is the model salinity at the head at the previous time step, S^r is the fresh water salinity set to 0.4 psu, V^c is the volume of the
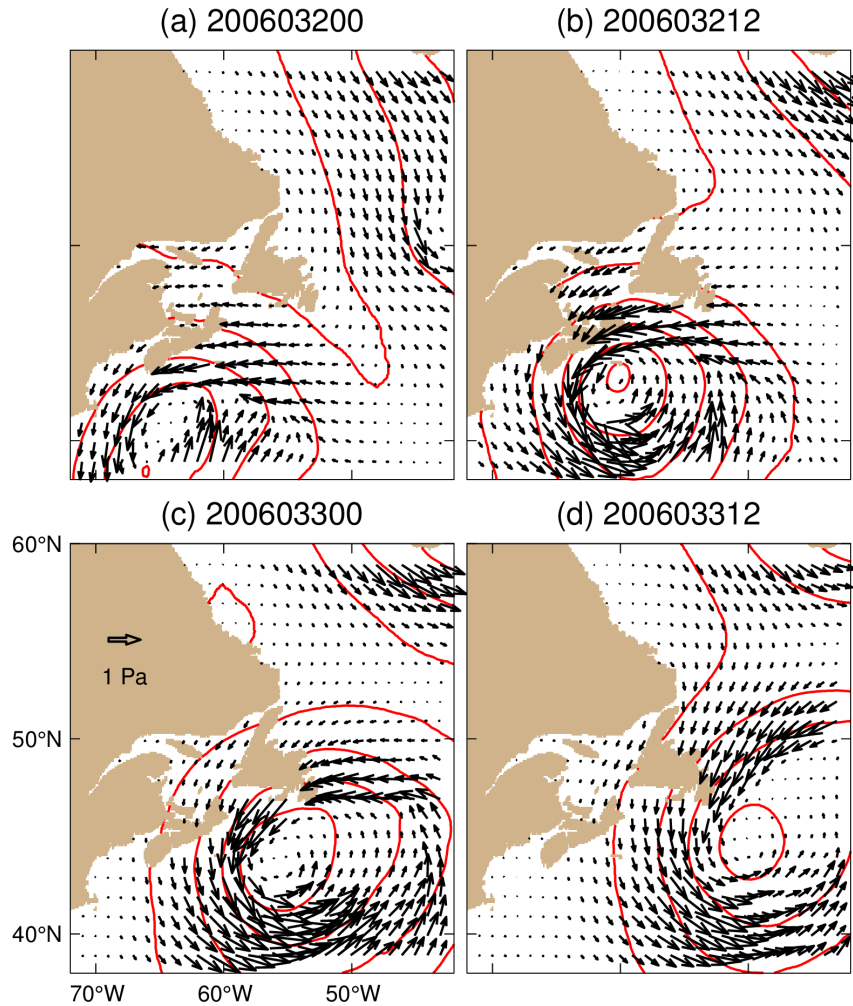
Figure 3.3: Wind stress (black arrows) and sea level pressure (red contour lines) over the eastern Canadian shelf during a winter storm taken from three hourly numerical weather forcasts produced by the Meteorological Service Canada at (a) 00:00 February 1, (b) 12:00 February 1, (c) 00:00 February 2 and (d) 12:00 UTC February 2 of 2006.

model cell at the head, and V^r is the volume of freshwater discharge during one time step. The surface elevation at the head (η^h) is given by

$$\eta^h = \eta^m + \frac{V_r}{A_c} \tag{3.3}$$

where η^m is the model surface elevation at head at the previous time step, and A_c is the surface area of the model cell at the same location.

The following boundary conditions are used in the NCOPS-HFX. Along the open boundary of submodel L2, the model surface elevation and depth-averaged currents are a

combination of (a) wind-induced surface elevations and depth-averaged currents produced by submodel L1, (b) tidal elevations and tidal (depth-averaged) currents produced by WebTide and (c) climatological monthly mean baroclinic currents produced by a coarse resolution northwest Atlantic Ocean model (*Sheng et al.*, 2001). Hourly tidal forcing is specified along the open boundaries of submodel L2. Tidal forcing includes two parts: tidal surface elevations and depth-averaged tidal currents calculated using five major tidal constituents (M_2, K_1, N_2, S_2 and O_1). The amplitudes and phases of the five constituents are taken from the WebTide dataset for the northwest Atlantic coastal ocean (*Dupont et al.*, 2002). The T_TIDE MATLAB package (*Pawlowicz et al.*, 2002) is used to generate time series of hourly tidal forcing. The following one-way nesting technique is used to transfer information from upper-level submodels to lower-level submodels. The *Orlanski* (1976) radiation condition is first used to determine whether the open boundary is passive or active. For passive open boundaries, the model variables (i.e. temperature, salinity, and currents) at the open boundaries are restored to the model results produced by the upper-level submodels, with a restoring time scale of 12 hours. For active open boundaries, the model variables at the open boundaries are advected outward.

Temperature and salinity fields of submodel L2–L4 are initialized by a gridded ($1/6°$ by $1/6°$) monthly mean climatology generated by *Geshelin et al.* (1999). Submodel L5 is initialized by the fine-resolution ($\sim$110 by 110 m) monthly mean climatology discussed in Section 3.2. Surface temperature and salinity are relaxed to monthly mean climatologies with a time scale of 15 days. The spectral nudging method (*Thompson et al.*, 2007) is applied to model temperature and salinity in submodels L2 and L5 to reduce model drift in simulating the seasonal cycle of hydrography.

3.3 Model Validation

The NCOPS-HFX is initialized from a state of rest with the December mean hydrographic climatology and integrated for 13 months from the beginning of December 2005 to the end of December 2006 using the external forcing presented in Section 3.2. The model results in 2006 are used for the model validation and analysis.

3.3.1 Sea Surface Elevation

We first assess the performance of submodel L5 in simulating sea surface elevation in Halifax Harbour by comparing model results with tide gauge data. Figure 3.4 shows the simulated and observed tidal and non-tidal surface elevations at tide gauge CHS 491 in Bedford Basin and CHS 490 in the Narrows from January 10 to February 20 in 2006. During this period, the sea surface elevations are affected by both tides and meteorological forcing. Figures 3.4a and c demonstrate that tidal components of observed and simulated sea surface elevations are dominated by semi-diurnal tides with roughly two high and two low tidal elevations each day. The spring and neap tides are also evident due mainly to the combined effect of the M_2 and S_2 tidal constituents. During the neap tide period, the minimum range of tidal elevations is about 0.6 m. During the spring tide, the maximum range is about 2.0 m. Figures 3.4b and d present the simulated and observed non-tidal components of sea surface elevation. The storm surge including the inverse barometer effect[‡] can cause a sea surface rise of about 0.7 m as indicated by the grey shaded vertical bars during three storm events marked in Figure 3.4, which is not negligible compared to the maximum tidal range of $\sim$2.0 m in the Harbour during these storm events.

To quantify the performance of the nested-grid modelling system, we use the γ^2 value defined as (*Thompson and Sheng*, 1997)

$$\gamma^2 = \frac{Var\left(O - M\right)}{Var\left(O\right)} \tag{3.4}$$

where Var represents the variance, O and M represent the observed and simulated variables respectively. The smaller γ^2 is, the better performance of the nested model has. Normally, the threshold value of γ^2 is chosen to 1. For tidal components, the γ^2 values between observed and simulated sea surface elevations at CHS490 and CHS491 are less than 0.03 during this 40 days period, indicating that the NCOPS-HFX performs well in simulating tidal elevations in Halifax Harbour.

In comparison, there are relatively large discrepancies of non-tidal components between model results and observations (Figures 3.4b and d) with γ^2 values of 0.16–0.18. One of possible explanations is the accuracy of the MSC meteorological forecast products in representing the real meteorological conditions in Halifax Harbour during this period. The

---

[‡] $\eta_a = -\tilde{P}_a/\rho g$, where $\tilde{P}_a$ is atmospheric pressure perturbation, ρ is density of seawater and g is acceleration of gravity.
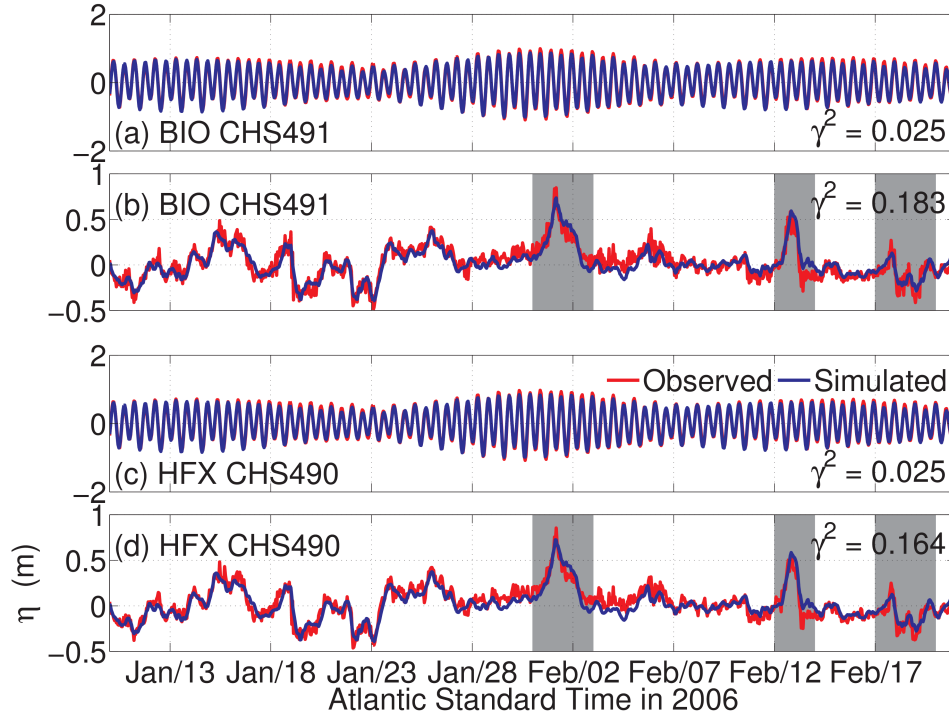
Figure 3.4: Time series of observed (red) and simulated (blue) tidal and non-tidal sea surface elevations at sites (a and b) CHS491 and (c and d) CHS 490 from January 10 to February 20, 2006. The simulated results are produced by submodel L5. The observed and simulated sea surface elevations are decomposed into tidal (a and c) and non-tidal (b and d) components using T_TIDE MATLAB package (*Pawlowicz et al.*, 2002). The grey shaded vertical bars indicate three storm events in February 2006.

other explanation is the model deficiency in reproducing high-frequency variations such as seiche oscillations in the harbour. A quarter-wave seiche model for an open-mouth inlet can be used to describe seiche oscillations in Halifax Harbour. The periods of seiches are given by (*Rabinovich*, 2009)

$$T_n = \frac{4L}{(2n+1)\sqrt{gH}}, \text{ for mode } n = 0, 1, 2, 3, \cdots \quad (3.5)$$

where L is the length of the inlet, H is the water depth, g is acceleration of gravity. For Halifax Harbour, giving an estimated length of $L \sim 30$ km, $H \sim 20$ m and $g \sim 9.8$ m/s^2, the period of the primary oscillation mode ($n = 0$) is about $T_0 \sim 2.4$ hours, which is very close to 2.2 hours estimated from tide gauge observations for 2006 in Halifax Harbour using power spectrum analysis.

We also compared model-calculated sea surface elevations with tide gauge records at these two tide gauges for other periods in 2006 and found that submodel L5 performed similarly in simulating tidal and non-tidal surface elevations in Halifax Harbour. This also confirms that the one-way nesting technique works well in passing transport information from larger domain models to smaller domain models, since sea surface elevations and depth mean currents associated with tides and storm surge are only specified along open boundaries of submodel L2, and the generation of tides and remote-generated storm surges in submodels L3-L5 depends solely on the one-way nesting technique.

3.3.2 *Tidal Current*

To assess the model performance in simulating tidal currents in Halifax Harbour, we compare model-calculated tidal currents with tidal currents produced by WebTide. WebTide is a computer program designed to provide tidal elevations and depth-averaged tidal currents for a given area. It contains several datasets; in this study, the datasets for the Scotia Shelf (*Dupont et al.*, 2005) and Halifax Harbour (*Greenberg*, 1999) are used. We calculate the depth-averaged tidal current ellipses for each month of 2006 from the 3D model currents produced by submodels L4 and L5. The month-to-month variability of depth-averaged tidal current ellipses in Halifax Harbour and adjacent waters in the model is very small (not shown), indicating that barotropic tides dominate this study region. As a result, we examine only the model-calculated depth-averaged M_2 tidal current ellipses in March 2006, during which the upper water column is relatively well mixed.

Figure 3.5 shows that the magnitudes of the simulated M_2 tidal currents are roughly uniform over the inner Scotian Shelf adjacent to Halifax Harbour, except for those near the coast and inside inlets due mainly to constraints of local coastline and bathymetry. The depth-averaged tidal currents produced by submodel L4 are about 5 cm/s over the inner Scotian Shelf outside Halifax Harbour in March 2006. The simulated M_2 tidal current ellipses are oriented roughly in the southeast-northwest direction. The general patterns of M_2 tidal current ellipses outside Halifax Harbour produced by submodel L4 are in rough agreement with the Scotia Shelf WebTide results.

The depth-averaged tidal currents in March 2006 produced by submodel L5 are shown in Figure 3.6a. They are relatively weak in Bedford Basin and relatively strong in the Narrows. The simulated M_2 tidal current ellipses in the Narrows are nearly rectilinear.
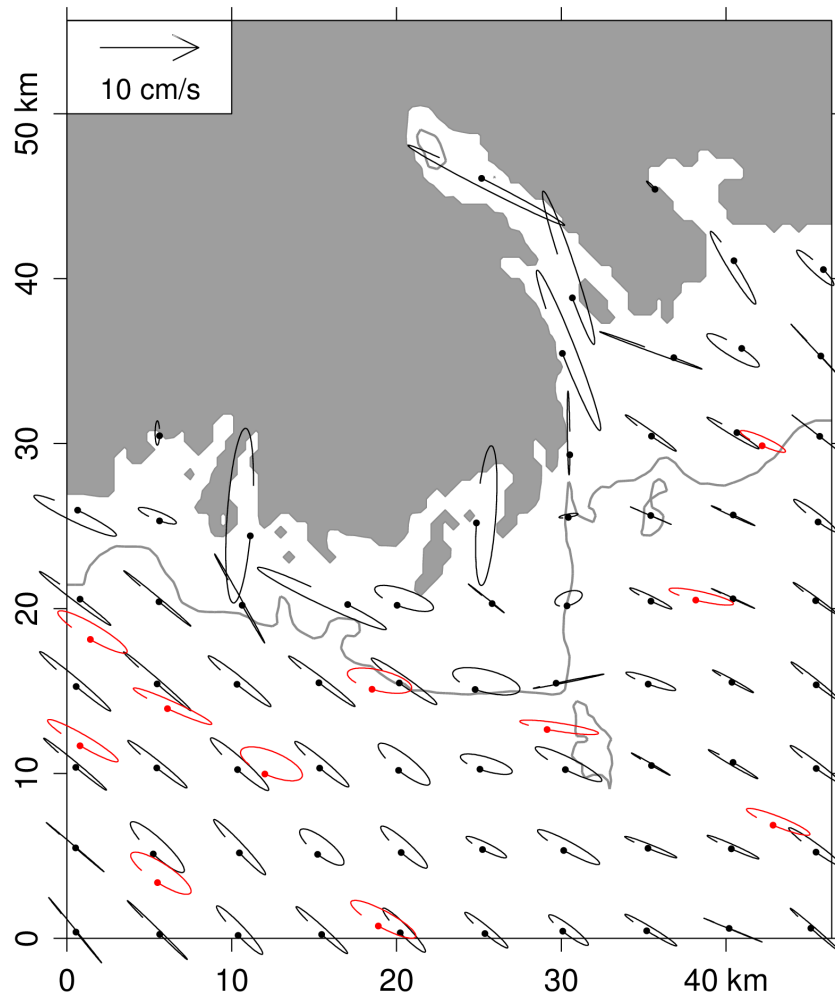
Figure 3.5: Comparison of depth-averaged M$_2$ tidal current ellipses calculated from model currents produced by submodel L4 in March 2006 (at each ten model grid in black) and WebTide (red). Contours for the 50 m isobath are shown.

Circular-shaped tidal current ellipses occur over areas to the southeast of Lawlor Island. Based on the semi-major axis, eccentricity, inclination and phase, tidal currents in Halifax Harbour can be divided into three areas. The first area is Bedford Basin, featuring relatively weak depth-averaged tidal currents. The second area is the Narrows where tidal current ellipses have large semi-major axes with very small eccentricity and are nearly rectilinear. The third area is the area to the southeast of Lawlor Island where tidal currents are more circular than in other areas. In comparison with WebTide's Halifax Harbour dataset, the general patterns of M$_2$ tidal current ellipses in Halifax Harbour produced by submodel L5 agree reasonably well with the Halifax Harbour WebTide (Figure 3.6).
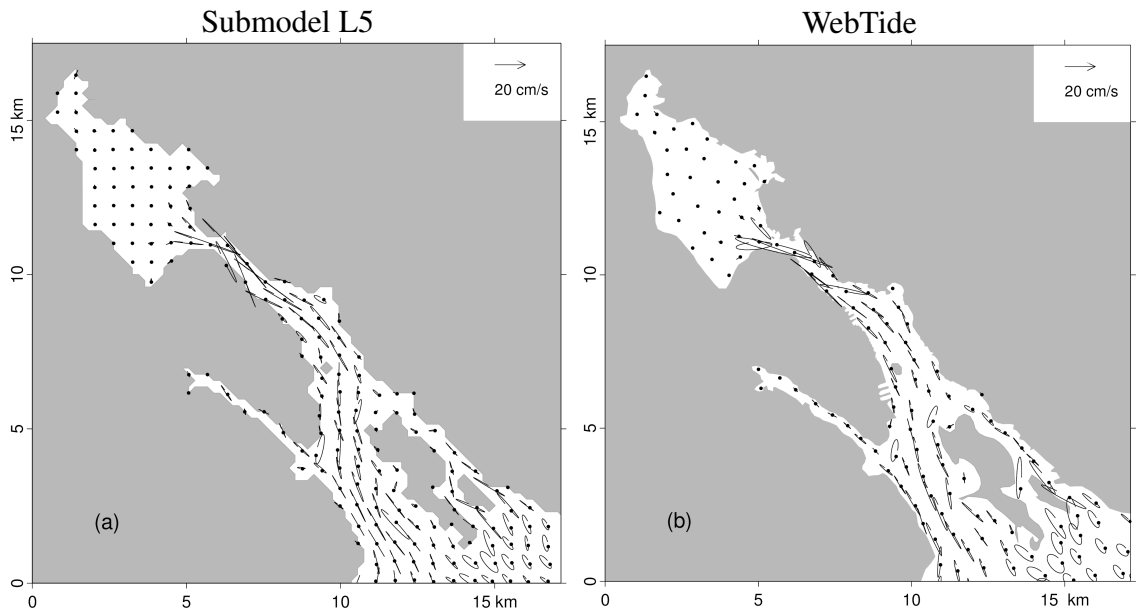
Figure 3.6: Comparison of depth-averaged M_2 tidal current ellipses calculated from (a) model results in March 2006 produced by submodel L5 (at each 3 model grid) and (b) WebTide for Halifax Harbour (for clarity, the minimum distance of each point is 600 meters).

The major differences of M_2 tidal current ellipses between our model results and WebTide can be attributed to several factors. Submodel L4 of the nested-grid modelling system resolves local topography and coastlines better than the Scotian Shelf WebTide. WebTide results for Halifax Harbour are based on model results produced by a limited area tidal circulation model with an ad hoc open boundary condition (*Greenberg*, 1999), while dynamic downscaling is used for model variables at open boundaries of submodel L5 of the NCOPS-HFX. In addition, the nested-grid model is baroclinic while WebTide datasets are based on barotropic model results.

3.3.3   General Mean Circulation

We next examine the model performance in simulating annual and monthly currents in the inner Scotian Shelf adjacent to Halifax Harbour. Figure 3.7 shows the annual mean currents from submodel L4 at a depth of 14 m in 2006. The annual mean currents flow from east to west along the coast as part of the Nova Scotia Current over the inner shelf near the eastern open boundary of submodel L4. These westward currents flow southwestward over the inshore area to the south of the headland of Sambro. The strong southwestward currents turn westward with a flow separation near the tip of the headland, with an anti-cyclone eddy to the west of this headland. The flow separation and general circulation around Sambro are similar to the previous finding of transient eddies around headlands (*Signell and Geyer*, 1991). In comparison with historical current observations (Figure 2.9) at depths between 10–20 m, submodel L4 has some skill in reproducing the general features of annual mean currents in the region. It should be noted that the observed currents were made before 1990 with different record lengths varying from 2 weeks to 8 months; it is not clear how representative the time-mean current observations are to the annual mean circulation in 2006.

Figure 3.8 shows the monthly mean near-surface (2 m) currents produced by submodel L4 and demonstrates the month-to-month variability of the Nova Scotia Current in 2006 over the inner Scotian Shelf adjacent to Halifax Harbour. The simulated Nova Scotia Current is relatively strong in February and November and relatively weak in May and August, which agrees in general with the current meter mooring data made at the Halifax Line (*Anderson and Smith*, 1989; *Loder et al.*, 2003).
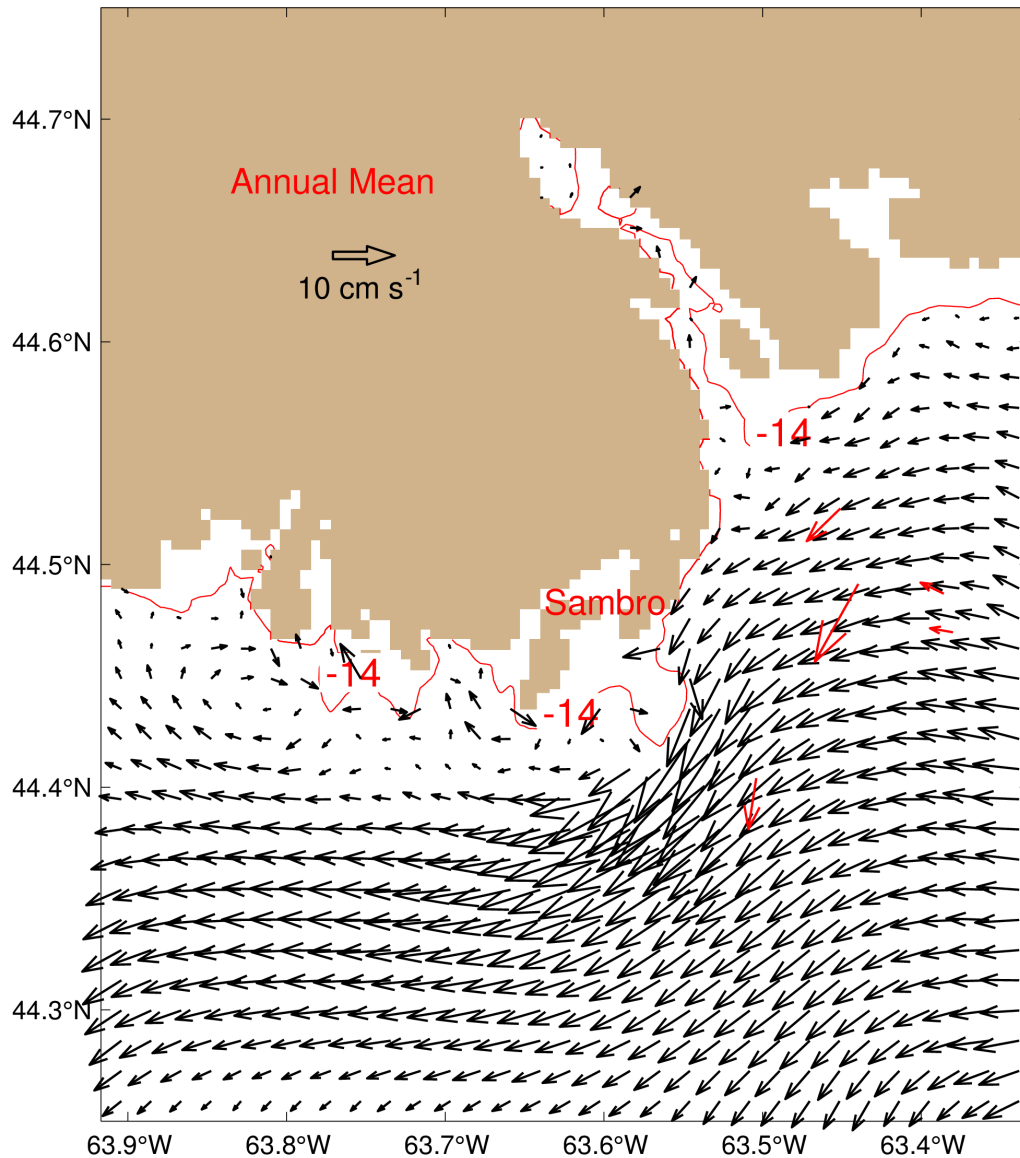
Figure 3.7: Annual mean currents (black arrows) at a depth of 14 m over the inner Scotian Shelf off Halifax Harbour calculated by submodel L4 of the nested-grid modelling system. For clarity, velocity vectors are plotted at every 3rd model grid point. Red arrows are mean currents based on observations collected prior to 1990 at depths between 10–20 m. Contours for the 14 m isobath are shown.
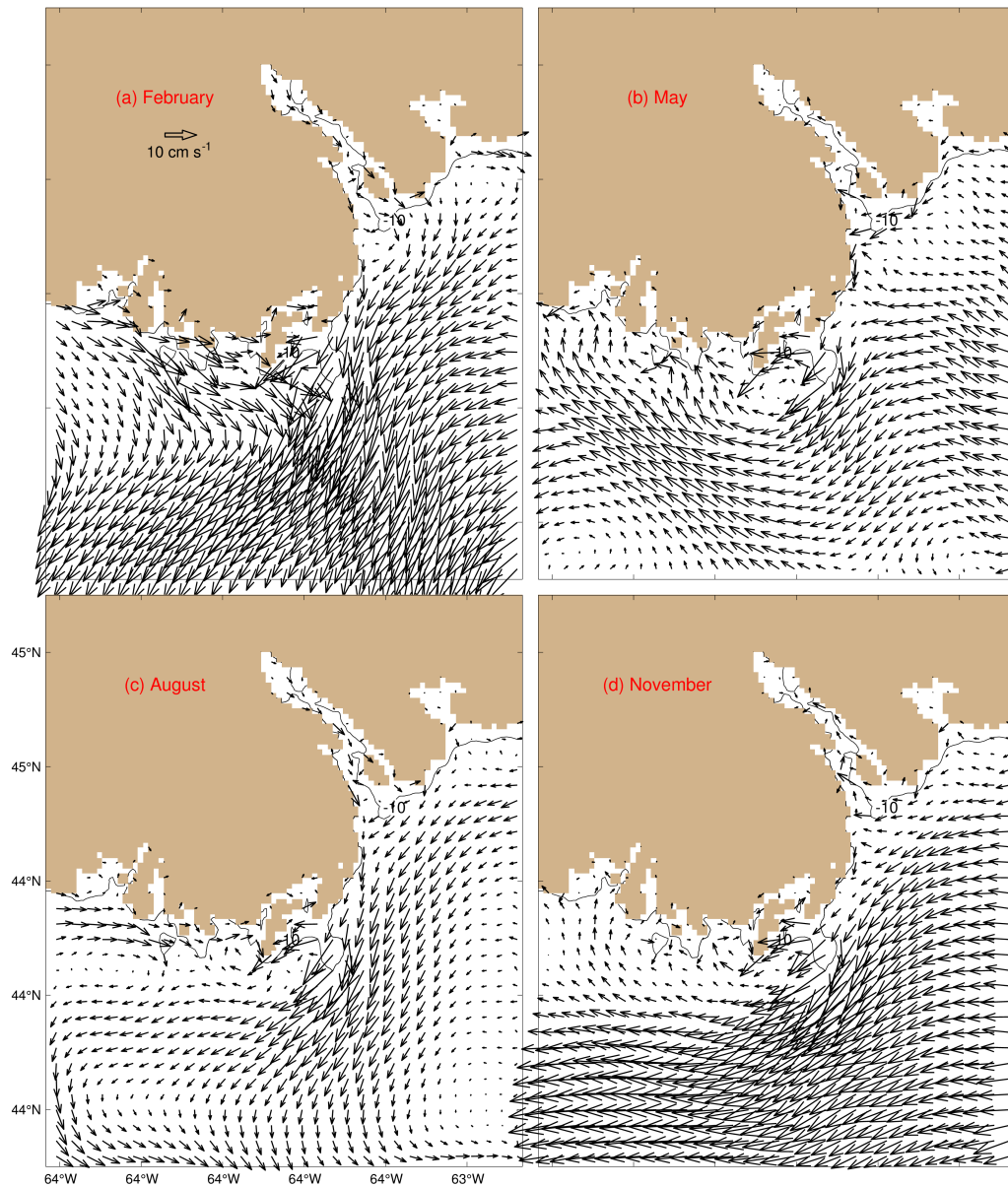
Figure 3.8: Monthly mean near-surface (2 m) currents over the inner Scotian Shelf off Halifax Harbour in (a) February, (b) May, (c) August and (d) November in 2006. Model results produced by submodel L4 of the nested-grid modelling system. For clarity, velocity vectors are plotted at every 3rd model grid point.

The annual mean currents at 2 m and 10 m in Halifax Harbour in 2006 produced by submodel L5 are characterized by a typical estuarine circulation with seaward flow in the upper layer, and landward return flow in the lower layer (Figure 3.9). Historical current observations made at station i at depths of 2 m and 10 m (Figure 2.9) confirm the general circulation features produced by submodel L5 of the nested-grid modelling system.
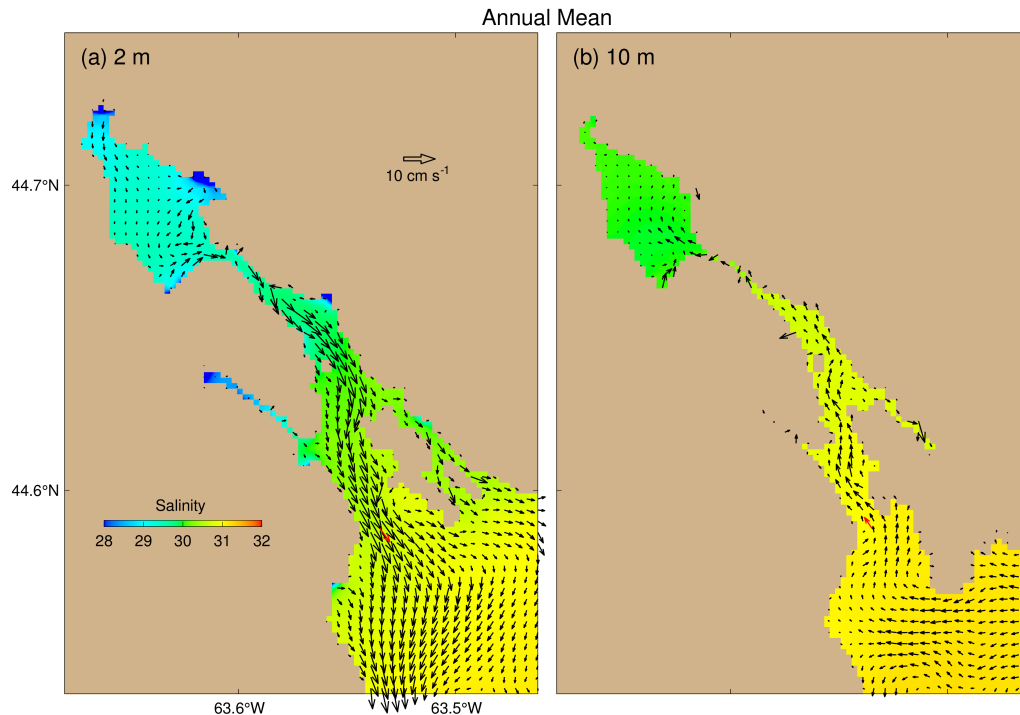
Figure 3.9: Annual mean currents and salinities at a depth of 2 m and 10 m in 2006 in Halifax Harbour calculated from model results produced by submodel L5. For clarity, velocity vectors are plotted at every 2nd model grid point. Red arrows are the time-mean current observations.

The horizontal structure of the two-layer circulation in the Harbour also has significant month-to-month variability. Figure 3.10 shows the monthly mean circulation at 2 and 10 m in the Halifax Harbour in February, May, August and November of 2006 calculated from model results produced by submodel L5. The monthly mean near-surface currents flow seaward (southwestward) all year round. The monthly mean near-surface currents are relatively weak in Bedford Basin, and relatively strong in the Narrows and the Inner and Outer Harbour. The seaward flow at 2 m is relatively strong in winter due mainly to the predominant westerly or northwesterly wind along the longitudinal axis of the Harbour. In February and August, the near-surface salinity gradients are relatively large between Bedford Basin and the Outer Harbour associated with relatively strong seaward

50

near-surface currents near the Lawlor Island. In May and November, the near-surface salinities are relatively low, especially in Bedford Basin and the Northwest Arm due mainly to ice and snow melt in spring and relatively large precipitation in late fall. The monthly mean sub-surface currents flow landward and are relatively weak in comparison with the near-surface currents. Over the Outer Harbour, the inshore branch of the Nova Scotia Current at 10 m flows westward from the eastern open boundary (Figure 3.10). Due to topographic steering, the current bifurcates, with one branch flowing into the Harbour as the landward flow, the other flows seaward. There is a small cyclonic eddy along the southern open boundary in the Outer Harbour. The sub-surface salinities are relatively high in comparison with the near-surface salinities. A sharp sub-surface salinity gradient is located around the Inner Harbour in February and May, and in the Narrows in August. In November, sub-surface salinities are relatively uniform and fresh in comparison with those in other months.

51
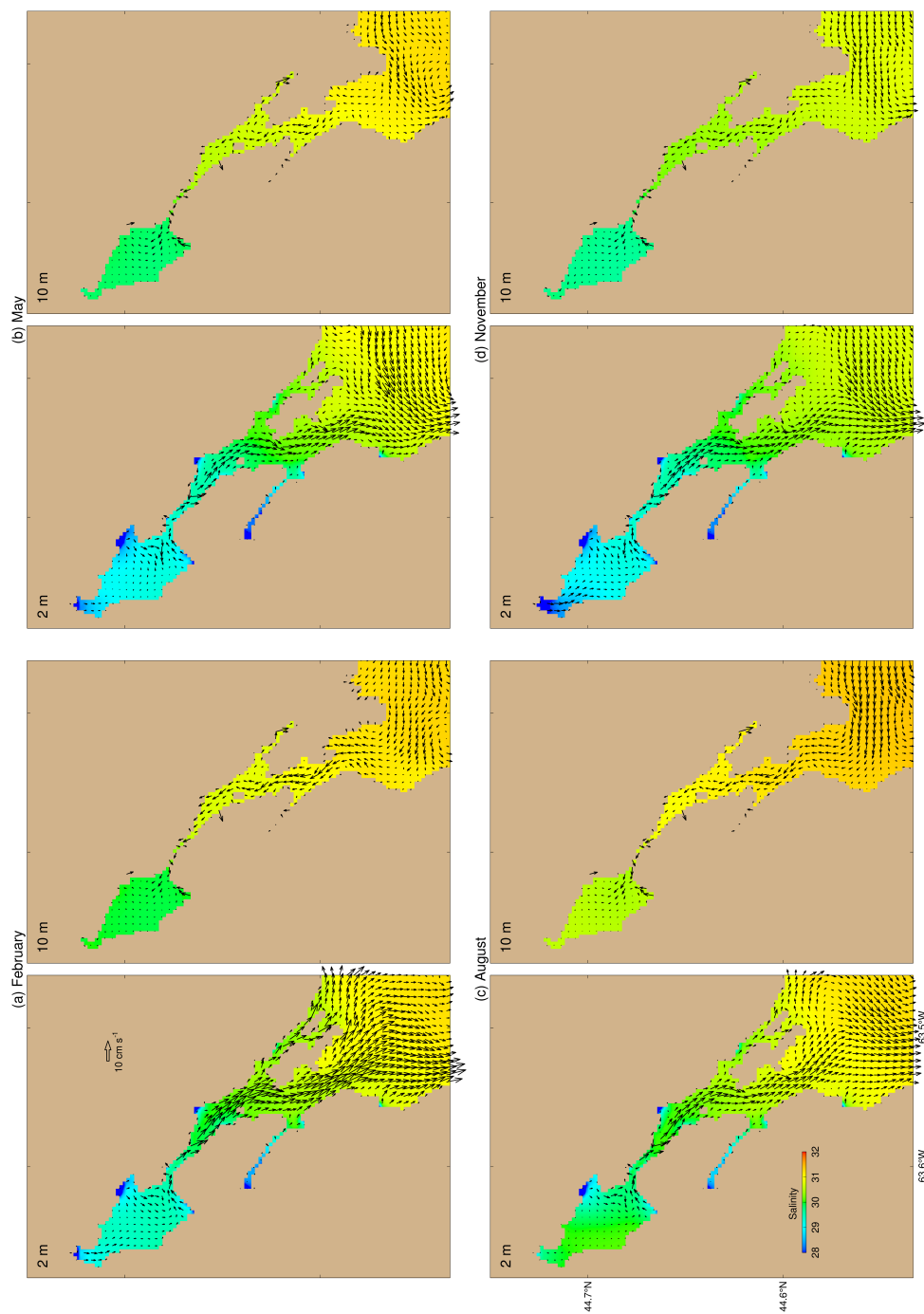
Figure 3.10: Monthly mean currents and salinities in Halifax Harbour at a depth of 2 m and 10 m in (a) February, (b) May, (c) August and (d) November of 2006 calculated from results produced by submodel L5 in the control run. For clarity, velocity vectors are plotted at every 2nd model grid point.

We also compare vertical profiles of annual mean currents produced by submodel L5 with historical observed currents (Figure 2.9) in Halifax Harbour presented in *Petrie and Yeats* (1990). Figure 3.11 shows the comparison of annual mean currents produced by submodel L5 with the time-mean observations at four stations in the Outer Harbour. The model-calculated mean current profiles are similar to observations, particularly at stations h, i and j. At these three stations, both the model results and observations demonstrate that strong velocity shears occur in the top 10 m. In the near-surface layer, the northward components of the simulated time-mean currents are negative and relative large, while the eastward components are positive or near zero, indicating that the near-surface currents flow nearly southward or southeastward (seaward) at these three stations. At station h, the eastward components are weak and the northward components have strong shear in the top 10 m and relatively weak below 20 m. At station i, velocity has strong shear in the near-surface layer with a turning point at about 20 m. At station j, there are relatively strong currents in the top 10 m and weak below 10 m. At station k, the eastward components are negative in the whole water column and the northward components are relatively strong in the near-surface layer and near zero below 10 m. The vertical profiles of simulated and observed currents at station i are in a good agreement. The modelled velocities at stations h and j have similar amplitudes of the observations, although there are only one or two observations made at these two stations, which provide limited verification of the vertical structure of model currents. At station k, there are large differences in the simulated and observed eastward components of time-mean currents, for which the exact reasons are unknown. One possible explanation is that the observed record length is relatively short. The model results represent the annual mean currents in 2006 under different forcing than those when the records were collected. Nonetheless, the overall qualitative agreement between model and observation is encouraging.
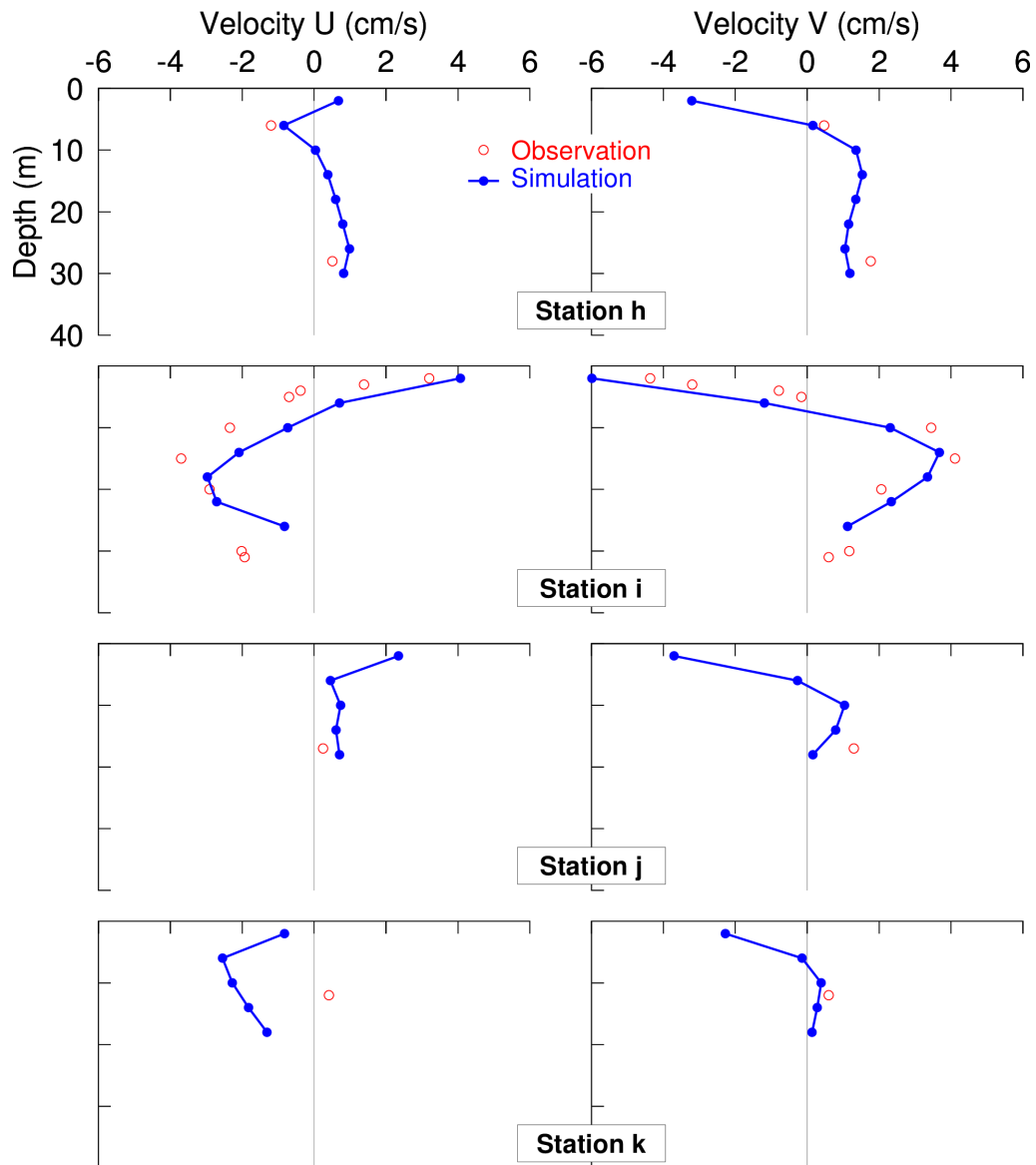
Figure 3.11: Vertical profiles of annual mean currents in 2006 (solid curves with bullets) calculated by submodel L5. Open circles represent the time-mean observed currents discussed in *Petrie and Yeats* (1990). Here U and V represent the eastward and northward components of currents, respectively. Observation records vary from about 3 weeks to 8 months. The station locations are marked in Figure 2.9.

To further examine the vertical variability of model-calculated currents, we present the along-transent and vertical components of monthly mean currents produced by submodel L5 along the transent from the Sackville River to the open sea in Figure 3.12. The vertical profiles of monthly mean currents produced by submodel L5 along the transect are characterized by a typical two-layer estuarine circulation (Figure 3.12) with near-surface waters flowing seaward (southeastward) and sub-surface waters flowing landward (northwestward). The seaward flow occurs in the top 5 m, and the landward flow occurs in the water column below 5 m from the surface. In Bedford Basin, the monthly mean currents are relatively large in the upper 20 m and much weaker at depths below 30 m. Another interesting feature is a current jet centred at about 5 m which overshoots from the Narrows into Bedford Basin (Figure 3.12). The Narrows is a dynamically active region in the Harbour with strong upwelling at about 10 km from the mouth of the Sackville River. This upwelling plays an important role in enhancing the near-surface seaward water transport, which corresponds to the "amplification" of the river input based on the classical two-layer estuarine circulation formulation. Over the Inner Harbour, the two-layer flow structure is well defined, with the flow direction changing from seaward to landward at depth of about 5 m. Below this depth, the landward flow over the Inner Harbour increases with depth to reach a maximum value at about 15 m, and then decreases with depth. Over the Outer Harbour, the circulation is largely influenced by the offshore large-scale circulation and hydrographic distributions of offshore waters. Figure 3.12 also demonstrates that the two-layer circulation has significant month-to-month variability. The intensity of the two-layer circulation is relatively strong in winter and relatively weak in summer, which is consistent with the previous finding by *Tee and Petrie* (1991) that the wind could intensify the two-layer circulation in winter.

Caution should be taken when interpreting Figure 3.12. First, the transect from the Sackville River to the open sea used in this study roughly follows the deep channel in Halifax Harbour (the red dashed line in Figure 2.3), and this is not the central line of the Harbour. Therefore the cross-transect component is not zero in general and the horizontal velocities in the transect have both non-zero along-transect and cross-transect components. In Figure 3.12 we present only the along-transect and vertical components of the model-calculated currents. Second, the ratio of along-transect currents to the vertical currents is not equal to the ratio of the horizontal distance to the vertical distance shown in

Figure 3.12. Therefore the effect of the vertical currents is exaggerated in the figure for eased visualization.

Figure 3.12: Vertical distributions of monthly mean currents in 2006 along a transect from the Sackville River to the open sea (see Figure 2.3) based on model results produced by submodel L5.

To compare the model results with the box model results produced by *Petrie and Yeats* (1990), volume averaged currents are also calculated for the five subareas defined in Figure 2.3 from the 3D model current fields produced by submodel L5 for 2006. Based on the typical vertical distribution of currents shown in Figure 3.12, we choose the depth range of 0–4 m to represent the near-surface layer. Figure 3.13 shows the volume averaged two-layer estuarine circulation. In comparison with box model results of *Petrie and Yeats* (1990) based on salt and mass conservation, the general circulation patterns shown in

Figure 3.13 are similar except that the volume averaged flow produced by the NCOPS-HFX is seaward in the sub-surface layer in May, August and November over the Outer Harbour, which is due mainly to variations of the thickness of near-surface layer (Figure 3.12) and the large influences of offshore waters. The maximum volume averaged current speed occurs over the Inner Harbour in February, which is about 4.3 cm/s. In the Northwest Arm, volume averaged circulation also has the two-layer estuarine circulation pattern.
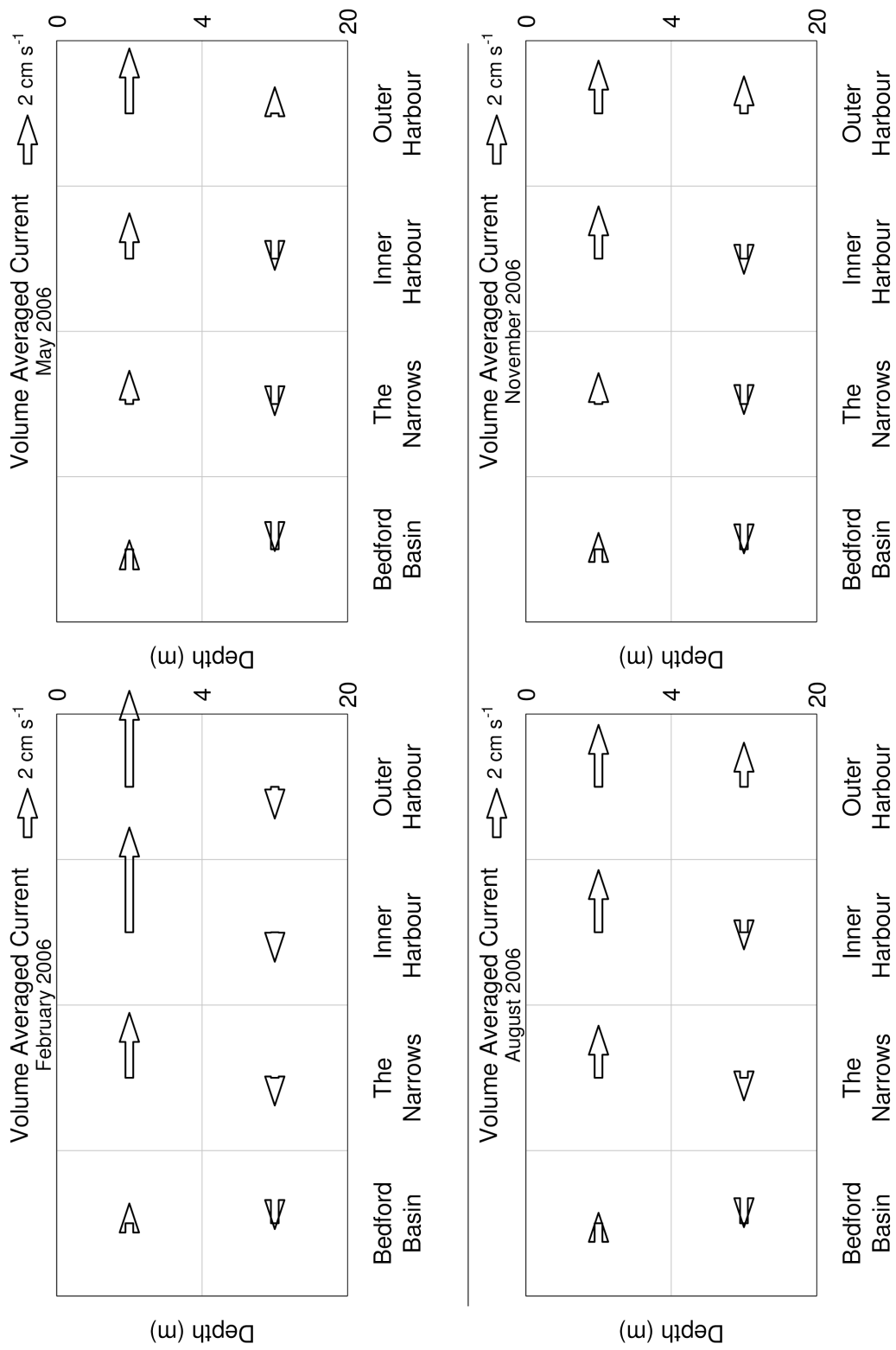
Figure 3.13: Volume averaged currents calculated from monthly mean 3D flow fields in February, May, August and November of 2006 produced by submodel L5. The thickness of the surface layer is set to 4 m in the calculation.

3.3.4 Temperature and Salinity

The model-calculated temperature and salinity produced by submodel L5 have significant variability over a wide range of time scales. We first examine the performance of submodel L5 in generating seasonal cycles of hydrography in the study region by comparing the monthly mean temperatures and salinities produced by the model (Figures 3.14 and 3.15) with monthly mean climatology (Figures 2.12 and 2.14) along the transect from the Sackville River to the open sea. A comparison of model results in Figure 3.14 with the climatology in Figure 2.12 demonstrates that submodel L5 has reasonable skill in reproducing the seasonal cycle of water temperatures in Halifax Harbour, particularly in late fall, winter and spring. In summer, the model-calculated surface water is cooler than the monthly mean climatology, which may be due to the coarse resolution heat flux forcing in representing the realistic air-sea interaction in Halifax Harbour, particularly in summer in the nested-grid modelling system. It should be noted the use of the spectral nudging method ((*Thompson et al.*, 2007)) ensures the success of the model in simulating the seasonal cycle of the hydrography in the study region.

A comparison of monthly mean salinities produced by submodel L5 shown in Figure 3.15 with monthly mean salinity climatology shown in Figure 2.14 demonstrates that the simulated monthly mean salinities have more small-scale features than the monthly mean climatology, especially in the Narrows. This is expected since the simulated monthly mean salinity is calculated by the NCOPS-HFX, which solves the primitive equation numerically based on realistic coastline and bathymetry, while the climatology was constructed using the Barnes' algorithm which is not explicitly constrained by coastline and bathymetry.

To demonstrate the model performance in simulating the high frequency variability of hydrography in Halifax Harbour, we examine time-depth distributions of temperature and salinity at stations G2 in Bedford Basin and B2 in the Outer Harbour based on daily model output produced by submodel L5 in 2006. Figure 3.16a and c show that cold water is generated first in the surface layer in winter, and this cold water in Bedford Basin sinks into the deeper layer associated mainly with vertical convection (Figure 3.16a). In summer, the seasonal thermocline is developed in the upper water column in Bedford Basin; in the Outer Harbour, the warm water column is frequently replaced by cooler water due mainly to upwelling. Figure 3.16b shows that relatively fresh water occupies the upper water column in Bedford Basin. The thickness of the fresh upper layer varies with time. The salinity of
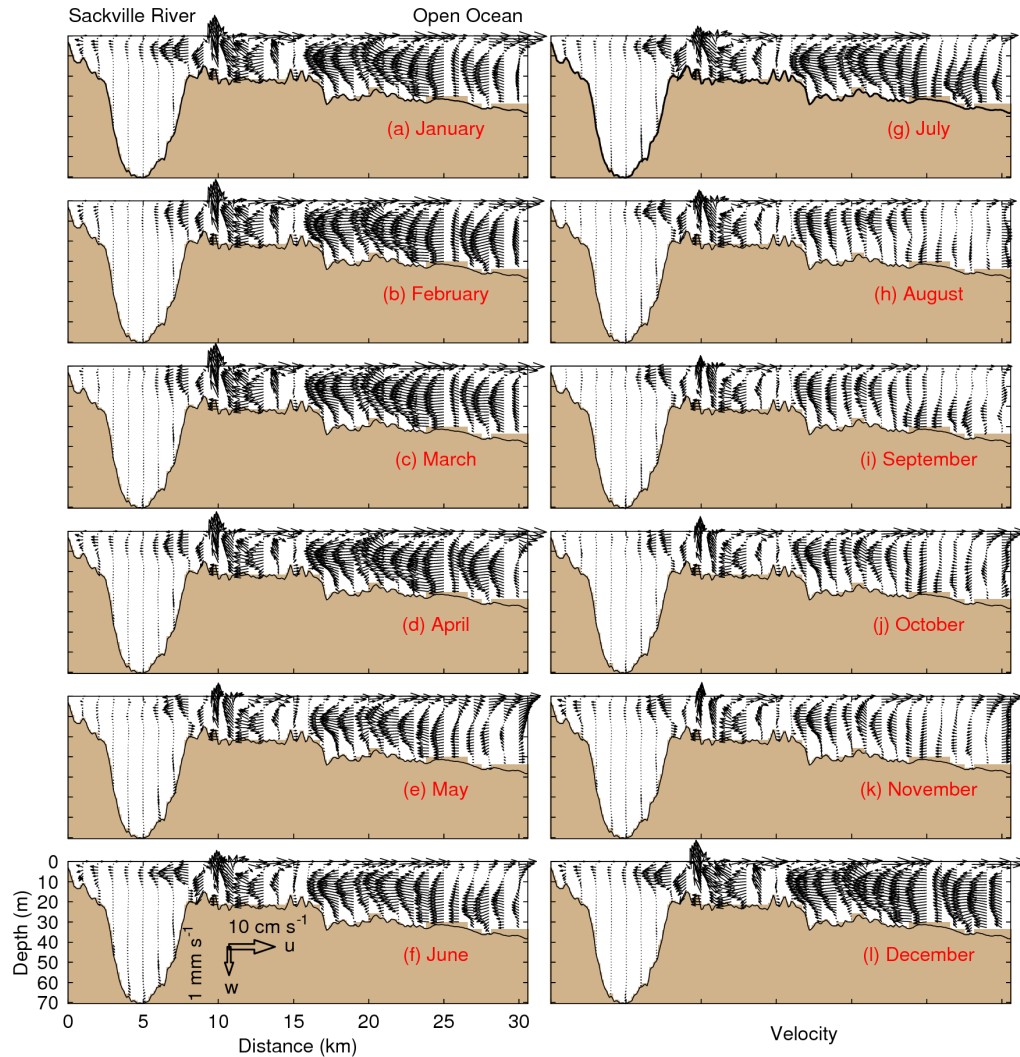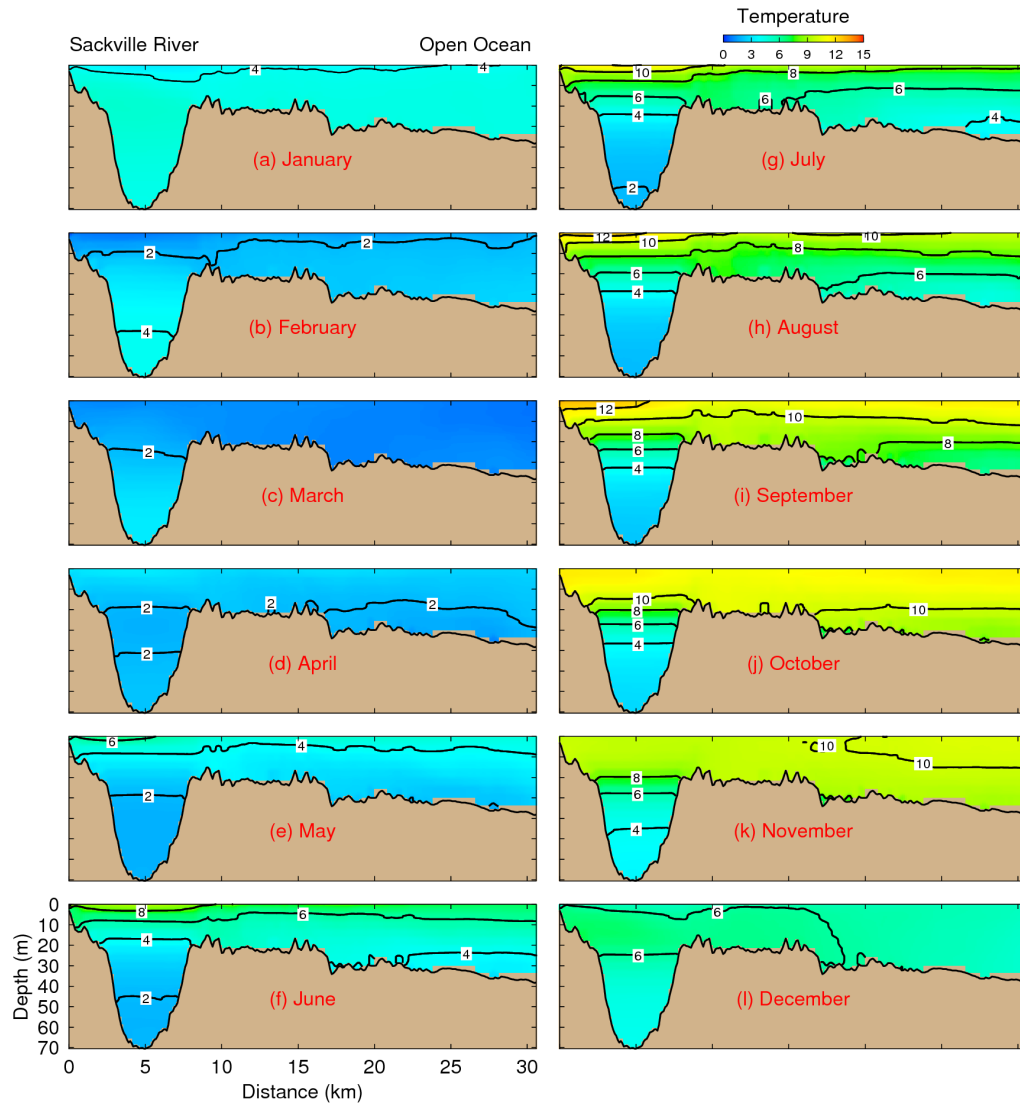
Figure 3.14: Vertical distributions of monthly mean temperatures in 2006 along the transect from the Sackville River to the open sea (see Figure 2.3) based on model results produced by submodel L5.

the lower water column is relatively high in late fall and winter compared to spring and summer. In comparison with the time-depth distributions of hydrographic climatology, the simulated hydrography has significant variability due mainly to the wind-induced upwelling and downwelling to be discussed in Chapter 4.

Time series of near-surface temperature and salinity (Figure 3.17) produced by submodel L5 show the modelling system is able to capture the seasonal variability of temperature and salinity in Halifax Harbour in comparison with the hydrography climatology. There are significant fluctuations of near-surface temperature and salinity at station B2 in the
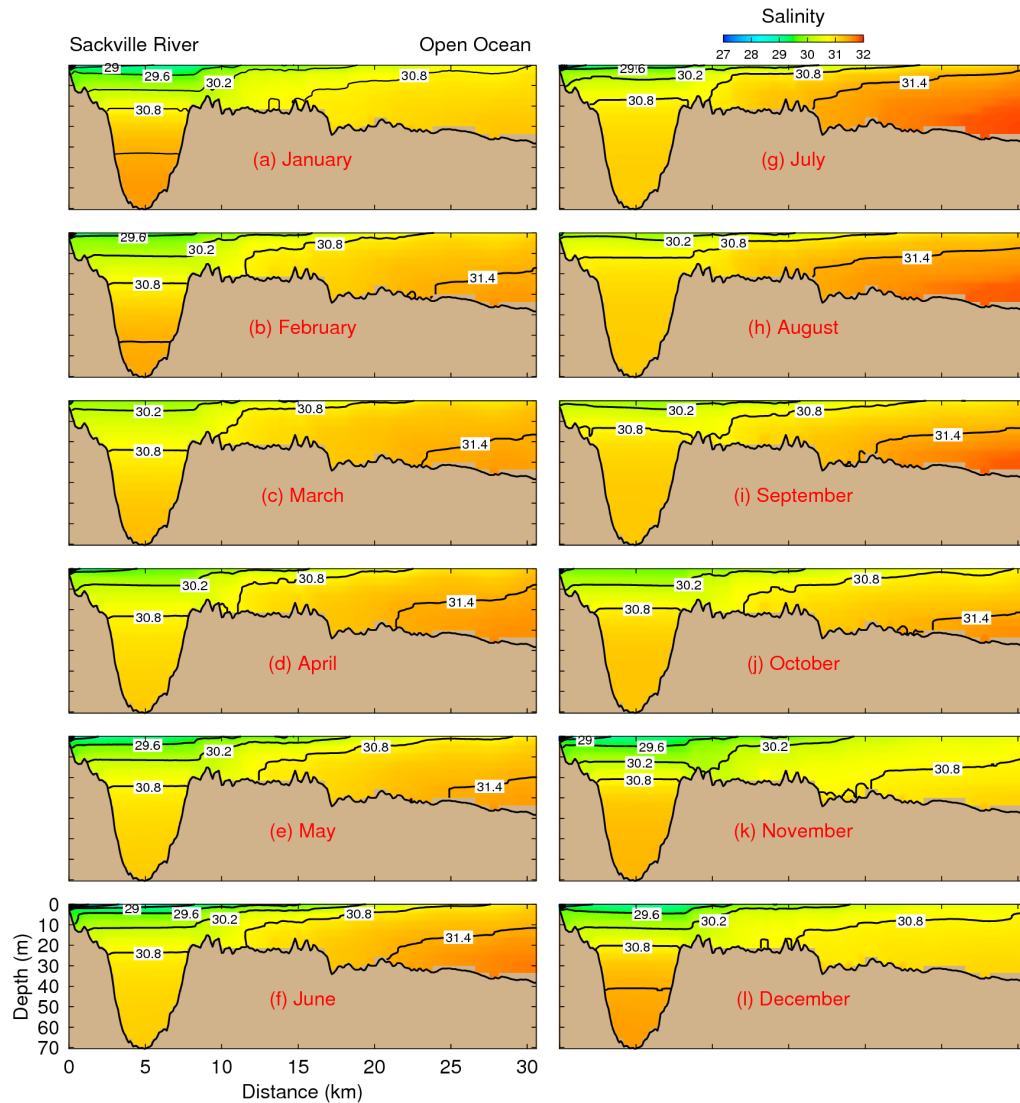
Figure 3.15: Vertical distributions of monthly mean salinities in 2006 along the transect from the Sackville River to the open sea (see Figure 2.3) based on model results produced by submodel L5.

Outer Harbour in summer due mainly to local upwelling and downwelling. There is a short period of low near-surface salinity in February 2006 at station G2 in Bedford Basin which is related to a peak freshwater discharge event as shown from the daily discharge of the Sackville River in 2006 (Figure 2.4). Figure 3.18 shows time series of observed and simulated near-surface temperature in Halifax Harbour. The simulated near-surface temperature roughly agrees with observations in January, February, November and December in 2006. However, the submodel L5 underestimates the near-surface temperature with relatively small high frequency variability in summer. The differences of near-surface

temperature between submodel L5 results and observations can be attributed largely to the low quality of surface heat flux fields and the lack of high frequency wind forcing, such as sea breeze, in this coastal region.

Finally temperature and salinity profiles (Figure 3.19) produced by submodel L5 show the model has some skill in simulating the variabilities of temperature and salinity in Bedford Basin in the top 20 m and in the Outer Harbour. However, in the lower water column of Bedford Basin the model-calculated temperature is cooler and salinity is fresher than the observed values. The close relationship between the model-calculated and climatological hydrography in the lower water column of Bedford Basin is due mainly to the use of the spectral nudging of which nudging parameters might be too strong for this particular area. Bedford Basin is a relatively deep area connected to the open sea via the shallow and narrow channel known as the Narrows. A non-hydrostatic model, high horizontal and vertical model resolution, high spatial and temporal resolution and reliable heat flux, precipitation, evaporation, local wind, better initial temperature and salinity fields, special and reliable mixing parameterization over the Narrows and Bedford Basin may be needed in order to further improve the performances of the NCOPS-HFX in simulating the intra- and inter-annual variabilities of temperature and salinity in Halifax Harbour, especially in Bedford Basin.
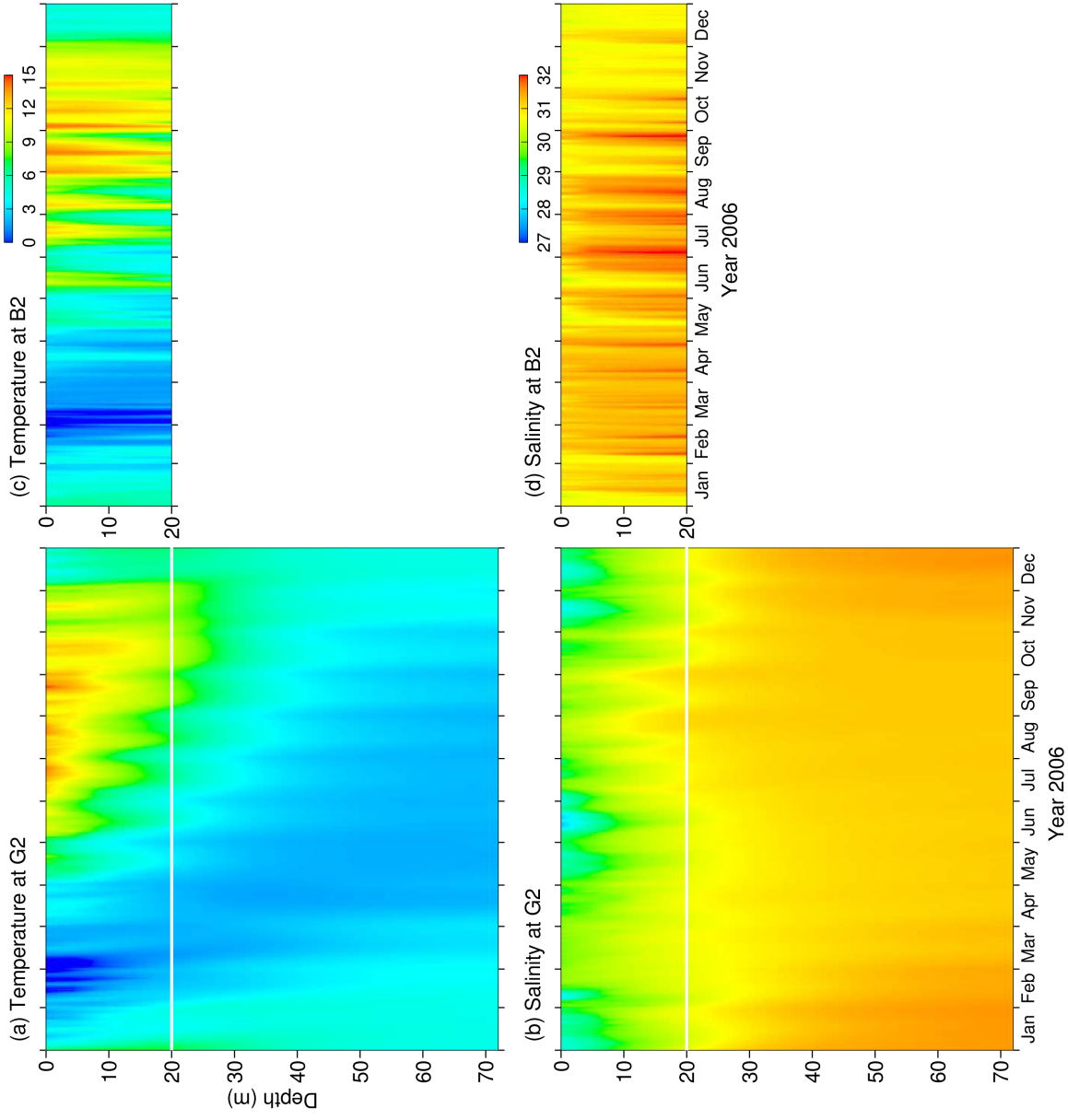
Figure 3.16: Time-depth distributions of model-calculated temperature and salinity at (a, b) station G2 in Bedford Basin and (c, d) station B2 in the Outer Harbour in 2006. Locations of these two stations are marked in Figure 2.3.
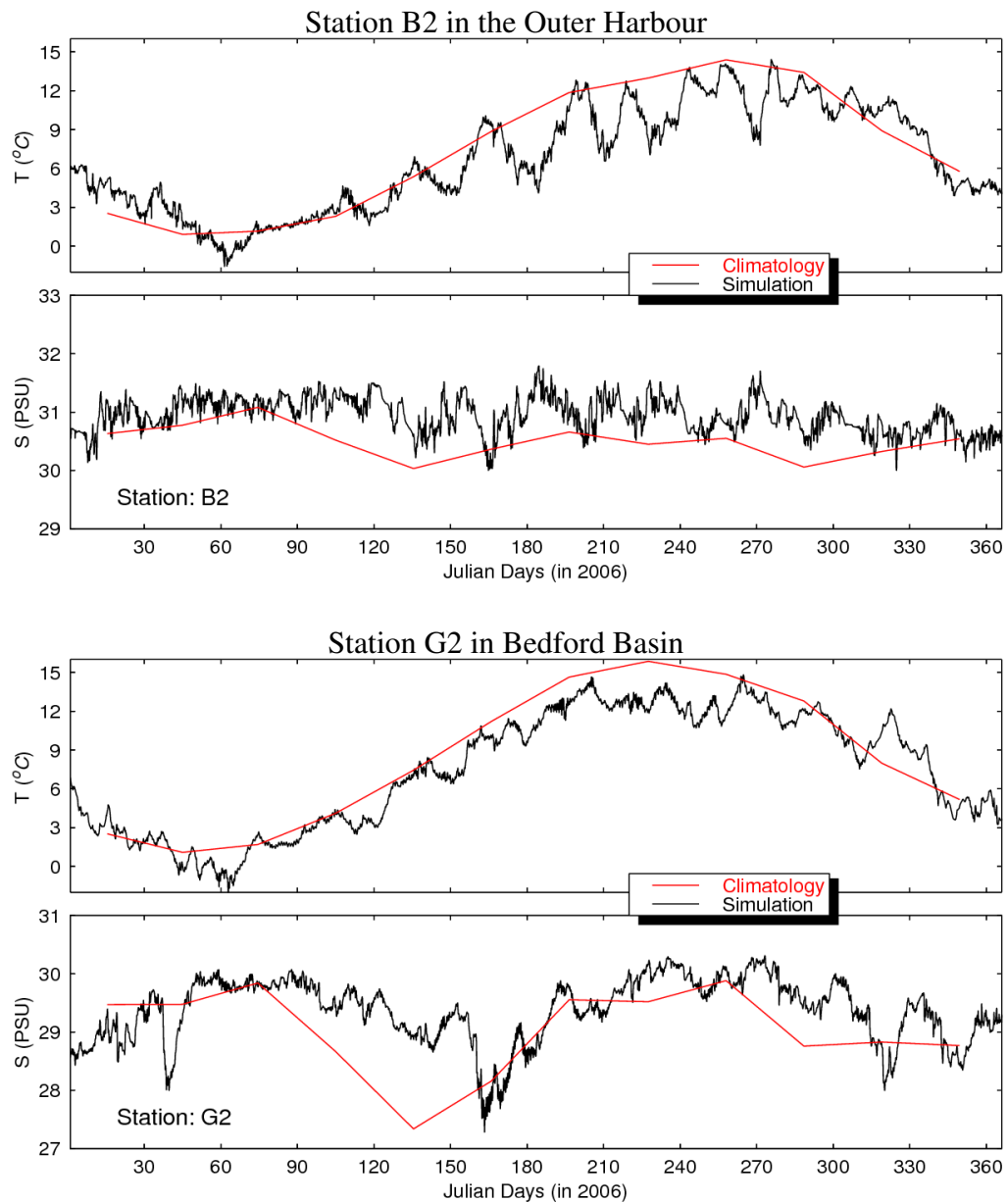
Figure 3.17: Time series of model-calculated near-surface (2 m) temperature and salinity at station G2 in Bedford Basin and at B2 in the Outer Harbour in 2006. Locations of these two stations are marked in Figure 2.3.
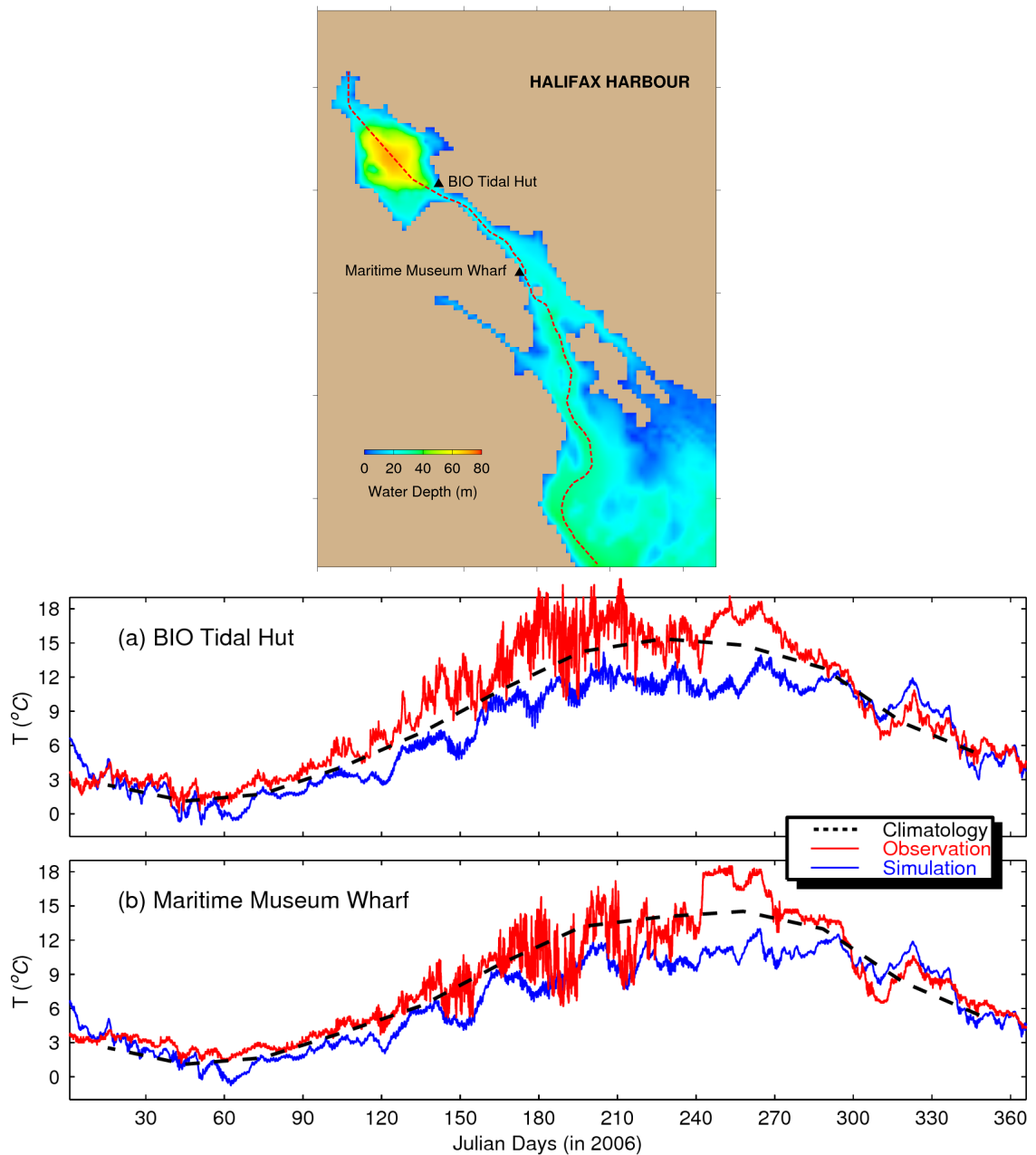
Figure 3.18: Time series of observed (red) and simulated (blue) near-surface (2 m) temperature at (a) BIO tidal hut and (b) Maritime Museum wharf in 2006. The simulated results are produced by submodel L5. The observations are extracted from the Oceanographic Databases of Fisheries and Oceans Canada, http://www.mar.dfo-mpo.gc.ca/science/ocean/database/data_query.html.
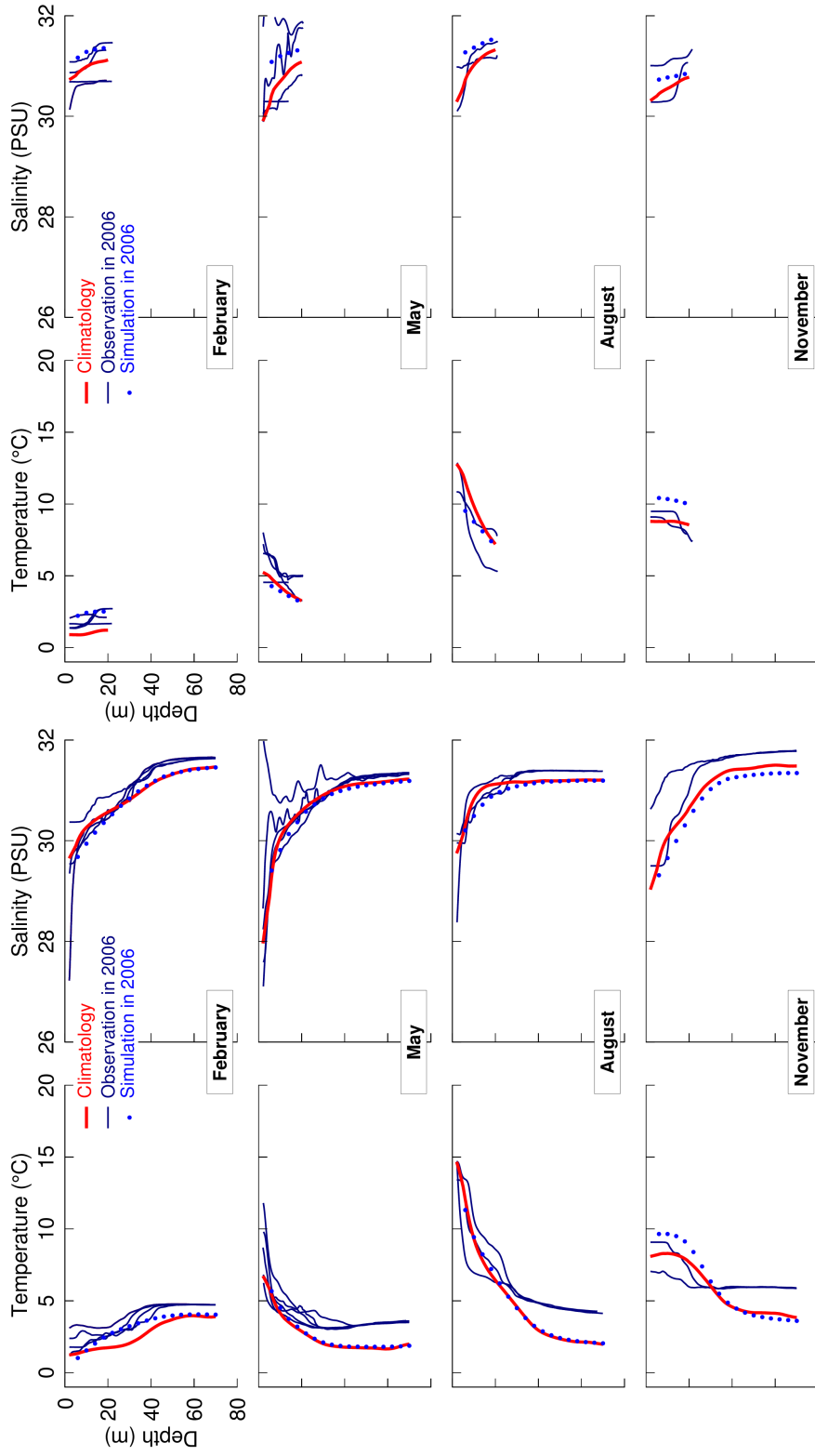
Figure 3.19: Vertical profiles of observed and simulated temperature and salinity at station G2 in Bedford Basin and B2 in the Outer Harbour.

CHAPTER 4

PROCESS STUDIES OF CIRCULATION AND HYDROGRAPHY IN HALIFAX HARBOUR

As discussed in the previous chapters, the circulation and hydrography of Halifax Harbour are affected by many forces including tides, wind and water discharge. A set of process studies is now conducted to determine the main physical mechanisms affecting circulation and hydrography in Halifax Harbour. Model results in the following four different numerical experiments are presented in this chapter.

i) Case-CR (Control-Run): The nested-grid modelling system is driven by all the forcing discussed in Chapter 3: tides, wind, sea surface heat and freshwater fluxes and freshwater discharges.

ii) Case-NoLocalWind: The modelling system has the same model setup as Case-CR except for zero wind forcing in submodels L3, L4 and L5. Since the domains of submodels L3-L5 are relatively small in comparison with the domain of submodel L2. The purpose of this experiment is to examine how the remotely generated wind-driven currents on the Scotian Shelf and the Gulf of St. Lawrence influence circulation and hydrography in Halifax Harbour and adjacent coastal waters.

iii) Case-NoTide: The modelling system has the same model setup and forcing as Case-CR except that the tidal sea surface elevations and tidal depth-averaged currents produced by WebTide are not specified along the open boundaries of submodel L2. Therefore the tidal forcing is set to zero in this experiment.

iv) Case-NoDischarge: The modelling system has the same setup and forcing as Case-CR except that freshwater discharge from the Sackville River, distributed inflows throughout the Harbour, and sewage are not specified in submodel L5.

4.1 Main Physical Processes Affecting Circulation During a Winter Storm Event

We first examine the main physical processes affecting the 3D circulation of Halifax Harbour and adjacent shelf water during winter storms. A major winter storm swept over the Scotian Shelf and adjacent waters on February 1, 2006. The spatial distributions of wind forcing during this storm are shown in Figure 3.3. The model results at 12:00 UTC February 1, 2006 produced by the nested-grid modelling system in Case-CR are shown in Figure 4.1. The total sea surface elevations produced by submodel L1 are large and positive, reaching about 55 cm around the storm centre on the Scotian Shelf. Depth-averaged currents produced by submodel L1 are characterized by large divergent currents over the area affected directly by the storm. There are relatively large depth-averaged currents over the Labrador and Newfoundland Shelves which were excited by an earlier storm that swept through the region. The surface circulation on the Scotian Shelf and Gulf of St. Lawrence produced by submodel L2 (Figure 4.1b) at this time is characterized by strong northwestward surface currents over the Laurentian Channel between the Grand Banks and the Scotian Shelf, and strong southwestward surface currents over the Scotian Shelf at this time. Relatively low surface salinity waters occur over the western Gulf of St. Lawrence and inner Scotian Shelf (Figure 4.1b). As shown in Figures 4.1c and 4.1d, the model-calculated near-surface currents over the inner Scotian Shelf adjacent to Halifax Harbour are southwestward due to strong wind forcing, and the surface salinity is nearly uniform at about 31 psu. Near the eastern open boundary of submodel L5 (Figure 4.1e), there is an intense westward through-flow as part of the Nova Scotia Current. A flow jet produced by the local topography can be seen in the Narrows (Figure 4.1e). A salinity front due to the freshwater discharges from the Sackville River, sewage and distributed water occurs in Bedford Basin and the Narrows.

Figure 4.2 shows the evolution of wind forcing and near-surface water temperatures and currents produced by submodel L4 in Halifax Harbour and adjacent inner Scotian Shelf during this storm event. Since shallow waters have a relatively low heat storage capacity
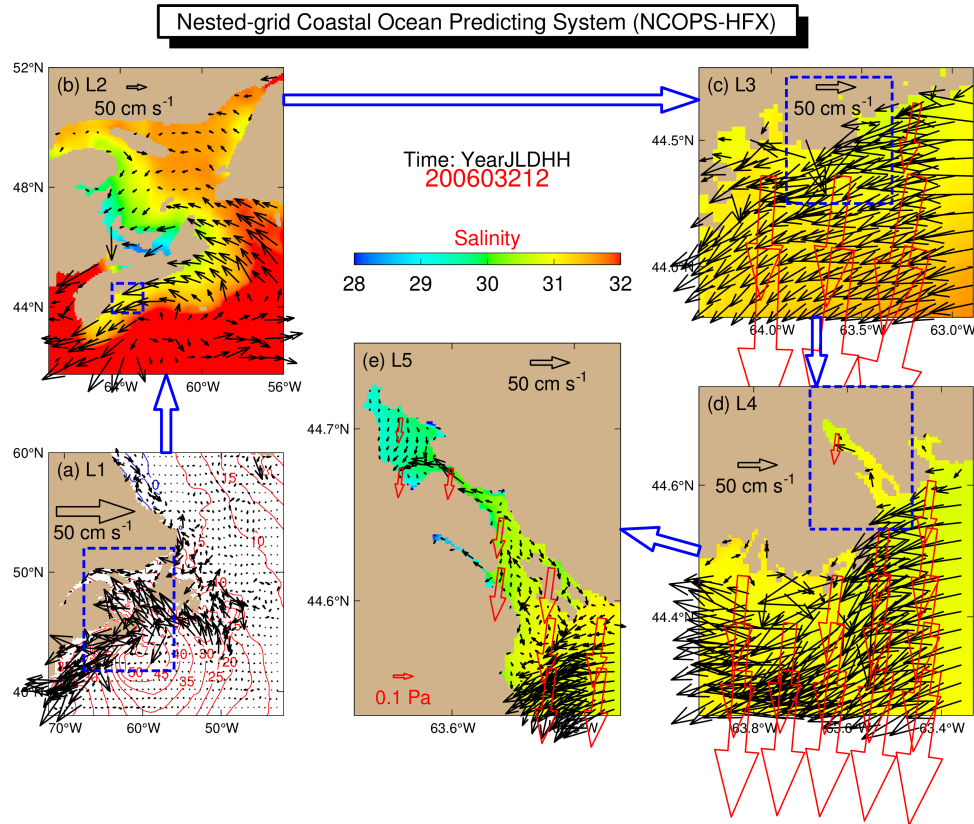
Figure 4.1: A snapshot of (a) depth-averaged currents (black arrows) and total surface elevation (red/blue contours for positive/negative values with the contour interval of 5 cm) produced by submodel L1; (b) surface currents (black arrows) and sea surface salinity (images) produced by submodel L2; and (c-e) near-surface (2 m) currents and salinities produced by submodels L3-L5. Time is day 32.5 (12:00 UTC February 1) in 2006. Red open arrows are wind stress vectors. For clarity, velocity vectors are plotted at every (a) 9th, (b) 10th, (c) 4th, (d) 6th, and (e) 3rd model grid point.

in comparison to deeper waters, the near-surface temperature in inlets should normally be cooler than offshore waters in winter. During this storm period, the storm-induced currents in the model flow from east to west over the inner Scotian Shelf, transporting relatively warm shelf waters to Halifax Harbour. After this storm event, model-calculated near-surface water temperature outside Halifax Harbour increases by about 2 °C.
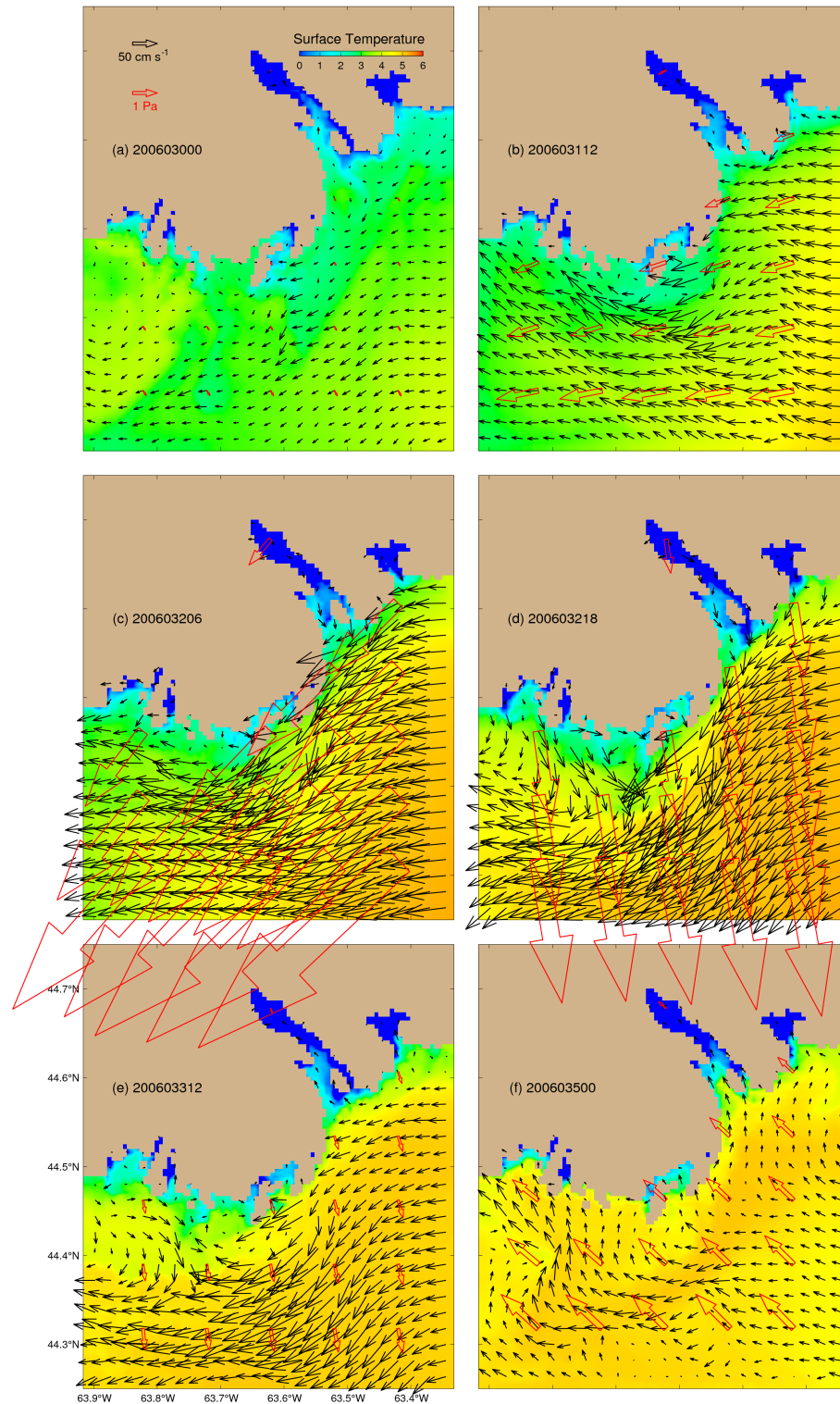
Figure 4.2: Evolution of near-surface (2 m) temperatures and currents at (a) 00:00 January 30, (b) 12:00 January 31, (c) 06:00 February 1, (d) 18:00 February 1, (e) 12:00 February 2, (f) 00:00 February 4 UTC in 2006, based on submodel L4 results in Case-CR. Red open arrows are wind stress vectors. For clarity, velocity vectors are plotted at every 4th model grid point.
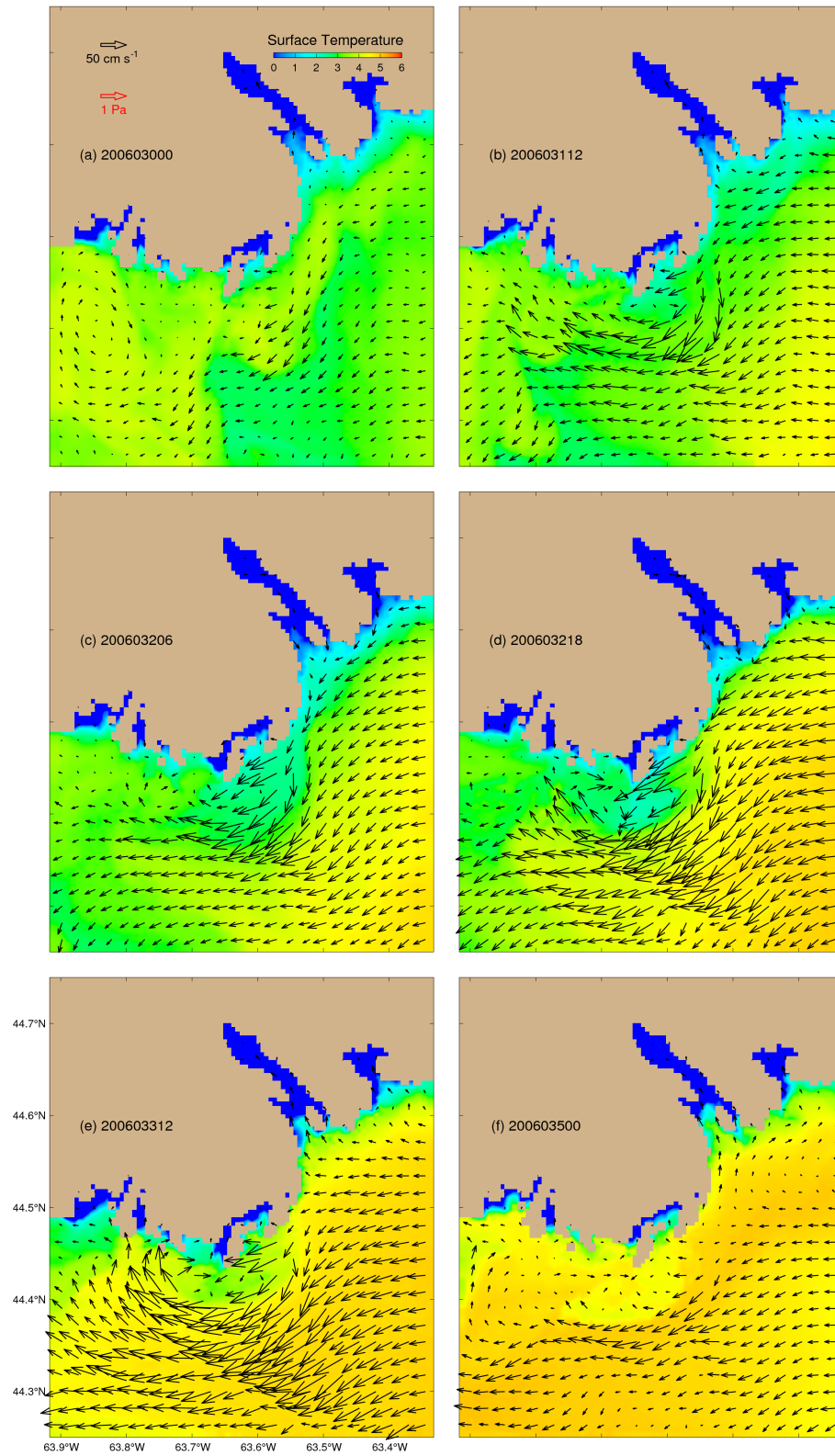
Figure 4.3: Same as Figure 4.2, except for model results in Case-NoLocalWind.
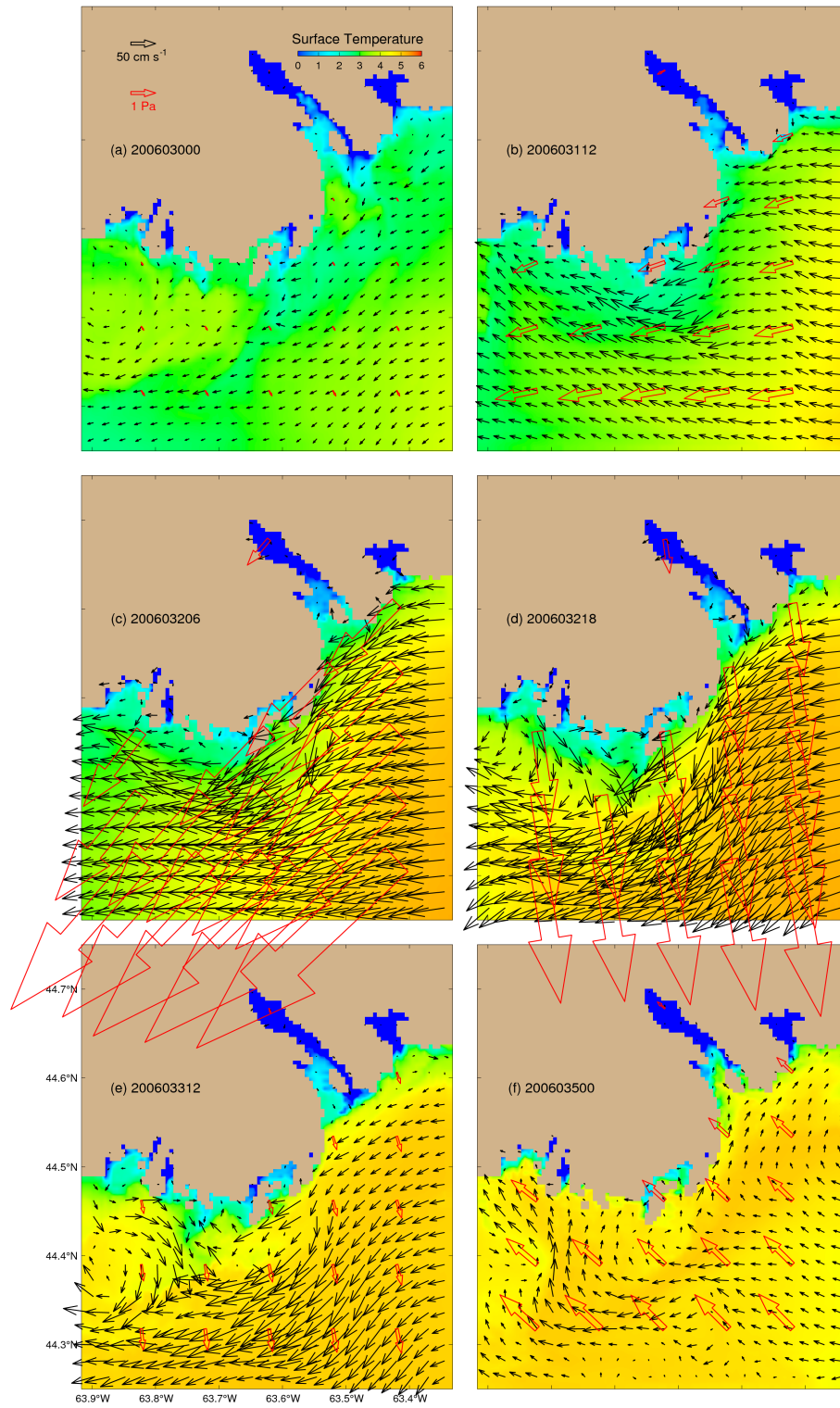
Figure 4.4: Same as Figure 4.2, except for model results in Case-NoTide.

To demonstrate the importance of wind forcing during this storm event, we compare the model results in Case-CR and Case-NoLocalWind during the same period. Prior to the storm, the near-surface currents and temperature in Case-NoLocalWind have similar horizontal distributions over the inner Scotian Shelf adjacent to Halifax Harbour as in Case-CR (Figures 4.2a and 4.3a). Differences between the two experiments become larger as wind increases. During the peak of this storm, the near-surface temperature produced by submodel L4 is relatively warmer in Case-CR than in Case-NoLocalWind, with much stronger westward near-surface currents in Case-CR due to the effect of local wind forcing (Figures 4.2c, d and 4.3c, d). After the peak of the storm, the wind gradually dies down and the model-calculated near-surface currents and temperature distributions outside Halifax Harbour become similar between Case-NoLocalWind and Case-CR model results, except that the near-surface temperatures in the shallow coastal regions are warmer in Case-CR compared to Case-NoLocalWind. The Nova Scotia Current in Case-NoLocalWind (Figures 4.3a, d and f) is relatively stronger around the peak of the storm and carries relatively warm and salty offshore waters to the Outer Harbour and adjacent waters, indicating the important role of the remote wind forcing outside of the domain of submodel L3. The model results in Case-NoTide (Figure 4.4) have large-scale features similar to these in Case-CR, with differences mainly in small-scale features in the study region, particularly in coastal areas and bays.

We next compare the near-surface currents and salinities produced by the submodel L5 at 12:00 UTC February 1, 2006 in the three experiments of Case-CR, Case-NoLocalWind and Case-NoTide (Figure 4.5). At this time, the storm reaches its highest intensity with the wind stress of about 0.2 Pa at the tide gauge CHS 490 in the Narrows and the tidal currents flood into Halifax Harbour. As mentioned earlier, the model results in Case-CR (Figure 4.5a) are characterized by weak and spatially uniform southward near-surface currents over Bedford Basin and the eastern side of McNabs Island, landward (northwestward) currents in the Narrows and strong southwestward flow in the Outer Harbour. Low salinity waters occur in Bedford Basin due to the freshwater discharge from the Sackville River, sewage and distributed water sources in Bedford Basin and the Narrows. Without local wind forcing (Case-NoLocalWind), Figure 4.5b shows that relatively uniform landward near-surface currents occur inside the Harbour with relatively large magnitudes at the Narrows and over the western side of McNabs Island, similar to flood M_2 tidal currents as shown in the atlas

of tidal currents for Halifax Harbour produced by *Greenberg* (1999). Major differences in the near-surface currents between Case-CR and Case-NoLocalWind occur over the Outer Harbour where the currents are much stronger in Case-CR than Case-NoLocalWind, indicating the important role of local wind forcing. The other differences between Case-CR and Case-NoLocalWind are the relatively stronger wind-induced near-surface currents in Bedford Basin and the relatively weaker landward jet in the Narrows in Case-CR compared to Case-NoLocalWind, which indicates that currents in the Harbour are dominated by strong wind-driven currents during this storm event, especially in Bedford Basin and over the east side of McNabs Island. The near-surface circulation patterns in Case-CR and Case-NoTide are similar except that there is no landward jet in the Narrows at this time in Case-NoTide. The through-flow over the Outer Harbour is more intense in Case-CR in comparison with Case-NoLocalWind results due mainly to the enhancement by the local wind forcing. Figure 4.5 also demonstrates the importance of the coastal currents generated by remote winds over the Scotian Shelf that propagate into Halifax Harbour through the domains of submodels L3 and L4.

In summary, local wind forcing can significantly modulate the near-surface tidal circulation patterns in Halifax Harbour. The strong through-flow in the Outer Harbour during this storm event is originally generated on the Scotian Shelf and enhanced by local wind forcing. The strong storm-induced currents associated with warm and salty waters have significant impacts on circulation and hydrography in the Outer Harbour. Without wind, the fresh water plume over Bedford Basin can spread farther offshore along the main navigation channel in Halifax Harbour. An intense tidal jet seen in the Narrows even during the peak of the storm can be modified by local wind forcing.
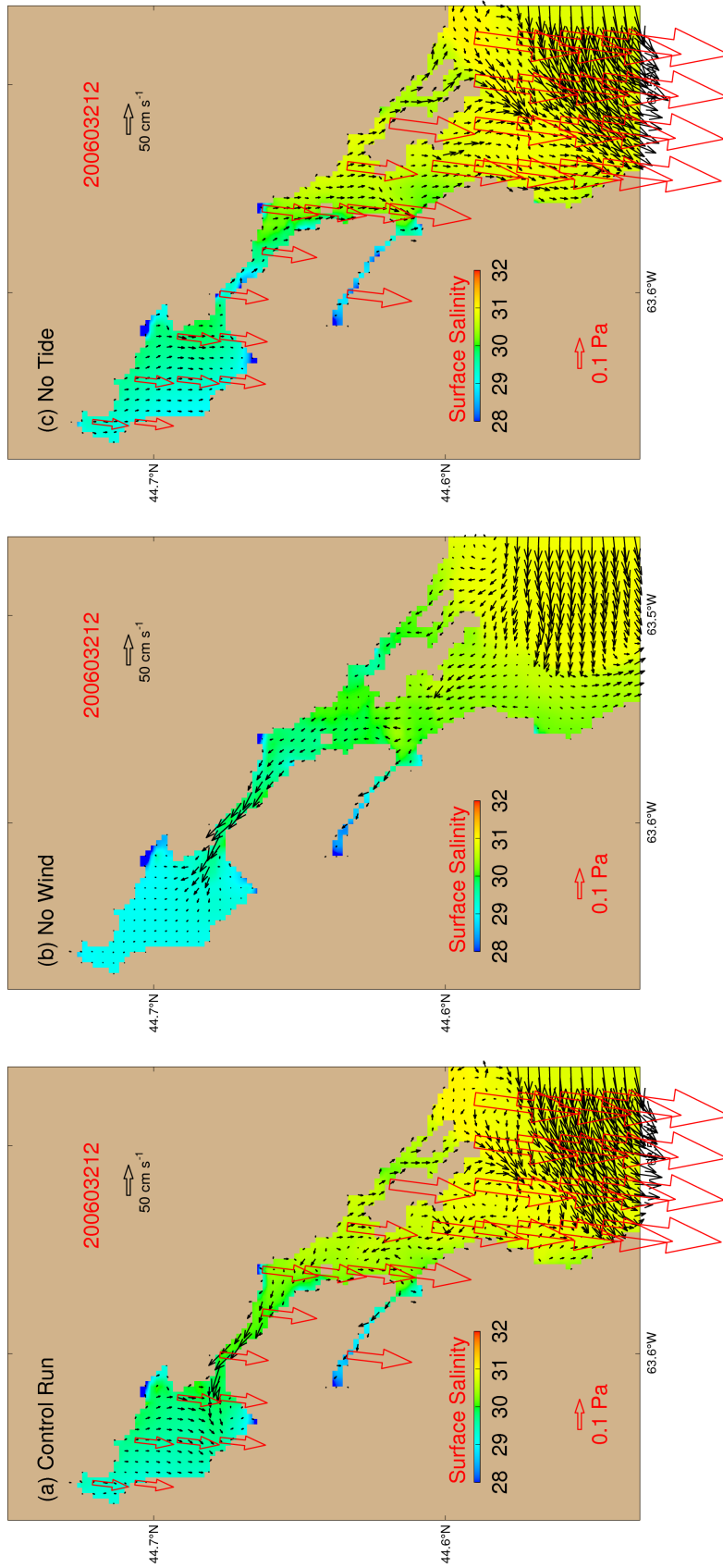
Figure 4.5: Near-surface (2 m) currents and salinities produced by submodel L5 to day 32.5 of 2006 (12:00 UTC February 1, 2006) for (a) the Case-CR, (b) Case-NoLocalWind and (c) Case-NoTide. Red open arrows are wind stress vectors.

4.2   Main Physical Processes Affecting Monthly Mean Circulation

Model results from the four experiments are now used to determine the mean physical processes affecting monthly mean circulation and hydrographic distributions and associated month-to-month variability in Halifax Harbour. The monthly mean currents and salinities at 2 and 10 m calculated for Case-NoLocalWind and Case-NoTide are shown in Figure 4.6 and Figure 4.7. One of major differences between monthly mean currents in the three experiments is the strength and direction of the time-mean current in the Narrows. The Narrows is a dynamically active area with an intense tidal jet even during storm events as discussed earlier. Monthly mean currents produced by the model in Case-CR (Figure 3.10) demonstrate that relatively strong landward (northwestward) flows occur at 10 m over the connection area between the Narrows and Bedford Basin. This kinds of flow pattern do not exist in Case-NoTide results. Additionally, the upwelling in the Narrows produced by Case-NoTide (Figure 4.9) is weaker than Case-CR upwelling (Figure 3.12), which suggests the important role of tides on the 3D mean circulation in the Narrows.

Monthly mean vertical temperature distributions between Case-NoTide (Figure 4.13) and Case-CR (Figure 3.14) are quite similar over the Outer Harbour and Bedford Basin. Over the connection area between the Narrows and Bedford Basin, the temperature in the upper layer produced by Case-NoTide is cooler than Case-CR model in February, May, August and November, indicating that tidal mixing plays a role in affecting the temperature distribution over this area. Salinity distributions for these two cases are also different in the Narrows. Without strong tidal currents and mixing in the Narrows, the low salinity waters in the upper layer are prevented from mixing with the high salinity waters in the lower layer over the connection area between the Narrows and Bedford Basin (compare Figures 3.15, 4.14). The large salinity gradient over the connection area between the Narrows and Bedford Basin generates a large flow which can be seen in the velocity transect (Figure 4.9), indicating again that tidal circulation and mixing are important factors in controlling the development of the salinity front and water renewal in Bedford Basin on a relatively longer time scale.
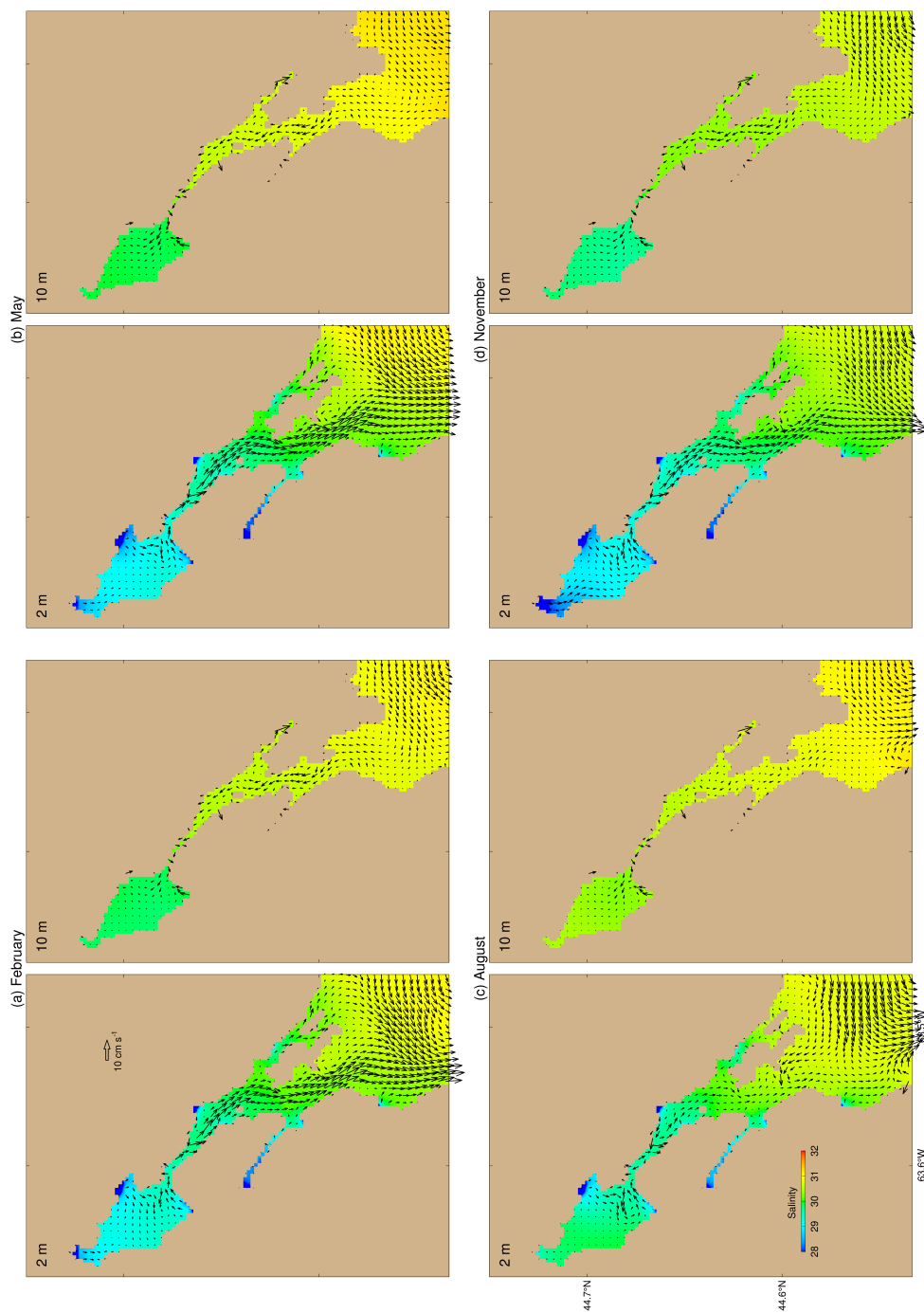
Figure 4.6: Monthly mean currents and salinities in Halifax Harbour at a depth of 2 and 10 m for (a) February, (b) May, (c) August and (d) November in 2006 calculated from submodel L5 for Case-NoLocalWind. For clarity, velocity vectors are plotted at every 2nd model grid point.
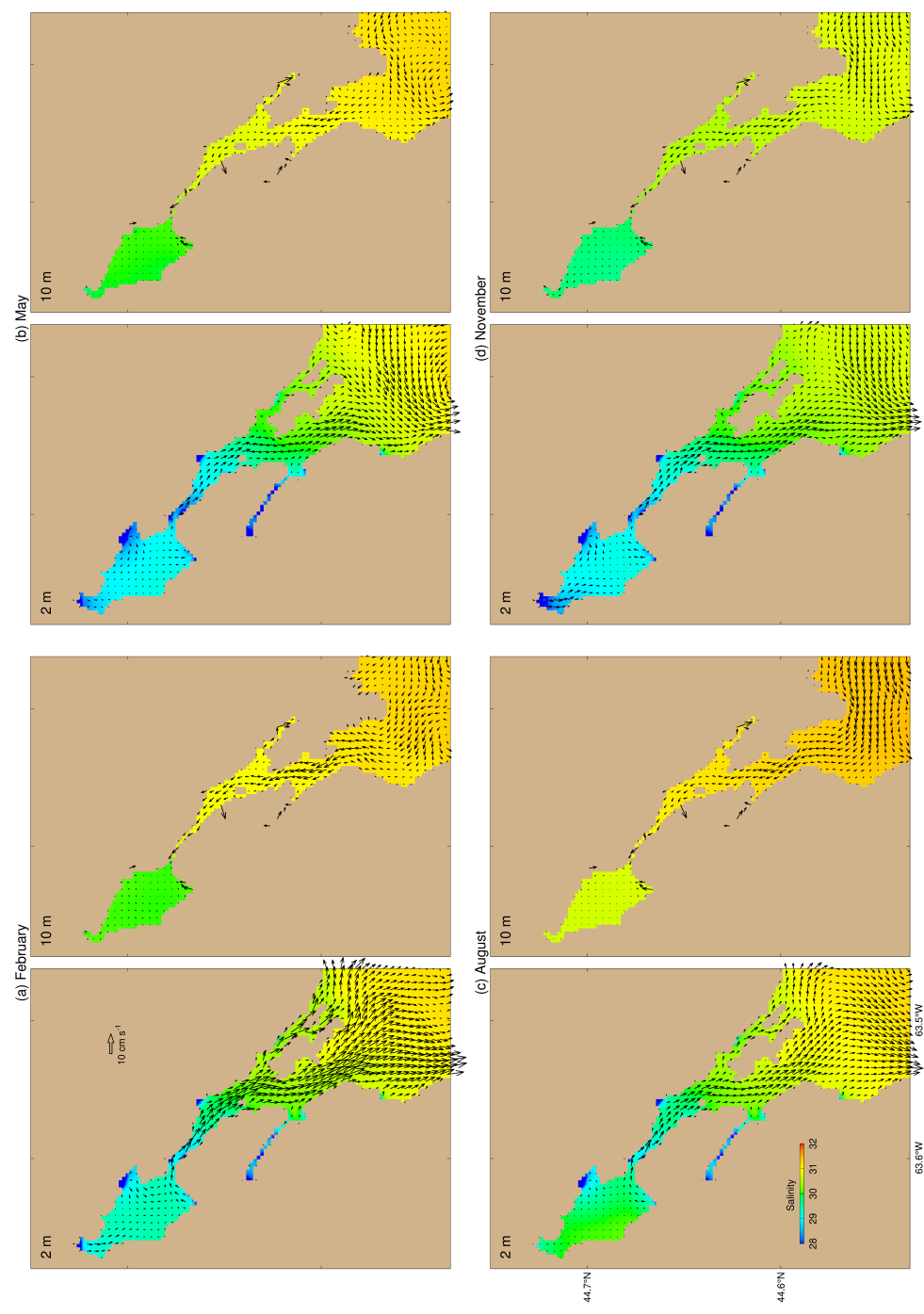
Figure 4.7: Same as Figure 4.6, except for Case-NoTide.
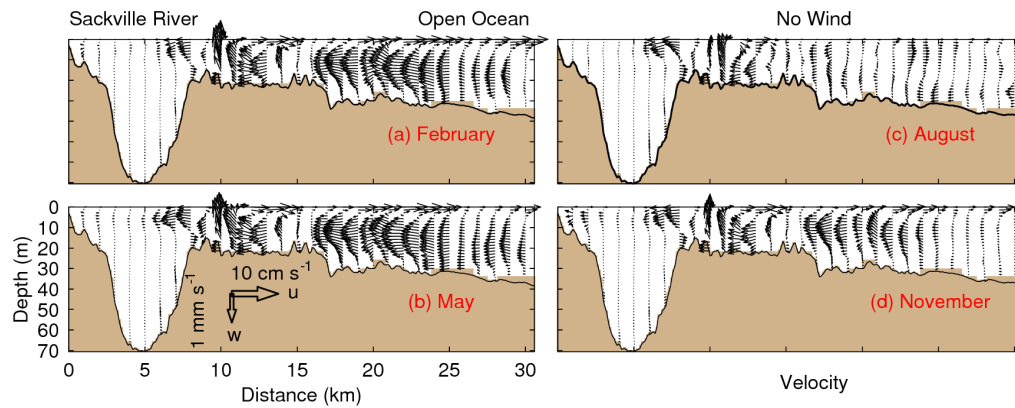
Figure 4.8: Vertical distributions of model-calculated monthly mean velocities for 2006 along a transect from the Sackville River to the open sea based on submodel L5 results for Case-NoLocalWind.

Figure 4.9: Same as Figure 4.8, except for Case-NoTide.
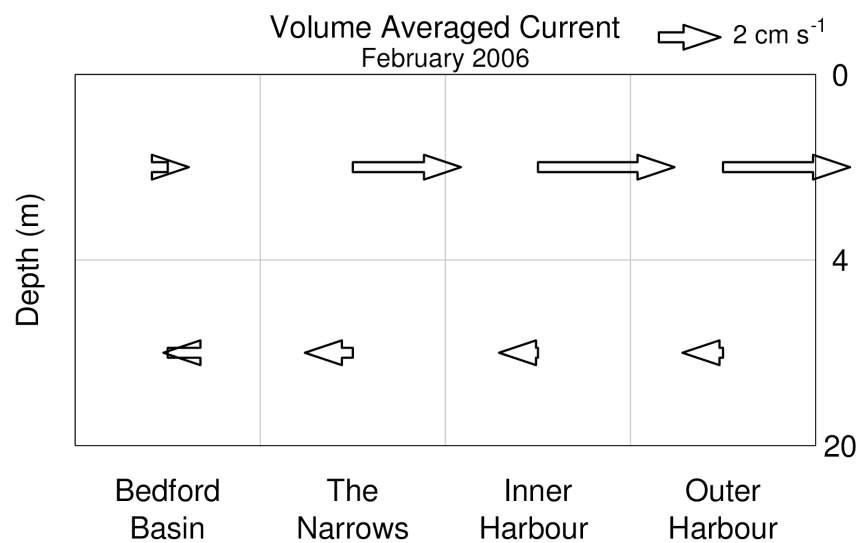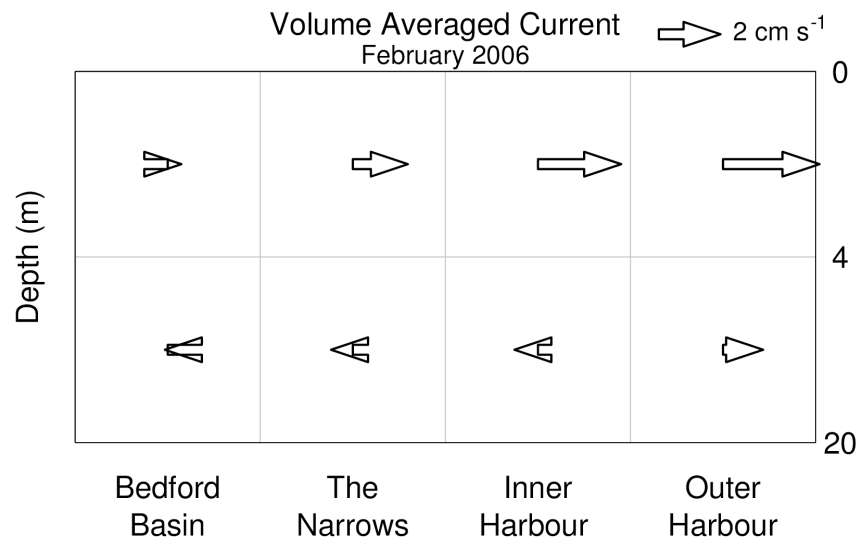
Figure 4.10: Volume averaged currents in Halifax Harbour for February, 2006 for Case-NoLocalWind (upper panel) and Case-NoTide (lower panel).

For the monthly mean circulation and hydrography, tides are important over the Narrows; the wind forcing plays an important role over the Outer Harbour. Comparison of monthly mean velocities on the transect from the Sackville River to the open ocean for Case-NoLocalWind and Case-CR (Figure 4.8 and 3.12) demonstrate that predominant westerly and northwesterly winds in winter enhance the two-layer estuarine circulation, leading to strong intrusion of offshore waters which are relatively warm and salty in winter. The volume averaged currents shown in Figure 4.10 calculated from monthly mean currents produced by Case-NoLocalWind and Case-NoTide clearly demonstrate that wind forcing could enhance the two-layer circulation in winter. The monthly mean salinities in Case-NoLocalWind (Figure 4.12) do not show a significantly increasing trend with time over the lower water column of the Outer Harbour in winter, particularly in February and March. The monthly mean temperatures in Case-NoLocalWind (Figure 4.11) are relatively cooler than Case-CR in the upper layer, especially over the Outer Harbour, which is explained by the relatively weaker intrusion of warm offshore waters to compensate for the local negative heat flux for the ocean and convection in winter in Case-NoLocalWind. In summer, the monthly mean near-surface temperatures and sub-surface salinities for Case-CR (Figure 3.14 and 3.15) over the Outer Harbour are relatively cooler and saltier than Case-NoLocalWind (Figure 4.11 and 4.12) due mainly to coastal upwelling. A detailed discussion of coastal upwelling is presented in Section 4.4. In spring and fall, the differences in monthly mean hydrography produced by Case-CR and Case-NoLocalWind are not as profound as those in winter and summer.
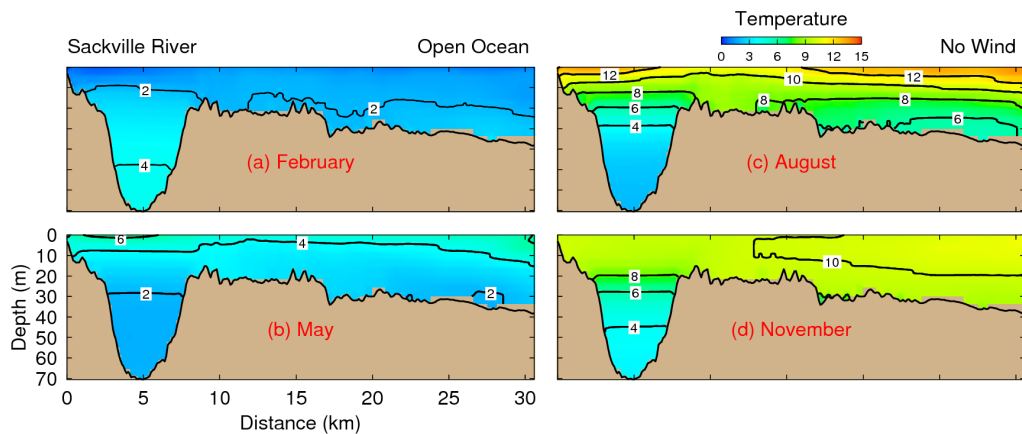
Figure 4.11: Vertical distributions of monthly mean temperatures for 2006 along a transect from the Sackville River to the open sea based on submodel L5 results for Case-NoLocalWind.
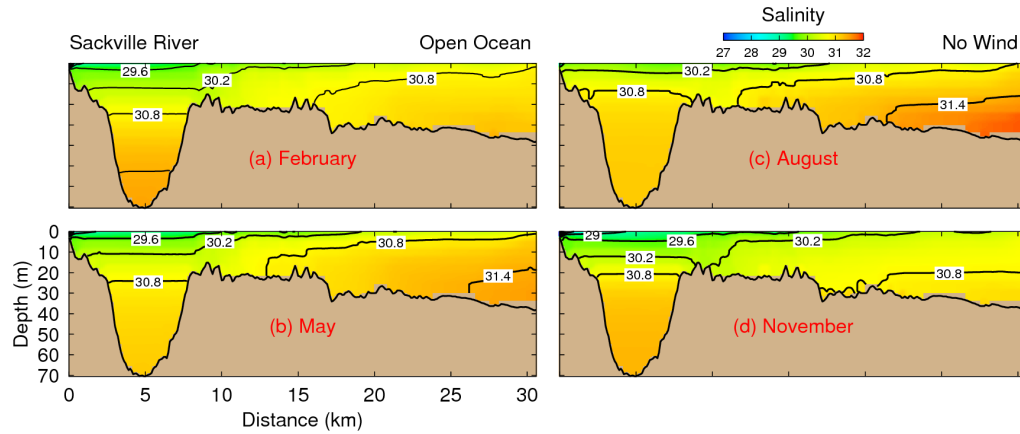
Figure 4.12: Vertical distributions of monthly mean salinities for 2006 along a transect from the Sackville River to the open sea based on submodel L5 results for Case-NoLocalWind.
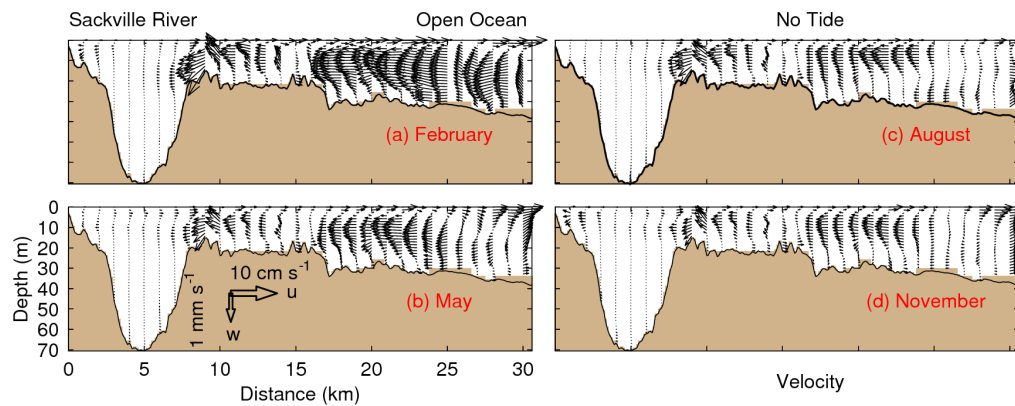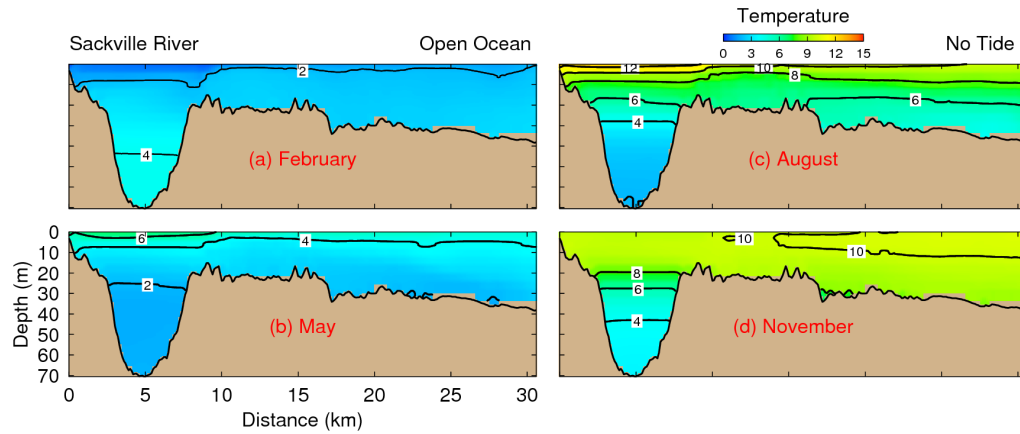

Figure 4.13: Same as Figure 4.11, except for Case-NoTide.

Although the annual mean discharge from the Sackville River is small, and only about 5 m³/s, it plays an important role in maintaining the salinity front in Bedford Basin. We examine the monthly mean model results for Case-NoDischarge. Figure 4.15 shows the salinity front is weaker in Bedford Basin for Case-NoDischarge than Case-CR (Figure 3.15). It should be noted that the seasonal variability of salinity in Case-NoDischarge is due mainly to the surface-salinity restoring to climatology, spectral nudging and the intrusion of offshore water.
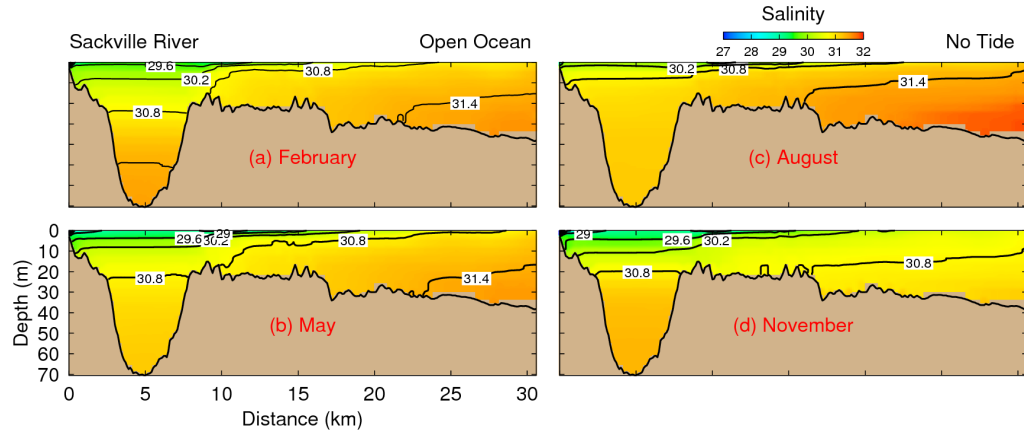
Figure 4.14: Same as Figure 4.12, except for Case-NoTide.
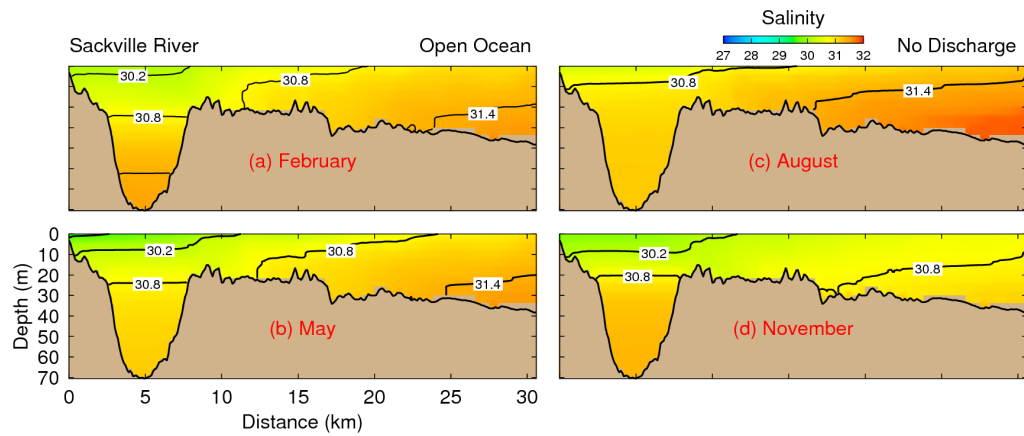
Figure 4.15: Same as Figure 4.12, except for Case-NoDischarge.

4.3   Density Driven Circulation

In order to quantify the density-driven circulation, we follow *Xing and Davies* (2001) and use submodel L5 to diagnose the density-driven currents associated with the monthly mean temperature and salinity in Case-CR. The model is run in diagnostic mode, in which the model hydrography are set to be the monthly mean hydrography produced by submodel L5 and invariant in time and other model external forcing is excluded. The density-driven circulation diagnosed from the model-calculated monthly mean temperature and salinity in Halifax Harbour is characterized by the two-layer estuarine circulation (Figure 4.16) and is highly comparable to the monthly mean circulation shown in Figure 3.10, indicating the importance of the baroclinic dynamics in affecting the monthly mean circulation in the region.

The role of the model external forcing in contributing to the monthly mean circulation can be examined by comparing the monthly mean model results for Case-CR shown in Figure 3.10 and the density-driven circulations shown in Figure 4.16. The relatively strong two-layer estuarine circulation in winter is due mainly to the westerly or northwesterly wind. The landward (northwestward) flows at 2 and 10 m over the connection area between the Narrows and Bedford Basin are due mainly to tides. The above circulation patterns do not occur in the density-driven circulation results. Furthermore the westward flows along the eastern open boundary of submodel L5 shown in monthly mean circulation (Figure 3.10), particularly at 10 m depth, do not occur in the density-driven circulation results, which indicates baroclinic currents over the Scotian Shelf also play a role in affecting the monthly mean circulation in Halifax Harbour.
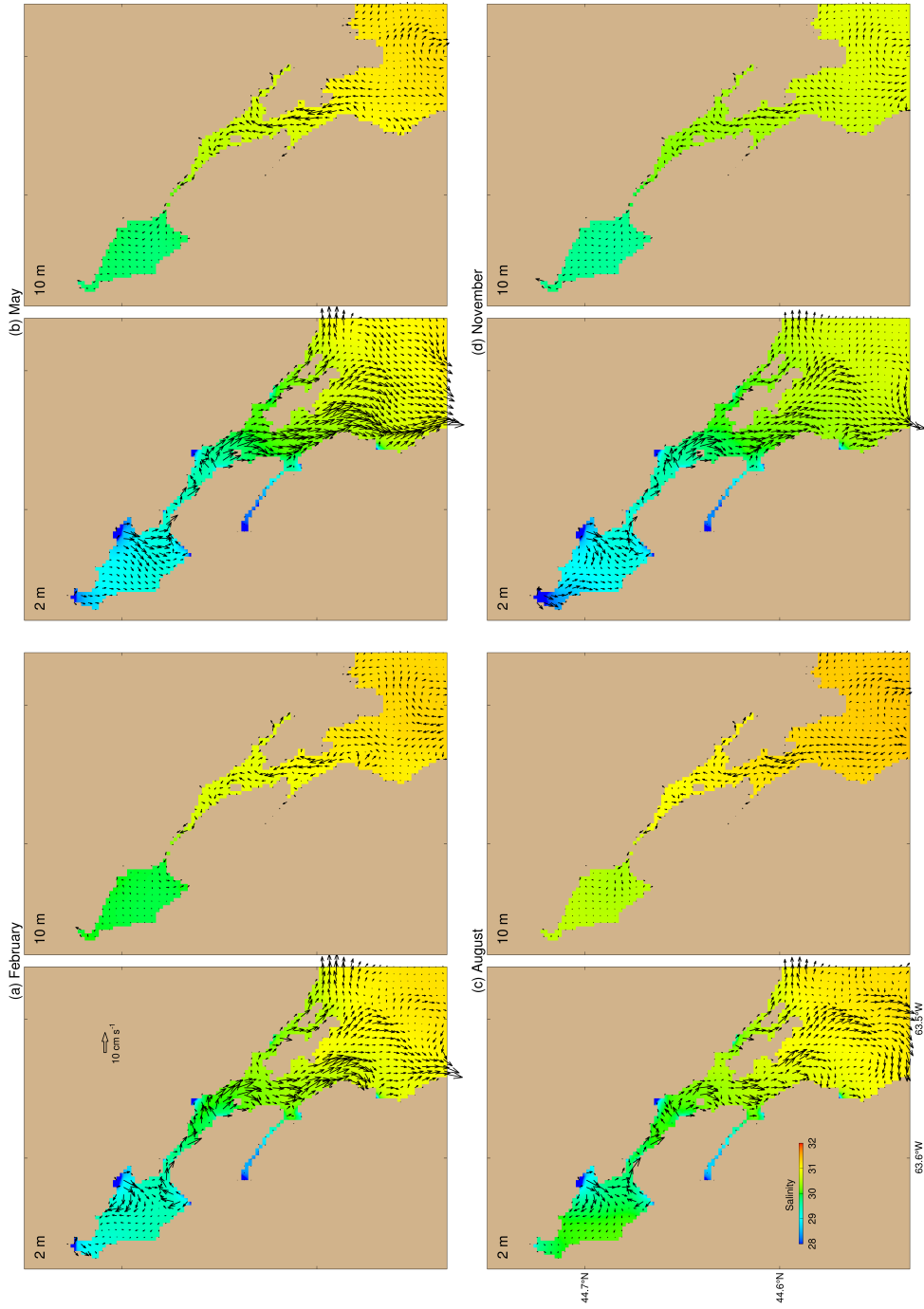
Figure 4.16: Monthly mean density-driven currents and salinities for (a) February, (b) May, (c) August, and (d) November 2006 at near-surface (2 m) and sub-surface (10 m) submodel L5, Case-CR. Velocity vectors are plotted at every 2nd model grid. The density-driven circulation model generating this plot is the same as submodel L5, which was initialized by temperature and salinity fields, and integrated diagnostically with no external forcing.

4.4 Coastal Upwelling

Coastal upwelling is a nearshore phenomenon in which denser subsurface waters are brought up to replace surface waters. Coastal upwelling on the Scotian Shelf has been studied by *Petrie et al.* (1987) and *Donohue* (2001). Temperature and salinity climatology of Halifax Section shows that coastal upwelling is the mean state over the Scotian Shelf through most of year (*Drinkwater and Taylor*, 1982). It is an important process which can influence hydrographic properties in Halifax Harbour. Wind forcing plays an important role in inducing coastal upwelling. Satellite images (Figure 2.8) show a strong month-long upwelling event in the summer of 1984. A band of cool water developed along the southshore of Nova Scotia; the water temperature south of Sambro (see Figure 2.8c,d in particular; see Figure 3.7 for location), had a relatively low value. This suggests outside Halifax Harbour is a favored place for upwelling in summer.

Time series of near-surface temperature and salinity at station B2 in the Outer Harbour produced by submodel L5 for Case-CR demonstrate that several coastal upwelling events occur from April to October in 2006 (Figure 4.17). There is a strong negative correlation between temperature and salinity variability during upwelling periods at station B2. However, time series of temperature at station G2 in Bedford Basin show small fluctuations in comparison with time series at station B2 in the Outer Harbour during the summer of 2006. The fluctuations of salinity in Bedford Basin are mainly due to the movement of the low salinity front in the upper Bedford Basin in response to tides and wind forcing. The effect of wind forcing in coastal upwelling can be shown based on a comparison of time series of near-surface temperature and salinity at station B2 in the Outer Harbour and G2 in Bedford Basin for Case-CR and Case-NoLocalWind. From April to October in 2006, Case-NoLocalWind results at station B2 in the Outer Harbour shown in Figure 4.17 have smaller fluctuations of temperature and salinity in comparison with Case-CR model results. At station G2 in Bedford Basin, the near-surface temperature and salinity in Case-CR and Case-NoLocalWind are very similar except that the time series of near-surface salinity in Case-NoLocalWind are relatively smooth in comparison with the results in Case-CR.

In comparison with Case-CR (Figure 3.16), the time-depth distributions (Figure 4.18) of model-calculated temperatures at B2 in the Outer Harbour for Case-NoLocalWind do not have significant alternations between warm and cold for the whole water column from April to October in 2006. For salinity of the whole water column at B2, the value in

Case-NoLocalWind is relatively low in comparison with Case-CR.

In summary, temperature and salinity variability in the Outer Harbour are significantly affected by wind forcing, especially from April to October. In Bedford Basin, high frequency fluctuations of salinity are mainly due to wind forcing, but low frequency variability is directly influenced by the movement of the low salinity front due to tides and wind forcing.
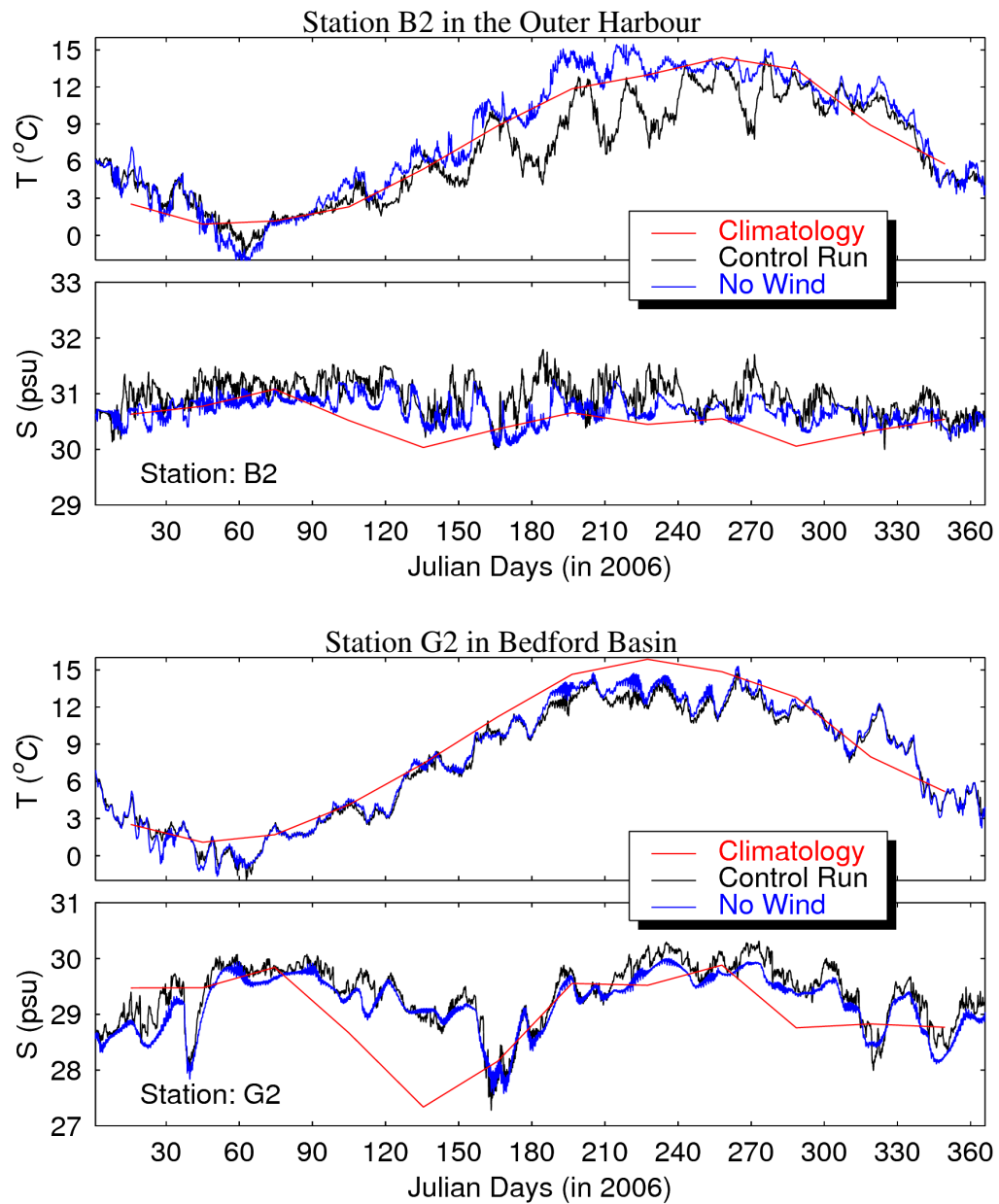
Figure 4.17: Time series of near-surface (2 m) temperature and salinity at station G2 in Bedford Basin and B2 in the Outer Harbour for 2006 produced by submodel L5 for Case-CR (black) and in Case-NoLocalWind (blue). The red curves represent monthly mean climatology. See Figure 2.3 for station locations.
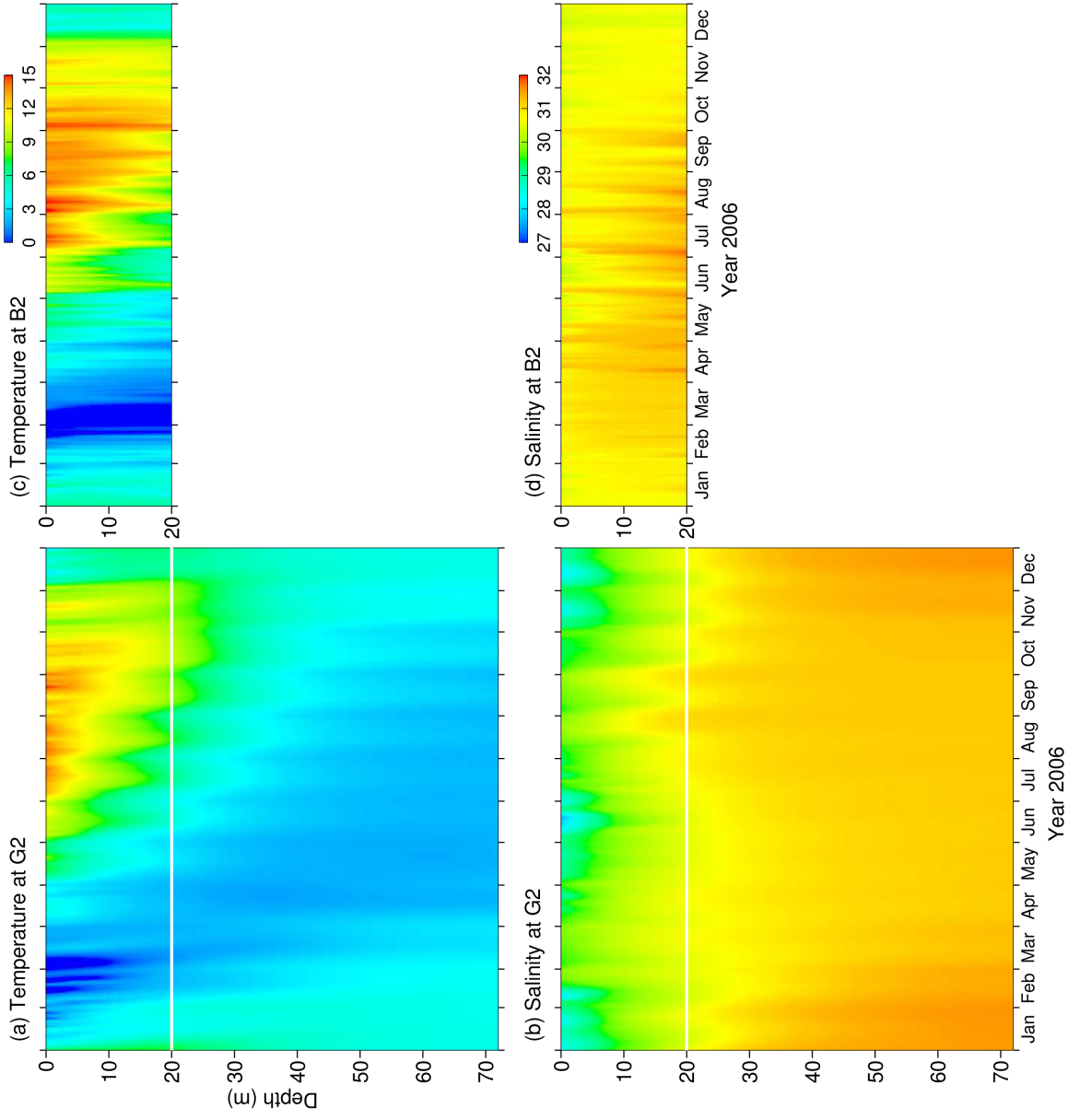
Figure 4.18: Time-depth distributions of model-calculated temperature and salinity at (a, b) station G2 in Bedford Basin and (c, d) B2 in the Outer Harbour in 2006 based on submodel L5 for Case-NoLocalWind. Locations of these two stations are marked in Figure 2.3.

CHAPTER 5

ESTIMATION OF FLUSHING TIME, DISPERSION AND RETENTION IN HALIFAX HARBOUR

Pollution control and sustainable development of Halifax Harbour require reliable information about how material is transported and dispersed within the Harbour and how the Harbour is flushed through water exchange with the open ocean. From the biological and chemical point of view, flushing time, dispersion and retention are important factors in determining levels of contamination and concentrations of nutrients in Halifax Harbour (*Platt et al.*, 1972). The time-dependent, 3D currents produced by the NCOPS-HFX are used to quantify flushing time, dispersion and retention in the Harbour. Both passive tracers and passive particles, which are carried by model-calculated currents, are used in this chapter. Passive tracer experiments correspond to the Eulerian approach, while passive particle tracking experiments correspond to the Lagrangian approach. In the passive tracer experiments, concentrations are calculated in the model using the tracer equation in the same manner as for model temperature and salinity fields. In the particle tracking experiments, the trajectories are tracked from the modelled velocity fields. Normally, tracer experiments are online calculations and particle tracking experiments are offline calculations.

5.1 Passive Tracers

The governing equation and model calculations for concentrations of passive tracers are the same as those for temperature and salinity (active tracers), except that concentrations of passive tracers do not affect the model density and flow fields and therefore have no effect on the flow dynamics. It should be noted that the CANDIE model uses fourth-order numerics and a flux limiter to discretize the nonlinear advection terms, which are very useful in simulating (passive and active) tracer concentrations (*Sheng et al.*, 1998).

Five different passive tracers are initialized over five different subareas of Halifax Harbour: (1) the entire Bedford Basin (tracer 1), (2) the upper layer of 20 m in Bedford Basin (tracer 2), (3) the Narrows (tracer 3), (4) the Inner Harbour (tracer 4) and (5) the Outer Harbour (tracer 5). The initial concentration of each tracer is set to one within the specific subarea and zero outside the given subarea. Figure 5.1a shows the initial distribution of concentrations for tracer 1 along the transect from the head of Sackville River to the open sea. In order to examine seasonal variations of tracer concentrations and flushing time over the specific subareas defined above, concentrations of the five tracers are reinitialized respectively on the first day in January, April, July and October in 2006 and evolved using the nested-grid modelling system.

Figures 5.1 and 5.2 present concentration distributions of tracer 1 and tracer 2 along the transect at days 0, 10, 20 and 30 after their release on January 1, 2006 in the entire and upper Bedford Basin, respectively. Figure 5.1b and c show a very thin layer near the sea surface with relative high concentrations of tracer 1 spreading seaward in the Narrows. In Bedford Basin, a sub-surface layer around a depth of 5 m with relatively low concentrations of tracer 1 forms from the Narrows to the head of Bedford Basin (Figure 5.1b and c). After 30 days, the concentrations of tracer 1 in the lower layer of Bedford Basin (Figure 5.1d) remain nearly unity. The tracer dispersion in the upper Bedford Basin is relatively fast and affected by the tidal currents and wind-induced mixing; the tracer dispersion in the lower layer of Bedford Basin is relatively slow and affected mainly by diffusion. In comparison with the evolution of concentrations of tracer 1, Figure 5.2 demonstrates concentrations of tracer 2 is dispersed to the open sea via the Narrows and also diffused to the lower layer of Bedford Basin. After 30 days, the concentrations of tracer 2 are reduced from unity to about 0.3 in the upper Bedford Basin (Figure 5.2d).

The flushing time is one of important parameters in understanding and predicting

the water quality level in coastal waters. We follow *Sheng et al.* (2009) and define the local flushing time is the e-folding time for the temporal decay of the volume averaged concentration (VAC) of each passive tracer. The VAC is defined as the volume integrated concentration of passive tracer concentrations over a specific subarea normalized by the total volume of the subarea. Figure 5.3a shows time series of the VACs during the 90 days period for tracer 1 over the entire Bedford Basin. The VACs of tracer 1 decrease exponentially with time due to the transport and dispersion of the passive tracer from Bedford Basin to the other areas. The four curves in Figure 5.3a represent four different seasons in 2006. The VACs of tracer 1 decay faster in winter than in other three seasons due mainly to the strong westerly or northwesterly winds in winter which enhance the two-layer estuarine circulation and mixing in the upper water column. Figure 5.3a also shows the high frequency variability of the VACs, with a typical period of about 12 hours, which is due mainly to the tracer patch flowing in and out of Bedford Basin due to the tides. The time series of VACs can be approximated by

$$C = C_o e^{-\frac{t}{T_e}} \tag{5.1}$$

where C is the VAC at time t, C_o is the initial value of the VAC and equal to 1, and T_e is the e-folding time. Based on the time series of VAC for the four seasons shown in Figure 5.3a, the estimated e-folding flushing time for the entire Bedford Basin is about 90.6 days.

The time series of VACs for tracer 2 (the initial concentration of the tracer is set to 1 in the upper 20 m of Bedford Basin) show a relatively faster decay (Figure 5.3b) in comparison to tracer 1. The estimated e-folding time of the upper Bedford Basin is about 39.2 days, which is shorter than the e-folding time to flush the whole basin. Figures 5.3c-e show the temporal decay of VACs in the Narrows, Inner and Outer Harbour, with estimated e-folding flushing times of about 1.1, 4.5 and 1.9 days, respectively. The estimated e-folding time for the Narrows is the shortest among the five subareas due to strong dispersion and advection of tracer concentrations associated with the intense, mainly tidal currents in the area.

The entire Bedford Basin: tracer 1
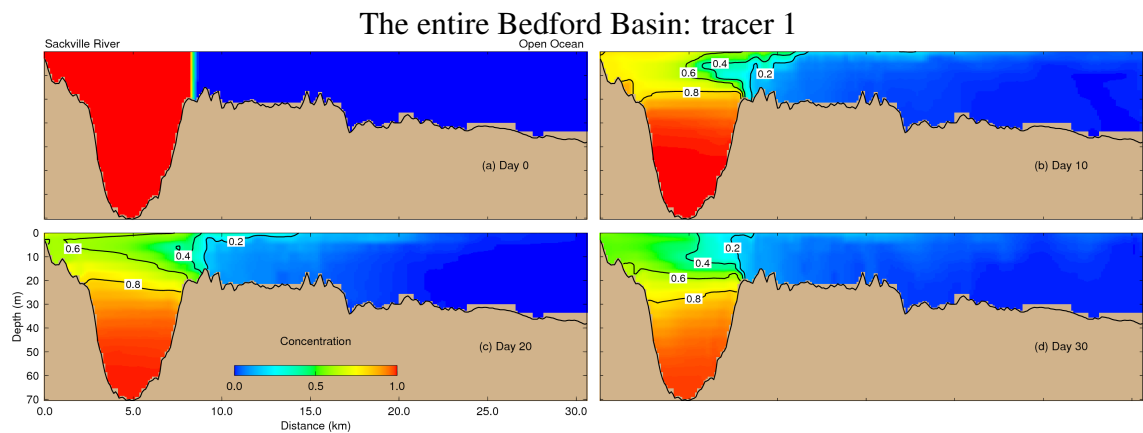
Figure 5.1: Transect view of passive tracer concentrations in Bedford Basin on (a) January 1, (b) January 11, (c) January 21 and (d) January 31, 2006. The tracer concentration is set to unity in the entire Bedford Basin on January 1, 2006. The model simulation is based on the Case-CR setup.

The upper layer of 20 m in Bedford Basin: tracer 2
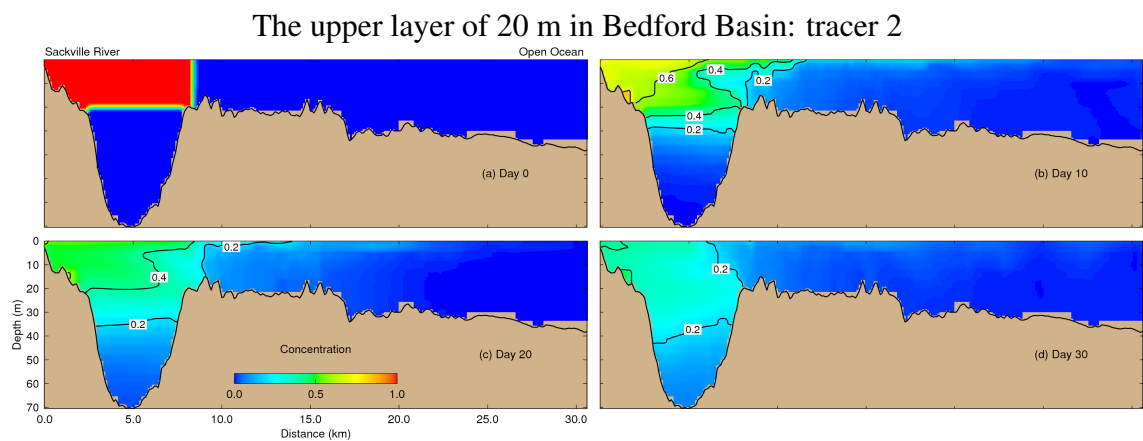
Figure 5.2: Same as Figure 5.1, except for tracer concentration is set to unity in the upper Bedford Basin.
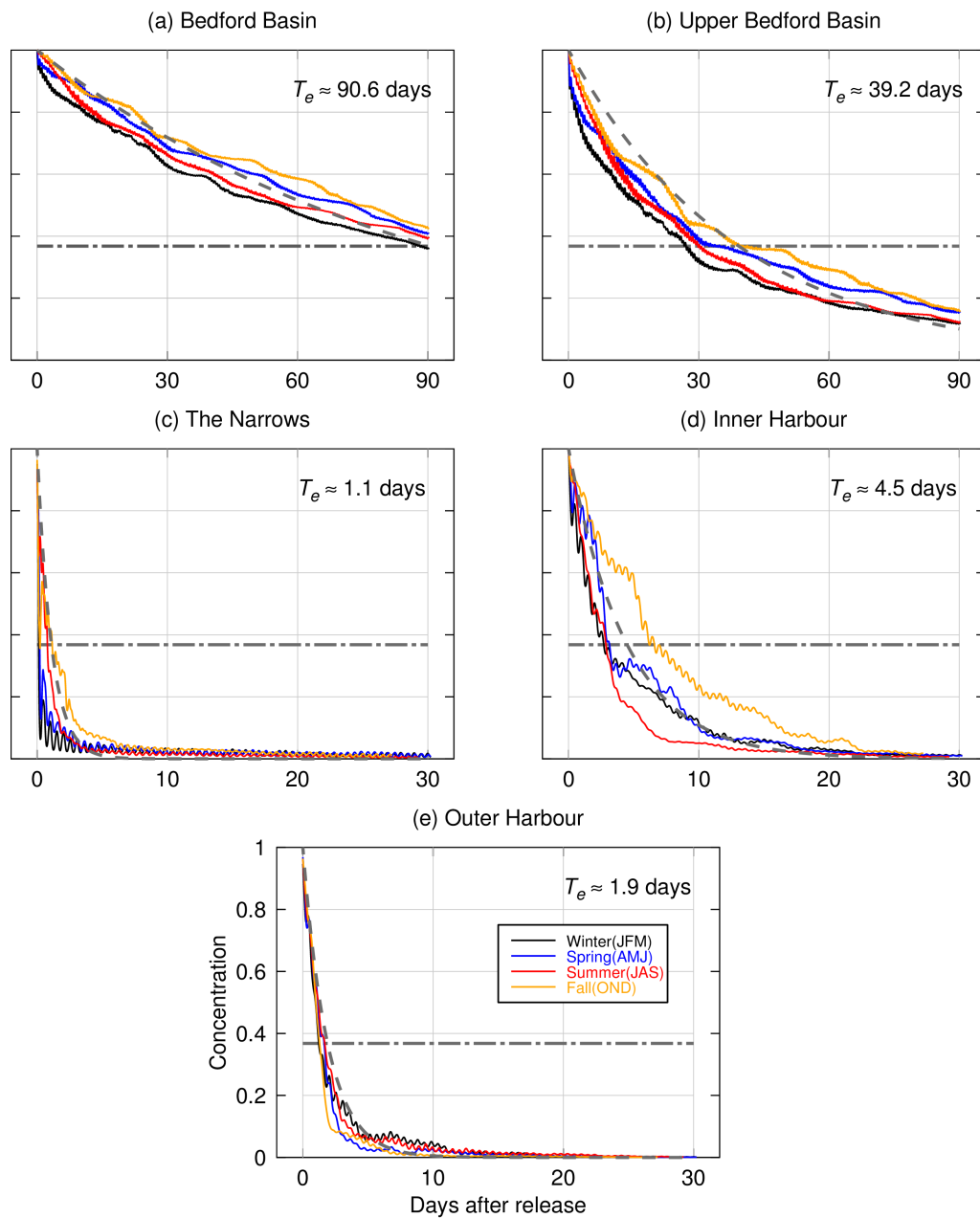
Figure 5.3: Time series of volume averaged concentrations (VACs) of passive tracer released in five different subareas of Halifax Harbour for the four seasons in 2006. The dashed line is the fit of $C = C_o e^{-\frac{t}{T_e}}$ to the seasonal model concentration.

In the next tracer experiment, the tracer concentrations are set to unity near sewage outfalls at each model time step; the initial concentration is zero everywhere in Halifax Harbour on January 1, 2006. The 3D distributions of tracer concentrations in this experiment can be used to identify which places in the Harbour will likely accumulate discharged material. Figure 5.4 shows the distributions of near-surface tracer concentrations in Halifax Harbour at the end of day 10, 100, 200 and 365 in 2006. The concentrations are characterized by relative higher tracer concentrations in the Northwest Arm, Bedford Basin and local areas near the sewage outfalls. At the end of year 2006, the tracer concentrations are about 0.45, > 0.5, 0.2, and < 0.15 in Bedford Basin, the Northwest Arm, Narrows and Inner Harbour, and Outer Harbour, respectively.

Figure 5.4: Tracer concentrations at the top z-level (centred at 2 m) at the end of days 10, 100, 200 and 365 in 2006 which tracer concentrations at water discharge outfalls are set to unity at each time step. The discharge locations are indicated by scaled arrows.

5.2 Particle Tracking

The movements of particles carried passively by the model currents are calculated using:

$$\overrightarrow{x}(t) = \overrightarrow{x}(t_0) + \int_{t_0}^{t} \overrightarrow{u}(\overrightarrow{x}, t)dt + \overrightarrow{\delta} \tag{5.2}$$

where $\overrightarrow{x}(t)$ and $\overrightarrow{x}(t_0)$ are position vectors of a passive particle at time t and initial time t_0, 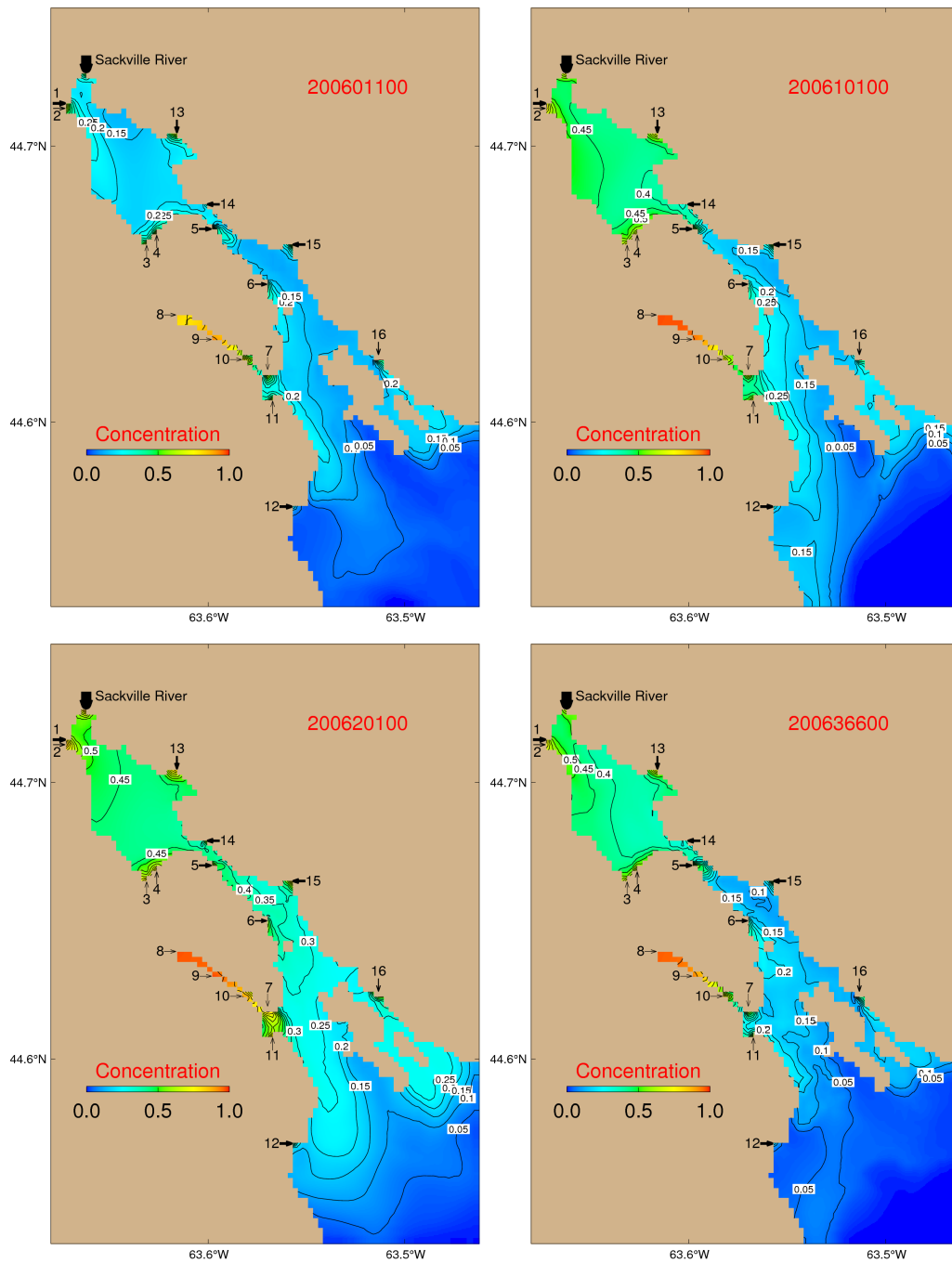respectively. Here $\overrightarrow{u}(\overrightarrow{x}, t)$ is the 3D velocity vector of model currents, and $\overrightarrow{\delta}$ is random walk to account for particle movements associated with turbulence in the ocean which is not captured by the model. We follow *Taylor* (1922) and express $\overrightarrow{\delta}(\delta x, \delta y, \delta z)$ as

$$\delta x = \xi_x \sqrt{2K_x \Delta t}, \qquad \delta y = \xi_y \sqrt{2K_y \Delta t}, \qquad \delta z = \xi_z \sqrt{2K_z \Delta t} \tag{5.3}$$

where ξ_x, ξ_y and ξ_z are uncorrelated Gaussian random variables, and K_x, K_y and K_z are additional eddy diffusivities in the x, y and z directions, and Δt (30 min) is the time step used in the integration of Equation 5.2. In this study, the horizontal diffusivity is homogeneous and isotropic ($K_x = K_y = 1.25$ m^2/s), and the vertical diffusivity is 10^4 smaller than the horizontal diffusivity ($K_z = 1.25 \times 10^{-4}$ m^2/s). The fourth-order Runge-Kutta scheme (*Press et al.*, 1993) is used to track trajectories of passive particles.

We first conduct a particle tracking experiment (TRACK-mean) using the 3D annual mean (time-independent) flow field in 2006 calculated from model results produced by submodel L5. The passive particles are released in the top z-level (centred at 2 m) (Figure 5.5) and tracked for five days. The initial separation distance between adjacent particles is 200 m. Figures 5.6–5.10 present spatial distributions of passive particles during five days of tracking. Most particles released in the near-surface of Bedford Basin and the Northwest Arm are retained within these areas with gradual seaward spreading due mainly to weak near-surface currents over these areas (Figure 5.10a). In the Narrows, Inner and Outer Harbour, only a small percentage particles remain in the near-surface layer with most of particles scattering along the deep channel of the harbour, suggesting most of particles in the near-surface layer move seaward (southeastward) and exit from the open boundary of submodel L5. A large number of particles are transported from the near-surface layer to the sub-surface layer (Figure 5.10b) indicating the model-calculated vertical velocity component plays an important role in diffusing passive particles in the

Harbour. In the sub-surface layer, the particles drift landward (northwestward) associated with the landward currents.

To understand the effects of tides, wind, freshwater discharge on the movements of passive particles in Halifax Harbour, we also conduct particle tracking experiments (TRACK-storm) on two stormy days: yearday 32 and yearday 49 of 2006 (see Figure 3.2). The initial positions of passive particles are the same as in experiment TRACK-mean (Figure 5.5). Particles are released in the top z-level at the beginning of each day and carried passively by time-dependent 3D currents produced by submodel L5 of the nested-grid modelling system. The major difference in wind forcing between these two days is that the wind direction in Halifax Harbour (Figure 3.2) changes anti-clockwise on day 32, and clockwise on day 49. This is because the storm track is on the eastern side of Halifax Harbour on day 32, and on the western side on day 49. It is also worth noting that tides in the Harbour are in the flood phase at the beginning of day 32, and in the ebb phase at the beginning of day 49. Figures 5.11–5.14 present spatial distributions of particles in Halifax Harbour during days 32 and 49 in 2006. For particles released at day 32, a large number of near-surface particles gather along the western side of Halifax Harbour from the Sackville River to the open sea (Figure 5.14a) due mainly to the strong storm-induced near-surface currents. Some of particles are carried from the near-surface layer to the sub-surface layer with most particles gathering along the coastlines in Halifax Harbour (Figure 5.14b). For particles released at day 49, most of particles in the near-surface drift seaward (Figure 5.14c). The near-surface particles in Bedford Basin converge along the southeastern part of the Basin and move into the Narrows. A large number of near-surface particles drift along McNabs Island and exit from the open boundary of submodel L5 (Figure 5.14c), due mainly to the storm-induced near-surface currents. Figure 5.14d shows that some particles are also transported from the near-surface layer to the sub-surface layer on day 49. The major factors affecting the trajectories of particles are flood or ebb tide and the local wind forcing in Halifax Harbour during storm events. Particle tracking results are sensitive to the release time.
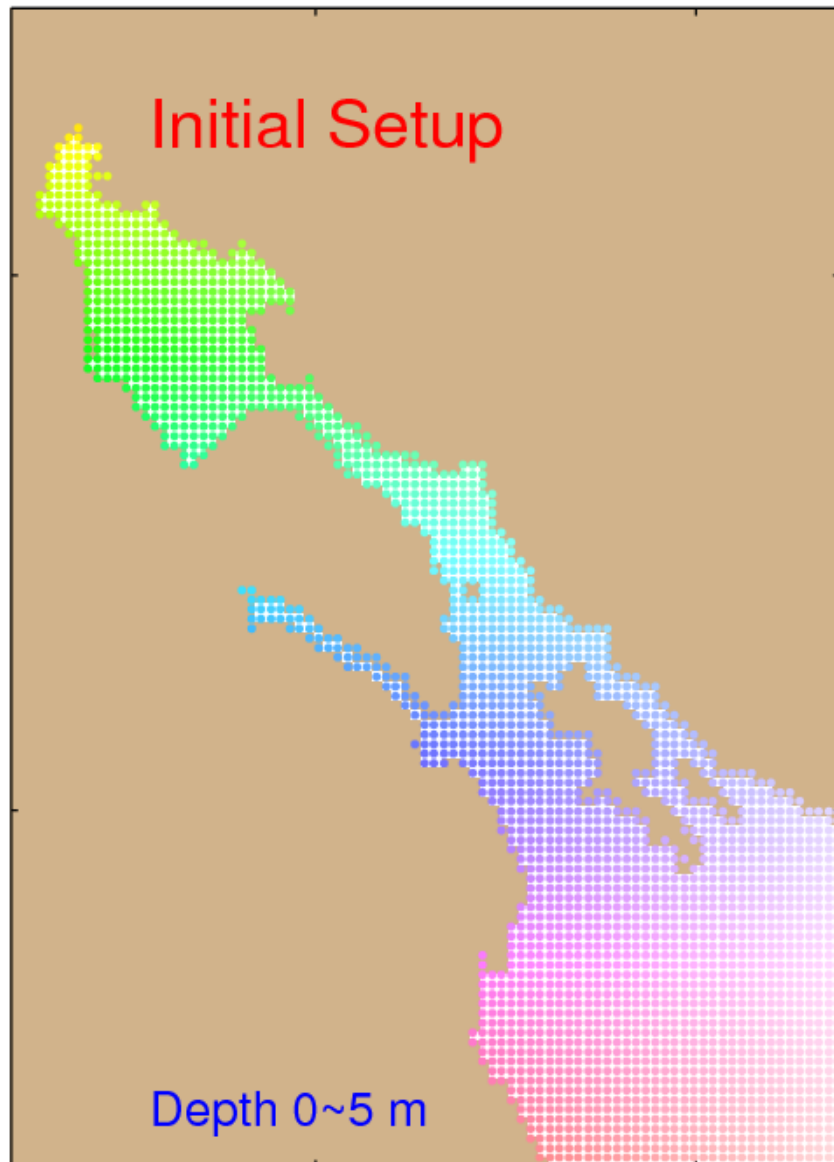
Figure 5.5: Initial positions of particles released in the top z-level (centred at 2 m) in Halifax Harbour. The initial separation distance between adjacent particles is 200 m.
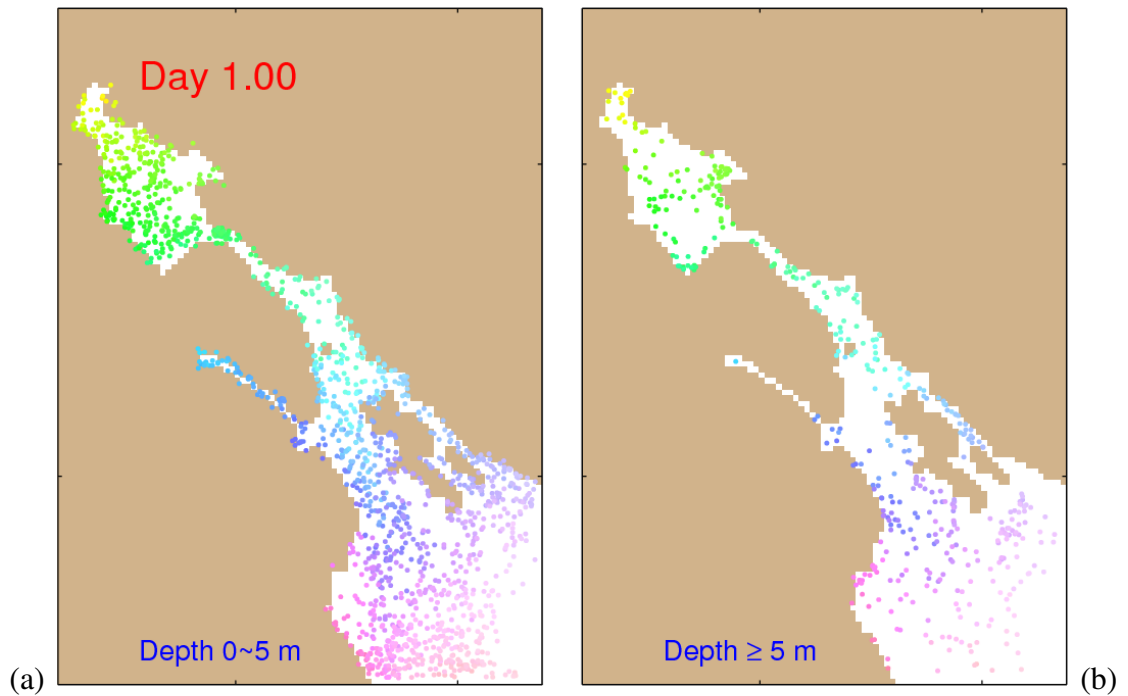
Figure 5.6: Distribution of particles in (a) the near-surface layer ($0 \sim 5$ m) and (b) the sub-surface layer (≥ 5 m) one day after their initial release in the near-surface layer. The time-independent 3D annual mean currents produced by submodel L5 are used.
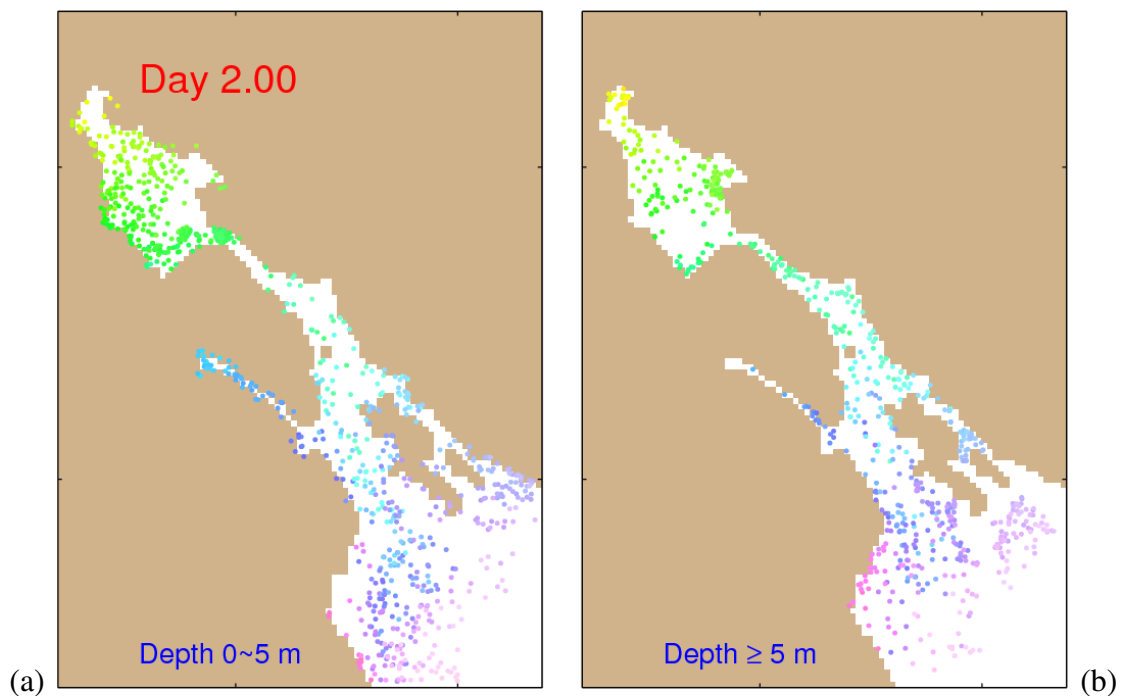
Figure 5.7: Same as Figure 5.6, except for two days after the initial release.

Day 3.00

Depth 0~5 m

Depth ≥ 5 m

(a)

(b)
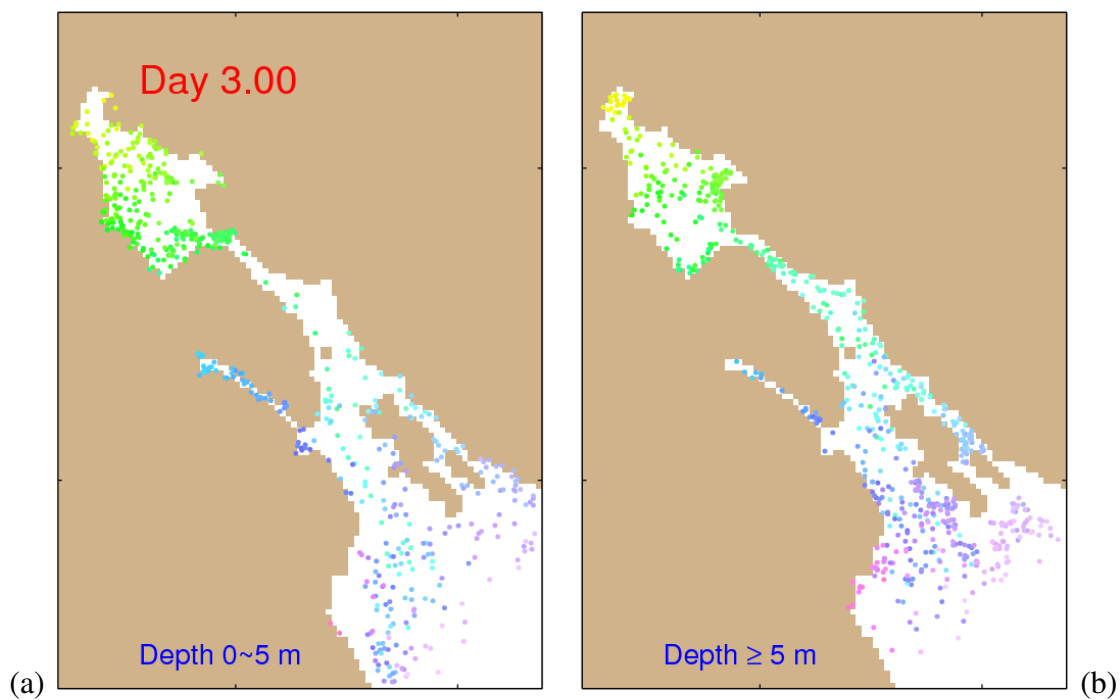
Figure 5.8: Same as Figure 5.6, except for three days after the initial release.

Day 4.00

Depth 0~5 m

Depth ≥ 5 m

(a)

(b)
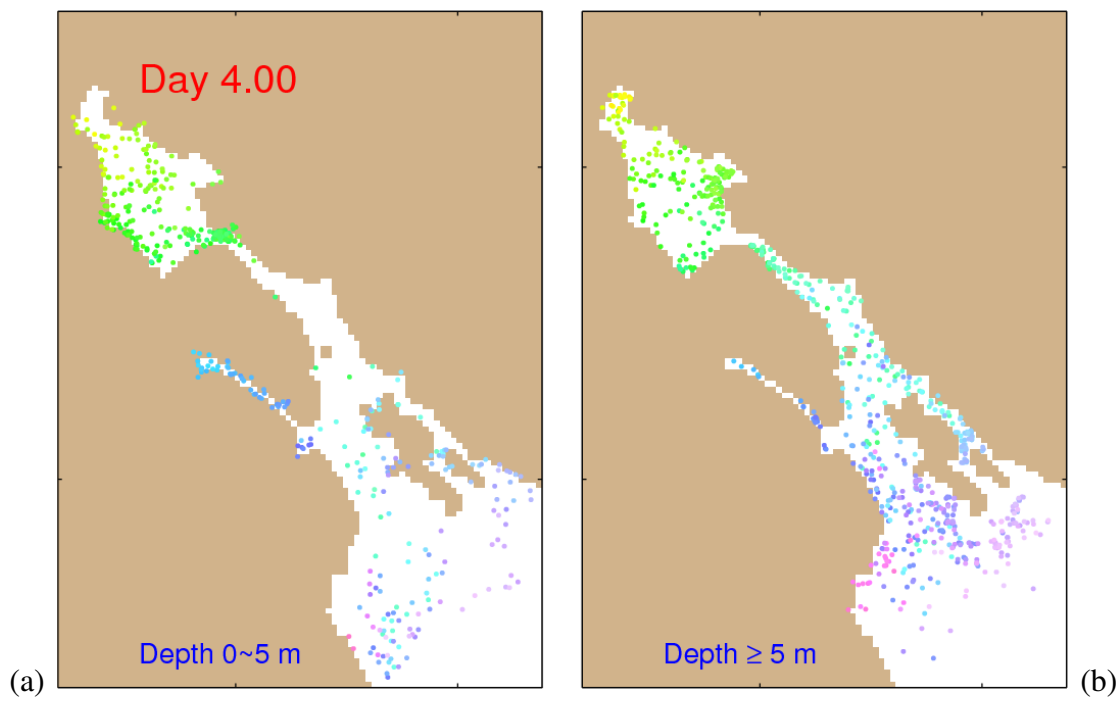
Figure 5.9: Same as Figure 5.6, except for four days after the initial release.
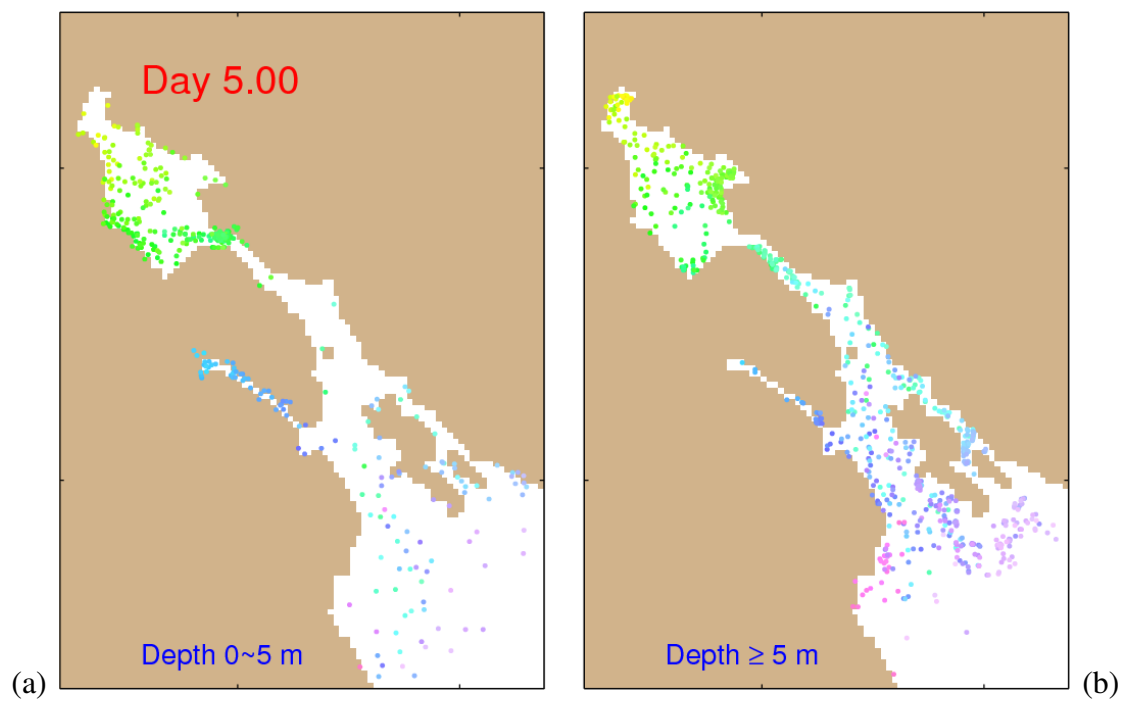
Figure 5.10: Same as Figure 5.6, except for five days after the initial release.

Figure 5.11: Distribution of particles in (a,c) the near-surface layer ($0 \sim 5$ m) and (b,d) the sub-surface layer (≥ 5 m) 1.5 hours after their initial release in the near-surface layer during two storm events (yeardays 32 and 49) in 2006. The time-dependent 3D currents produced by submodel L5 are used.

Figure 5.12: Same as Figure 5.11, except for 3.5 hours after the initial release.

Figure 5.13: Same as Figure 5.11, except for 5.5 hours after the initial release.
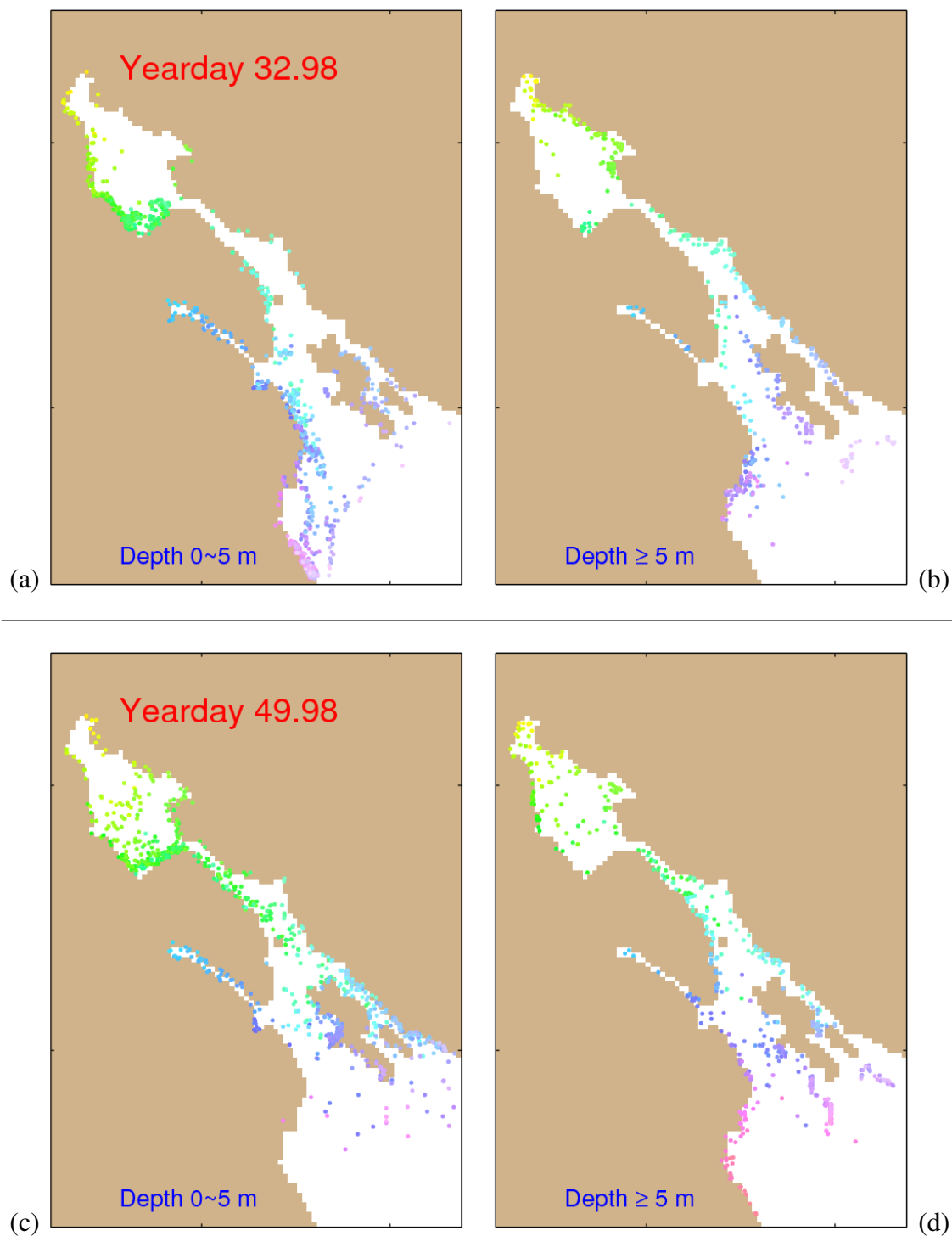
Figure 5.14: Same as Figure 5.11, except for 23.5 hours after the initial release.
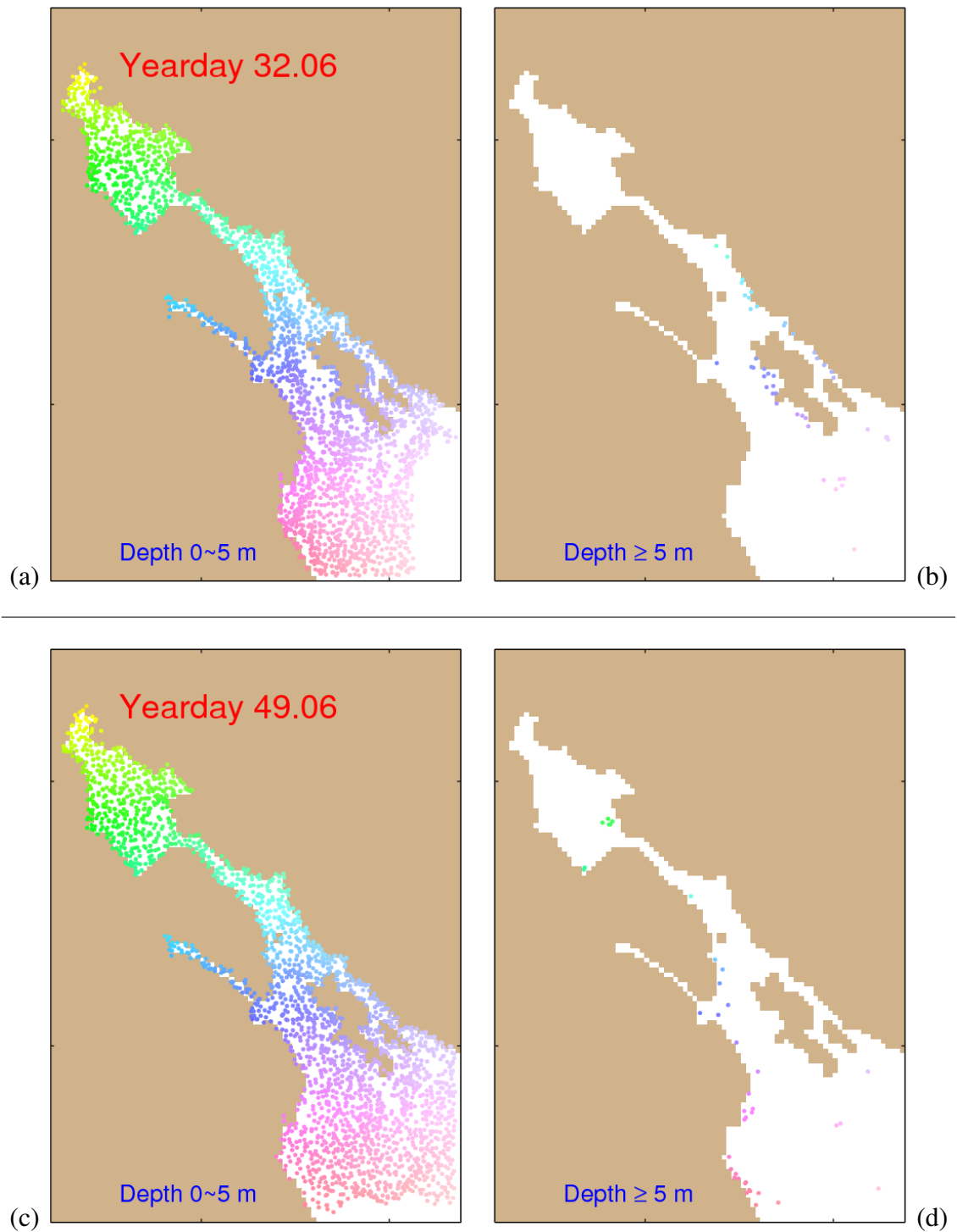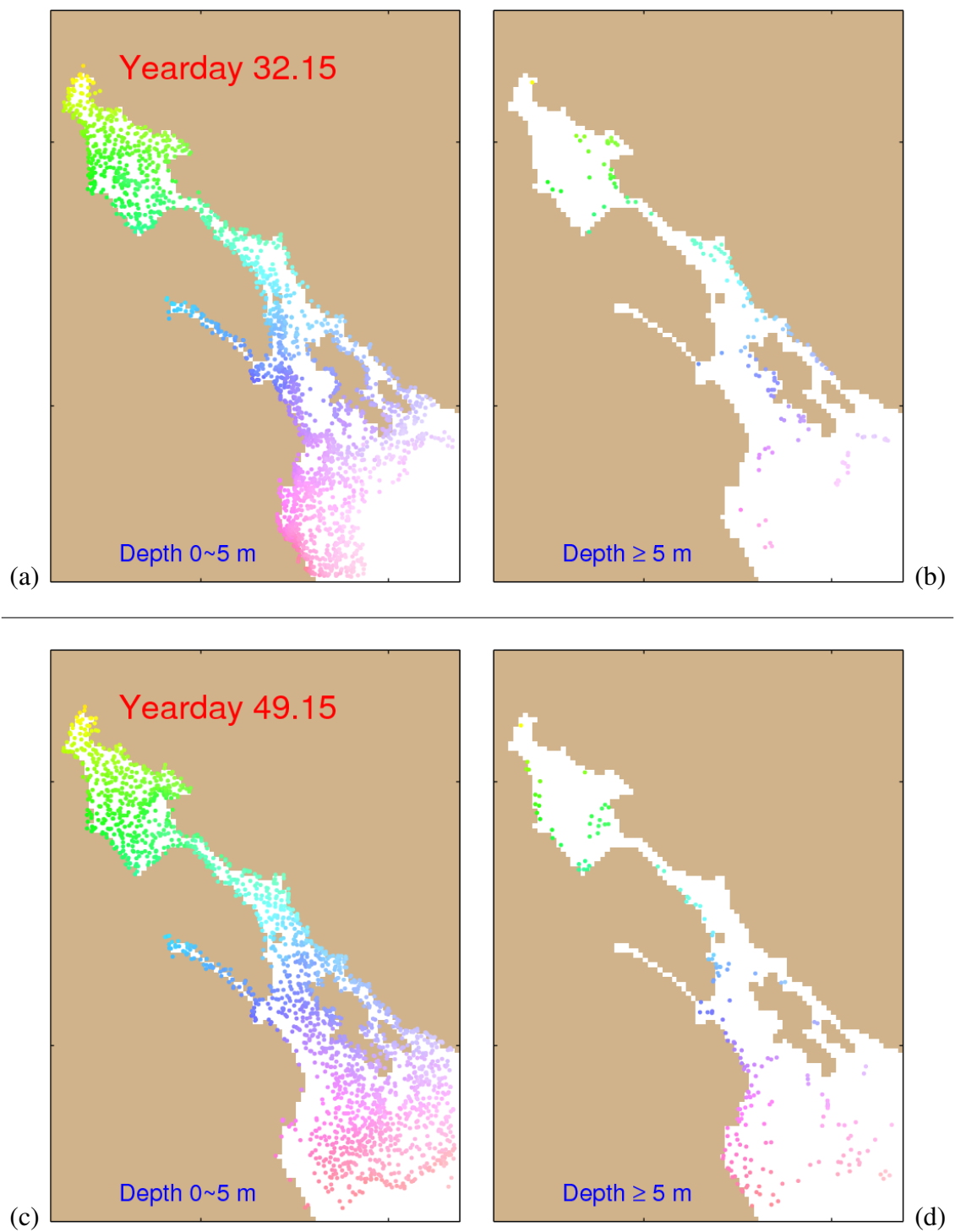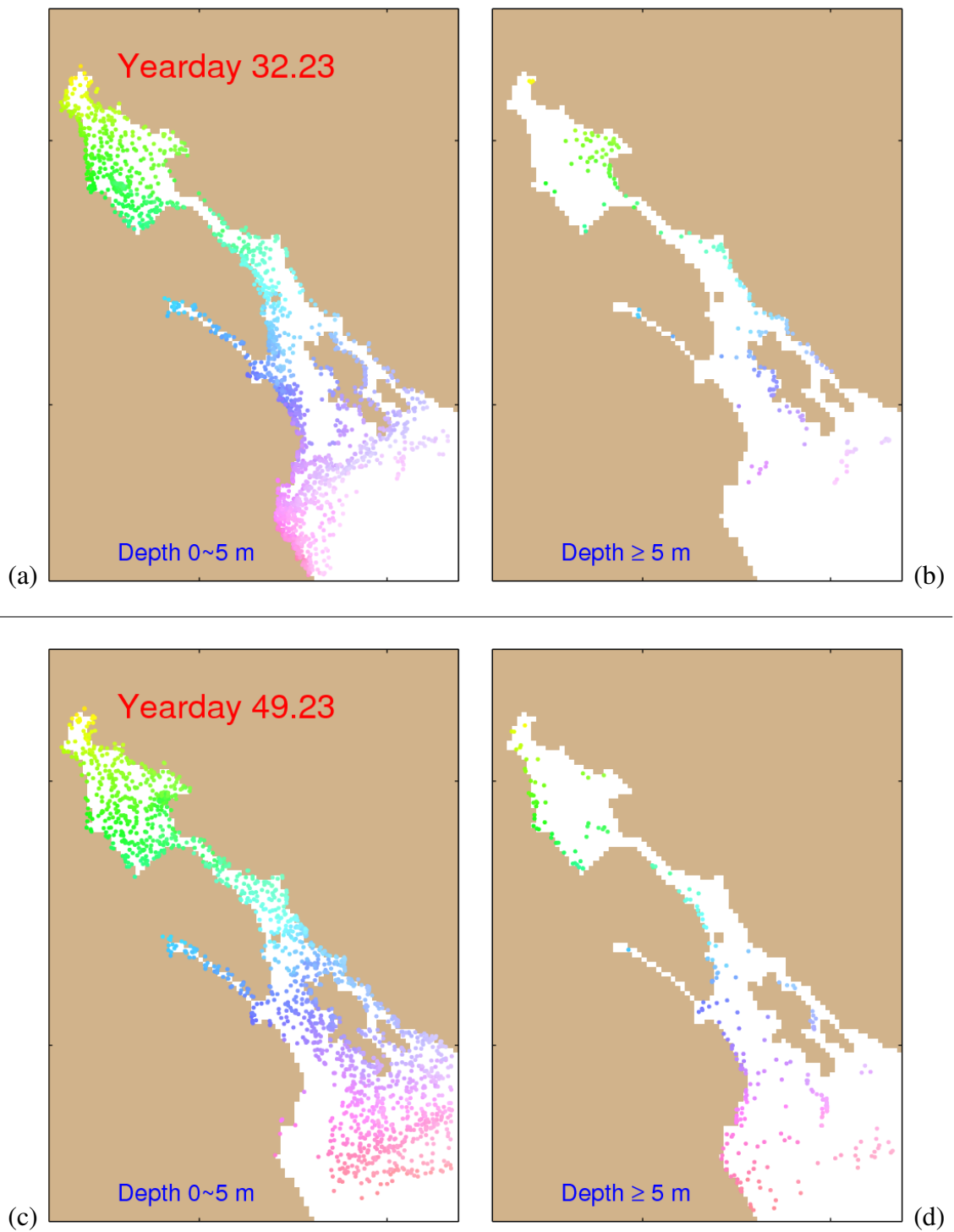
A connectivity matrix provides useful information of how each region hydrodynamically is connected to each other (*Thompson et al.*, 2002). To calculate the connectivity matrix from trajectories of passive particles, Halifax Harbour is divided into five subareas (Figure 2.3): Bedford Basin, the Narrows, Inner Harbour, Northwest Arm and Outer Harbour. The horizontal and vertical elements in the connectivity matrix shown in Figure 5.15 represent the sink and source region respectively in the TRACK-mean experiment. The diagonal elements of the matrix from bottom-left to top-right represent percentages of particles remaining in their original subarea during the experiment period. The horizontal elements (S_h) with respect to each diagonal element (S_d) in the matrix represent the percentages of the particles in a given subarea (S_d) reaching to other subareas (S_h, sink), and vertical elements (S_v) represent the percentages of the particles released in other subareas (S_v, source) moving to a given subarea (S_d) during the experiment period. About 75% and 85% of particles remain in Bedford Basin and the Northwest Arm, respectively in experiment TRACK-mean. In this experiment nearly 90% of particles are flushed to the open sea in the Outer Harbour. About 24%, 27% and 26% of particles travel from Bedford Basin to the Narrows, from the Narrows to the Inner Harbour, and from the Inner Harbour to the Outer Harbour, respectively, which indicates the model-calculated seaward currents carry particles from Bedford Basin to the open sea. The connectivity matrices calculated from the TRACK-storm experiments are shown in Figure 5.16. On day 32, nearly all the particles still remain in Bedford Basin. More than 70% of particles initially over the Outer Harbour are flushed to the open ocean. On day 49, nearly 30% of particles released from Bedford Basin drift to other areas. More than 80% of the Outer Harbour's particles are flushed to the open ocean.

Figure 5.15: Connectivity matrix over five subareas in Halifax Harbour (see Figure 2.3) based on passive particles carried by model-calculated annual mean currents produced by submodel L5 over 5 days.
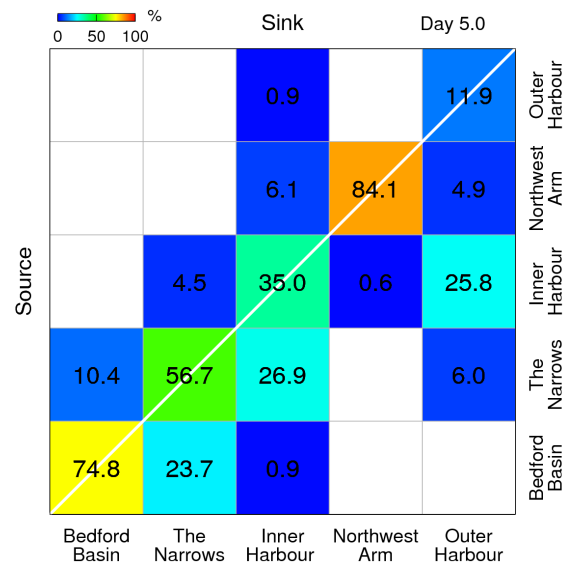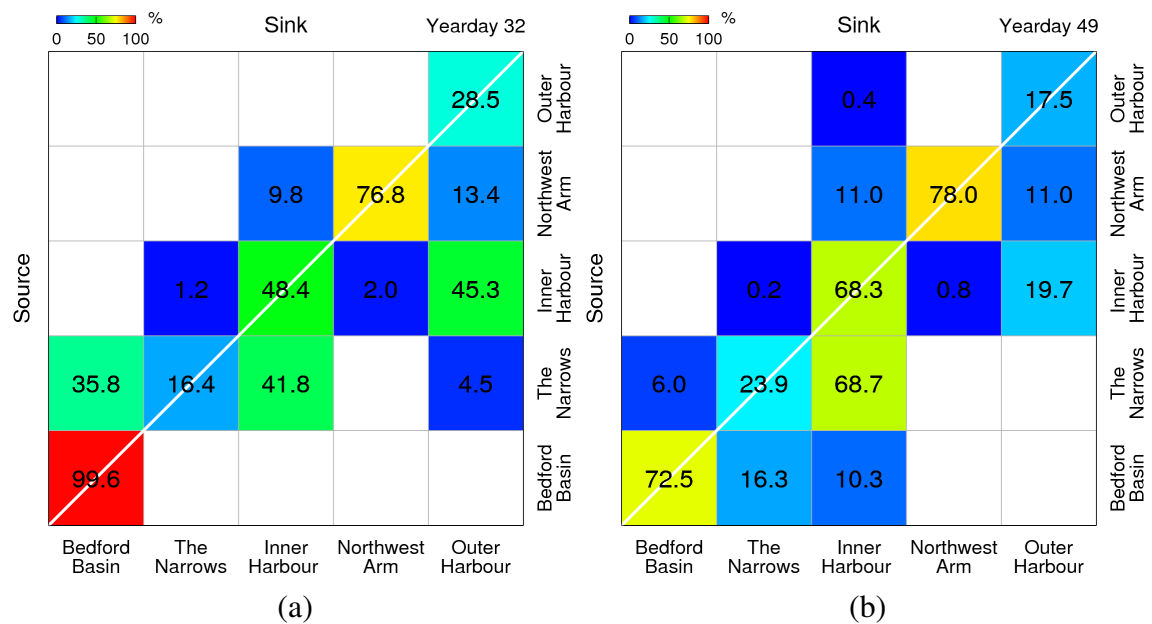

Figure 5.16: Connectivity matrices over five subareas in Halifax Harbour (see Figure 2.3) calculated from particle tracking experiments of (a) yearday 32 and (b) yearday 49 in 2006.

CHAPTER 6

SUMMARY AND DISCUSSION

A nested-grid ocean circulation modelling system was used to simulate circulation, hydrography and associated variability in Halifax Harbour in 2006. The modelling system was driven by tides, water discharges, atmospheric forcing, heat fluxes and initialized from newly generated monthly mean temperature and salinity climatology for Halifax Harbour. The nested-grid modelling system performance was validated against observations available to this study. The modelling system has reasonable skill in reconstructing sea surface elevation, including tidal and non-tidal components, in the Harbour. The depth-averaged M_2 tidal currents produced by the model are similar to the WebTide datasets for the Scotian Shelf (*Dupont et al.*, 2005) and Halifax Harbour (*Greenberg*, 1999). The time-mean currents profiles are in good agreement with some archived current meter records for Halifax Harbour discussed by *Petrie and Yeats* (1990). The time-mean circulation in the Harbour produced by the model is characterized by a typical two-layer estuarine circulation with seaward flow in the upper layer and landward flow in the lower layer. The modelling system also has skill in simulating temperature, salinity and associated seasonal and synoptic variability in Halifax Harbour.

Numerical process studies were conducted using the nested-grid modelling system to gain a better understanding of the hydrodynamic response of Halifax Harbour to tides, wind and buoyancy forcing associated with freshwater runoff. Our model results demonstrate that the freshwater discharge plays a very important role in maintaining a low salinity plume in the upper layer in Bedford Basin. The local wind forcing plays a very important role in affecting the movement and vertical structure of the low salinity front in Bedford Basin and also modulating the tidal circulation in the Narrows. The remotely generated coastal currents on the Scotian Shelf propagate into the Outer Harbour, carrying saline

108

offshore water masses into the Harbour. Tidal currents are strong in the Narrows. The dominant westerly or northwesterly winds in winter enhance the two-layer estuarine circulation. The dominant southwesterly winds in summer are a major cause of coastal upwelling outside Halifax Harbour.

Numerical passive tracer and particle tracking experiments were used to estimate the flushing time, dispersion and retention in Halifax Harbour. Based on the passive tracer experiments, we estimated the flushing time of the entire Bedford Basin to be about 90.6 days, 39.2 days in the upper Bedford Basin, and only about 1.1, 4.5 and 1.9 days in the Narrows, Inner Harbour and Outer Harbour, respectively. We calculated the movements of particles that are carried passively by the time-independent 3D annual mean currents (TRACK-mean) and time-dependend 3D currents (TRACK-storm) produced by submodel L5 of the NCOPS-HFX with an added random walk to approximate the sub-grid scale dispersion. The TRACK-mean experiment shows that within five days, about 75% and 85% of particles remain in Bedford Basin and the Northwest Arm, respectively; nearly 90% of particles are flushed to the open sea in the Outer Harbour. The TRACK-storm experiments demonstrate that particle movement and hydrodynamic connectivity in the harbour vary significantly during different storm events.

The development of the nested-grid ocean circulation modelling system for Halifax Harbour provides a framework for investigating a wide range of dynamic issues in the harbour, some of which have been discussed here. The modelling system reproduces many key features of sea surface elevations, currents and hydrography in Halifax Harbour. For the numerical study of sewage pollution and spring bloom in this region, more advanced numerical models, such as fully coupled physical-water quality and physical-biological models, are needed.

Over the next 100 years, climate change may have a significant impact on the oceanographic conditions in Halifax Harbour. For example, the North Atlantic Oscillation (NAO) is one of the most important manifestations of climate fluctuation in the North Atlantic. Both the positive and negative phases of the NAO are associated with changes in the intensity and location of the North Atlantic jet stream and storm tracks. *Li and Harrison* (2008) show that an atmospheric climate signal could propagate to phytoplankton in Bedford Basin.

A study presented to Halifax regional councillors on February 9, 2010 suggests that

local sea level could rise by 73 cm between 2000 and 2100 in Halifax Harbour (http: //www.thecoast.ca/general/pdfs/SeaLevelRise.pdf). The direct impact of sea level rise is that low-lying areas in the study region might be flooded in the future. The global change of atmospheric circulations could modify the wind forcing in the Harbour. An intensified westerly or northwesterly wind in winter over Halifax Harbour could enhance the two-layer estuarine circulation in the Harbour, which could also increase the exchange of the Harbour water with offshore water. Stronger wind fields in summer might lead to enhanced upwelling or downwelling along the south coast of Nova Scotia, affecting the hydrography in the Harbour. Changes of the atmospheric circulation might also change the frequency and intensity of storms passing the study regions. The surge associated with storms and hurricanes could cause significant damage to low-lying areas in the study region. Atmospheric circulation changes could also influence precipitation over Halifax Harbour that could affect the strength and position of the freshwater front in Bedford Basin. An increase in precipitation should lead to more storm water and sewage directly discharged into the Harbour, due to limited capacity of sewage treatment plants. The increase of the discharge of the St. Lawrence River in the Gulf of St. Lawrence could also decrease the salinity of the Nova Scotia Current which might reduce the impact of the intrusion of salty offshore water into Halifax Harbour in some degree. The Nova Scotia Current, the Labrador Current and the Gulf Stream all play an important role in affecting circulation over the Scotian Shelf and slope regions. The change of the circulation and hydrography on the Scotian Shelf could influence the circulation and hydrography in Halifax Harbour. Finally, the sewage discharge could increase in the Harbour as further developments associated with the increase of population and economic activities in the Halifax area.

The nested-grid modelling system for Halifax Harbour is an useful tool to quantify the impacts of climate change of external forcing on the oceanographic conditions in Halifax Harbour under different scenarios. The model results could be used for decision making under extreme events and further developments in the Harbour.

BIBLIOGRAPHY

Anderson, C., and P. Smith, Oceanographic observations on the Scotian Shelf during CASP, *Atmosphere-Ocean*, *27*, 130–156, 1989.

ASA Consulting Limited, Final report to Halifax Harbour Cleanup Inc. on water quality modelling in Halifax Harbour, *Technical Report*, Halifax, N.S., 1991.

Bousquet, T., How the sewage plant broke, http://www.thecoast.ca/halifax/how-the-sewage-plant-broke/Content?oid=1210451, 2009.

Buckley, D. E., and G. V. Winters, Geochemical characteristics of contaminated surficial sediments in Halifax Harbour: impact of waste discharge, *Canadian Journal of Earth Sciences*, *29*, 2617–2639, 1992.

CBC News, Harbour sewage woes prompt new diving rules, http://www.cbc.ca/canada/nova-scotia/story/2009/09/01/ns-navy-divers-harbour.html, 2009.

Daley, R., *Atmospheric data analysis*, Cambridge University Press, 1993.

DeIure, A. M., The effect of storms on sediments in Halifax Inlet, Nova Scotia, M.Sc. Thesis, Dalhousie University, 1983.

Donohue, S. M., A numerical model of an upwelling event off the coast of Nova Scotia, M.Sc. Thesis, Royal Military College of Canada, 2001.

Drinkwater, K., and G. Taylor, Monthly means of the temperature, salinity and density along the Halifax Section, *Canadian Technical Report of Fisheries and Aquatic Sciences 1093*, 1982.

Dupont, F., C. Hannah, D. Greenberg, J. Cherniawsky, and C. Naimie, Modelling system for tides for the Northwest Atlantic coastal ocean, *Canadian Technical Report of Hydrography and Ocean Sciences 221*, 2002.

Dupont, F., C. Hannah, and D. Greenberg, Modelling the sea level of the upper Bay of Fundy, *Atmosphere-Ocean*, *43*, 33–47, 2005.

Durski, S., S. Glenn, and D. Haidvogel, Vertical mixing schemes in the coastal ocean: Comparison of the level 2.5 Mellor-Yamada scheme with an enhanced version of the K profile parameterization, *Journal of Geophysical Research*, *109*, C01015, 2004.

Fader, G. B. J., and R. O. Miller, Surficial geology, Halifax Harbour, Nova Scotia, *Geological Survey of Canada Bulletin 590*, 2008.

Fogarty, C. T., R. J. Greatbatch, and H. Ritchie, The role of anomalously warm sea surface temperatures on the intensity of Hurricane Juan (2003) during its approach to Nova Scotia, *Monthly Weather Review*, *134*, 1484–1504, 2006.

Forrester, W. D., Canadian tidal manual, *Technical Report*, Department of Fisheries and Oceans, Ottawa, Ont., 1983.

Fournier, R. O., Halifax Harbour Task Force Final Report, *Technical Report*, Halifax, N.S., 1990.

Geshelin, Y., J. Sheng, and R. J. Greatbatch, Monthly mean climatologies of temperature and salinity in the western North Atlantic, *Canadian Data Report of Hydrography and Ocean Sciences 153*, 1999.

Greenberg, D. A., Atlas of tidal currents for Halifax Harbour, http://www.mar.dfo-mpo.gc.ca/science/ocean/coastal_hydrodynamics/atlas/atlas.pdf, 1999.

Greenberg, D. A., T. Murty, and A. Ruffman, A numerical model for the Halifax Harbour tsunami due to the 1917 explosion, *Marine Geodesy*, *16*, 153–167, 1993.

Hachey, H. B., The effect of a storm on an inshore area with markedly stratified waters, *Journal of the Biological Board of Canada*, *1*, 227–247, 1935.

Huntsman, A. G., Circulation and pollution of water near and around Halifax Harbour, *Contributions to Canadian Biology*, *2*, 71–81, 1924.

Jordan, F., Oceanographic data of Halifax Inlet, *BIO Data Series BI-D-72-8.*, 1972.

Large, W., and S. Pond, Open ocean momentum flux measurements in moderate to strong winds, *Journal of Physical Oceanography*, *11*, 324–336, 1981.

Lawrence, D., Physical Oceanography and Modelling in Halifax Harbour: A Review, in *Investigations of marine environmental quality in Halifax Harbour*, edited by H. Nicholls, 1989.

Li, W. K. W., and W. G. Harrison, Propagation of an atmospheric climate signal to phytoplankton in a small marine basin, *Limnology and Oceanography*, *53*, 1734–1745, 2008.

Loder, J., C. Hannah, B. Petrie, and E. Gonzalez, Hydrographic and transport variability on the Halifax section, *Journal of Geophysical Research*, *108*, 8003, 2003.

MacLaren Plansearch Limited, Final report to Halifax Harbour Cleanup Inc. on physical oceanography, *Technical Report*, Halifax, N.S., 1991.

MacLaren Plansearch Limited, and Martec Limited, Final Report to Halifax Harbour Cleanup Inc. on sediment transport modelling at Ives Point, *Technical Report*, Halifax, N.S., 1991.

McGonigal, D., R. Loucks, and D. Ingraham, Halifax narrows: Sample current meter data 1970-71, *BIO Data Series BI-D-74-5*, 1974.

Mellor, G., and T. Yamada, Development of a turbulence closure model for geophysical fluid problems, *Reviews of Geophysics and Space Physics*, *20*, 851–875, 1982.

Mullarney, J., A. Hay, and A. Bowen, Resonant modulation of the flow in a tidal channel, *Journal of Geophysical Research*, *113*, C10007, 2008.

Orlanski, I., A simple boundary condition for unbounded hyperbolic flows, *Journal of Computational Physics*, *21*, 251–269, 1976.

Paulson, C., and J. Simpson, Irradiance measurements in the upper ocean, *Journal of Physical Oceanography*, *7*, 952–956, 1977.

Pawlowicz, R., B. Beardsley, and S. Lentz, Classical tidal harmonic analysis including error estimates in MATLAB using T_TIDE, *Computers & Geosciences*, *28*, 929–937, 2002.

Petrie, B., and P. Yeats, Simple models of the circulation, dissolved metals, suspended solids and nutrients in Halifax Harbour, *Water Pollution and Resource Journal of Canada*, *25*, 325–349, 1990.

Petrie, B., B. Topliss, and D. Wright, Coastal upwelling and eddy development off Nova Scotia, *Journal of Geophysical Research*, *92*, 12979–12991, 1987.

Platt, T., A. Prakash, and B. Irwin, Phytoplankton nutrients and flushing of inlets on the coast of Nova Scotia, *Le Naturaliste Canadien*, *99*, 253–261, 1972.

Press, W., S. Teukolsky, W. Vetterling, and B. Flannery, *Numerical recipes in Fortran; the art of scientific computing*, Cambridge University Press, 1993.

Rabinovich, A. B., Seiches and harbor oscillations, in *Handbook of coastal and ocean engineering*, edited by Y. Kim, chap. 9, pp. 198–198, World Scientific Publishing Company, 2009.

Robichaud, B., and J. Mullock, The Weather of Atlantic Canada and Eastern Québec, http://www.navcanada.ca/ContentDefinitionFiles/publications/lak/atlantic/A34E-W.PDF, 2001.

Sheng, J., D. Wright, R. Greatbatch, and D. Dietrich, CANDIE: A new version of the DieCAST ocean circulation model, *Journal of Atmospheric and Oceanic Technology*, *15*, 1414–1432, 1998.

Sheng, J., R. Greatbatch, and D. Wright, Improving the utility of ocean circulation models through adjustment of the momentum balance, *Journal of Geophysical Research*, *106*, 16711–16728, 2001.

Sheng, J., J. Zhao, and L. Zhai, Examination of circulation, dispersion, and connectivity in Lunenburg Bay of Nova Scotia using a nested-grid circulation model, *Journal of Marine Systems*, *77*, 350–365, 2009.

Signell, R., and W. Geyer, Transient eddy formation around headlands, *Journal of Geophysical Research*, *96*, 2561–2575, 1991.

Smagorinsky, J., General circulation experiments with the primitive equations, *Monthly Weather Review*, *91*, 99–164, 1963.

Smith, B., and E. Miyaoka, Frequency domain identification of harbour seiches, *Environmetrics*, *10*, 575–587, 1999.

Song, Y., and D. Haidvogel, A semi-implicit ocean circulation model using a generalized topography-following coordinate system, *Journal of Computational Physics*, *115*, 228–244, 1994.

Spencer, P. L., P. R. Janish, and C. A. I. Doswell, A four-dimensional objective analysis scheme and multitriangle technique for wind profiler data, *Monthly Weather Review*, *127*, 279–291, 1999.

Taylor, G., Diffusion by continuous movements, *Proceedings of the London Mathematical Society*, *2*, 196–212, 1922.

Tee, K. T., and B. Petrie, A two-dimensional baroclinic model for the Halifax Harbour, in *Proceedings Second Halifax Inlet Research Workshop*, 1991.

Thompson, K. R., and J. Sheng, Subtidal circulation on the Scotian Shelf: Assessing the hindcast skill of a linear, barotropic model, *Journal of Geophysical Research*, *102*, 24987–25003, 1997.

Thompson, K. R., M. Dowd, Y. Shen, and D. A. Greenberg, Probabilistic characterization of tidal mixing in a coastal embayment: a Markov Chain approach, *Continental Shelf Research*, *22*, 1603–1614, 2002.

Thompson, K. R., K. Ohashi, J. Sheng, J. Bobanovic, and J. Ou, Suppressing bias and drift of coastal circulation models through the assimilation of seasonal climatologies of temperature and salinity, *Continental Shelf Research*, *27*, 1303–1316, 2007.

Wilson, S. J., Case study: The costs and benefits of sewage treatment and source control for Halifax Harbour, http://www.gpiatlantic.org/pdf/water/halharbour.pdf, 2000.

Xing, J., and A. M. Davies, A three-dimensional baroclinic model of the Irish Sea: Formation of the thermal fronts and associated circulation, *Journal of Physical Oceanography*, *31*, 94–114, 2001.

Yang, B., and J. Sheng, Process study of coastal circulation over the inner Scotian Shelf using a nested-grid ocean circulation model, with a special emphasis on the storm-induced circulation during tropical storm Alberto in 2006, *Ocean Dynamics*, *58*, 375–396, 2008.

Yang, B., J. Sheng, B. G. Hatcher, and B. Petrie, Numerical study of circulation and temperature-salinity distributions in the Bras d'Or Lakes, *Ocean Dynamics*, *57*, 245–268, 2007.

Zhang, H., The effects of frshwater inflow on the water quality of Bedford Basin Estuary: A modeling study, M.A.Sc. Thesis, Dalhousie University-DalTech, 1998.